INTEGRATION OF RENEWABLE ENERGY SOURCES:

RELIABILITY-CONSTRAINED POWER SYSTEM PLANNING AND

OPERATIONS USING COMPUTATIONAL INTELLIGENCE

A Dissertation

by

LINGFENG WANG

Submitted to the Office of Graduate Studies of
Texas A&M University
in partial fulfillment of the requirements for the degree of

DOCTOR OF PHILOSOPHY

December 2008

Major Subject: Electrical Engineering

INTEGRATION OF RENEWABLE ENERGY SOURCES:

RELIABILITY-CONSTRAINED POWER SYSTEM PLANNING AND

OPERATIONS USING COMPUTATIONAL INTELLIGENCE

A Dissertation

by

LINGFENG WANG

Submitted to the Office of Graduate Studies of
Texas A&M University
in partial fulfillment of the requirements for the degree of

DOCTOR OF PHILOSOPHY

Approved by:

Chair of Committee,	Chanan Singh
Committee Members,	Karen L. Butler-Purry
	Jim X. Ji
	Lewis Ntaimo
Head of Department,	Costas N. Georghiades

December 2008

Major Subject: Electrical Engineering

ABSTRACT

Integration of Renewable Energy Sources: Reliability-constrained Power System

Planning and Operations Using Computational Intelligence. (December 2008)

Lingfeng Wang, B.Eng, Zhejiang University, China;

M.Eng, Zhejiang University, China;

M.Eng, National University of Singapore

Chair of Advisory Committee: Dr. Chanan Singh

Renewable sources of energy such as wind turbine generators and solar panels have attracted much attention because they are environmentally friendly, do not consume fossil fuels, and can enhance a nation's energy security. As a result, recently more significant amounts of renewable energy are being integrated into conventional power grids. The research reported in this dissertation primarily investigates the reliability-constrained planning and operations of electric power systems including renewable sources of energy by accounting for uncertainty. The major sources of uncertainty in these systems include equipment failures and stochastic variations in time-dependent power sources.

Different energy sources have different characteristics in terms of cost, power dispatchability, and environmental impact. For instance, the intermittency of some renewable energy sources may compromise the system reliability when they are integrated into the traditional power grids. Thus, multiple issues should be considered in grid interconnection, including system cost, reliability, and pollutant emissions. Furthermore, due to the high complexity and high nonlinearity of such non-traditional power systems with multiple energy sources, computational intelligence based optimization methods are used to resolve several important and challenging problems in their operations and planning. Meanwhile, probabilistic methods are used for relia-

bility evaluation in these reliability-constrained planning and design.

The major problems studied in the dissertation include reliability evaluation of power systems with time-dependent energy sources, multi-objective design of hybrid generation systems, risk and cost tradeoff in economic dispatch with wind power penetration, optimal placement of distributed generators and protective devices in power distribution systems, and reliability-based estimation of wind power capacity credit. These case studies have demonstrated the viability and effectiveness of computational intelligence based methods in dealing with a set of important problems in this research arena.

v

To my family and friends

ACKNOWLEDGMENTS

Many people deserve special acknowledgment for their support throughout the duration of this work.

First, I must acknowledge my deep gratitude to my advisor, Dr. Chanan Singh, for his excellent professional guidance and constant assistance rendered in making this dissertation possible. His insightful comments and suggestions fueled the research. I want to say that working under his supervision during my Ph.D. study is one of the luckiest things in my life. His mentoring will benefit me in a long term.

Next, I would like to express great thanks to Dr. Karen Butler-Purry, Dr. Jim Ji, and Dr. Lewis Ntaimo for their effort in serving as members of my Ph.D. studies committee. They consistently provided strong support to my career development in the academic environment. I really appreciate their help during these years.

I am indebted to many friends for their assistance and advice. They have stood by and encouraged me when my productivity waned. I also wish to thank my family for their ever-present encouragement and for the moral and practical support given over the years before and throughout this endeavor. I dedicate this dissertation to them.

TABLE OF CONTENTS

      A. Introduction   29
      B. Reliability Evaluation of Hybrid Generating Systems   . . .   31
      C. Monte Carlo Simulation and Population-based Intelli-
         gent Search   32
            1. State space   33
            2. Monte Carlo Simulation   34
                  a. Computational procedure   35
                  b. Stopping criteria   36
                  c. Some remarks   36
            3. Population-based Intelligent Search   37
                  a. Computational procedure   37
                  b. Stopping criteria   38
                  c. Some remarks   39
                  d. Representative PIS algorithms   39
            4. Conceptual comparison between MCS and PIS   40
      D. PIS-based Adequacy Evaluation   41
      E. Simulations and Evaluation   48
      F. Summary   58

VI   RELIABILITY-CONSTRAINED OPTIMUM PLACEMENT
      OF RECLOSERS AND DISTRIBUTED GENERATORS IN
      DISTRIBUTION NETWORKS USING ANT COLONY SYS-
      TEM ALGORITHM   59

      A. Introduction   59
      B. Problem Formulation   60
      C. Ant Colony System Algorithms   62
            1. Basic principle   63
            2. Basic steps   63
      D. The Proposed Approach   65
            1. Search space   66
            2. Reliability evaluation   67
            3. Solution construction and pheromone updating   68
            4. Computational procedure   69
      E. Simulation Results and Analysis   70
      F. Summary   78

LIST OF TABLES

LIST OF FIGURES

FIGURE   Page

CHAPTER I

INTRODUCTION

This chapter first presents the background of the research reported in this dissertation. Then research objectives and the dissertation organization are given outlining an overall picture of this investigation.

A. Introduction

The optimum economic planning and operation of electric power systems play an important role in the modern electric power industry. In the face of depleting natural resources, the efficient use of available energy sources is becoming increasingly important in reducing operational costs while satisfying ever-tighter pollution regulations. Meanwhile, reliability analysis of the power system is being incorporated into various planning and operation strategies. Furthermore, in the recent years, renewable sources of energy have attracted much attention. They are highly advantageous with respect to the traditional fossil fuels in some respects. For instance, they are environmentally benign and do not consume depleting fuel reserves. However, some renewable sources of energy such as wind turbine generators and solar panels are time-dependent. This means that their availability in each time period cannot be precisely predicted ahead of time. As a result, when this type of energy sources is integrated into conventional power grids, some reliability problems may be introduced. For instance, when the wind speed drops, power deficiency may be caused in some regions due to insufficient generation and this may lead to power outage. Therefore, reliability issues in this type of power systems should be carefully addressed.

The journal model is *IEEE Transactions on Automatic Control.*

This research is intended to improve the utilization of natural resources, minimize the environmental pollution, and ensure the power system reliability. With the penetration of more significant amounts of time-dependent energy sources, more uncertain factors are involved in system reliability evaluation including equipment failures and stochastic characteristic of generation sources. For this purpose, probabilistic methods are used for reliability evaluation by taking into account various uncertainties. Meanwhile, power networks have become very large these days which involve numerous nodes and lines. As a result, traditional analytical methods oftentimes become less effective or even are unable to deal with these kinds of complex power systems. In this work, computational intelligence based optimization techniques are applied to deal with a set of challenging problems, which are usually able to derive an adequate solution within a reasonable amount of time. These methods are less sensitive to the system complexity and nonlinearity as compared with the analytical methods. In this study, several important real-world problems in this research arena are examined.

B.   Research Objectives

As indicated in the dissertation title, there are three major research objectives in this study, which are to be examined through several case studies.

- The impact of renewable energy integration on the traditional power systems, especially from the perspective of system planning and operations.

- Reliability-constrained designs accounting for renewable energy integration, especially time-dependent energy sources.

- Effectiveness of computational intelligence based optimization methods in dealing with highly complex and highly nonlinear problems in power system planning and operations.

C.   Organization of Dissertation

The dissertation can be broadly divided into two parts. The first four chapters present the background knowledge and motivation of this research, and the following four chapters are devoted to several important problems in this research arena. In the second chapter, some conventional and renewable sources of energy are presented focusing on their cost and environmental impact. The third chapter discusses the reliability-constrained planning and operations when the renewable energy is integrated into the power grids at both power generation and distribution levels. Chapter IV presents the major computational intelligence based optimization techniques used in this study. In Chapter V, reliability evaluation of hybrid generation systems is carried out based on population-based intelligent search, where the stochastic nature of wind power is also taken into account. In Chapter VI, the optimum placement schemes of distributed generators and reclosers for power distribution networks are derived by an outstanding discrete optimizer termed ant colony system. In Chapter VII, the economic power dispatch problem is readdressed when the wind power is integrated. An improved particle swarm optimization algorithm is developed to find out a set of tradeoff solutions in terms of operational cost and system security. Chapter VIII discusses the optimal design of hybrid generation systems including fossil-fuel-fired generators, wind turbine generators, solar panels, and storage batteries. A modified multi-objective particle swarm optimization algorithm is used to derive the tradeoff solutions measured by system cost, reliability, and pollutants emission. In Chapter IX, the wind power capacity credit is estimated through a particle swarm optimization algorithm. Loss of load probability is used as the reliability index in the calculation.

CHAPTER II

CONVENTIONAL AND RENEWABLE SOURCES OF ENERGY

Due to the ever-increasing demands on energy, energy consumption worldwide is rapidly increasing. As a result, fossil-fuel reserves are depleting and energy prices are skyrocketing especially in the past few years. Meanwhile, with increasing concerns on environmental protection, there are stricter regulations on pollutant emissions. The most important emissions considered in the power generation industry, due to their highly damaging effects on the ecological environment, are sulfur dioxide and nitrogen oxides. These emissions can be modeled through functions that associate emissions with power production for conventional generating units. Besides environmental pollution, global warming is another issue of much concern internationally in the current political climate, and it has become a highly pressing challenge. Human activity has been aggravating the emission of greenhouse gases, because the major portion of carbon dioxide is produced by combusting coal, oil, and gas. As a severe consequence, earth surface temperature has increased around 0.6°C since the late 19th century, and about 0.2°C to 0.3°C within the past 25 years (from National Oceanic and Atmospheric Administration). However, the consumption of electric power keeps growing dramatically on a worldwide basis. Many countries have specified goals to curb the emission of carbon dioxide to prevent or slow down further global warming. Basically, there are two major ways to achieve this goal, that is, implementing energy-saving measures and wide utilization of renewable energy. The renewable sources of energy have a much lower environmental impact than conventional energy sources, producing low or no emissions of carbon dioxide, particulates, and sulphur dioxide.

As said earlier, today we are also facing the environmental crisis caused by climate change and greenhouse/polluting gas emissions. Development of renewable energy

technologies will not only make energy independence feasible, but it will protect our Earth home and provide healthier environments for human beings. Nowadays, people from relevant fields are bringing a broad range of expertise to radically increase the utilization of renewable energy and alternative fuels. Most renewable energy comes directly or indirectly from the sun, thus, the energy resource will not be depleted in the foreseeable future. Furthermore, the energy security of a country can be significantly enhanced by fully utilizing renewable energy due to its decreased reliance on imported fossil fuels. In this section, the characteristics of several alternative sources of energy are discussed. Besides the traditional fuel-fired generation, renewable sources of energy including wind turbine generators, solar panels, wave and tidal power, biomass, fuel cells, and geothermal energy are discussed in this section.

A.   Fuel-Fired Generators

Most of the world energy consumption currently relies on conventional sources of energy including coal, oil, and natural gas. These fossil fuels are nonrenewable since they consume limited resources that are diminishing, becoming too cost-ineffective, or too environmentally detrimental to retrieve. In traditional FFGs, pollutant emissions are the major drawback. For instance, coal has been a reliable, abundantly available, and relatively inexpensive fuel source for a long time, but coal-fired power generation is facing increasing pressure since environmental regulations are becoming more stringent than ever around the world. An affordable control scheme for air pollution reduction is a deciding factor in fossil fuels continued role as a prime energy source in the power generation industry. As a result, combined use of fuel sources and other cleaner sources may be a viable way to abate pollutant emissions while still fulfilling certain cost and reliability requirements. In the restructured power market, DG using

renewable sources of energy is being connected to the utility grid at the distribution level, attempting to diminish the demerits in traditional central generation plants. Renewable power sources promise to play an important role in complementing the fossil-fuel-fired generation by reducing its negative environmental impacts.

B.   Wind Turbine Generators

Wind energy is ample, renewable, widely dispersed, and clean. The conversion of wind energy into electricity can be achieved using wind turbines installed onshore and offshore. It can be used by large-scale wind farms for nation-level power grids as well as small turbines for rural residences or grid-isolated locations. WTGs are powered by windmills, which are usually operated by utilities and independent power producers (IPPs). They are located in areas with rich wind resources onshore or offshore. Thus, effective utilization of wind energy is particularly attractive in spurring the reduction of pollutant emissions, which is a major drawback to the traditional fossil-fuel-based generation. However, the availability of wind power is primarily determined by weather conditions and thus can quite fluctuate in a year or even in a day. The volatility of wind power should be fully addressed when designing a renewable-based power plant. In our investigation, other power sources are also used in order to mitigate or even out the fluctuations caused by the intermittency of wind power. Wind power has been widely developed worldwide. For instance, the average U.S. wind energy growth rate for the past 5 years is 24%. The leading countries in wind power generation are Germany, Spain, Denmark, and the Netherlands, and they occupy 84% of the total European wind capacity. By year 2020, it is anticipated that wind power will fulfill the residential demands of about half of the region's population.

C. Photovoltaic Cells

Sunlight can be directly converted into electric energy by PV panels. PV panels use the photovoltaic effect of semiconductors to generate electricity from sunlight. Like wind power, the production of a solar system is also influenced considerably by varying meteorological conditions. Because of its intermittent power supply, other supplemental power sources such as storage batteries are usually needed to smooth out the fluctuations. PV panels produce no direct emissions and thus are environmentally friendly. The advance of manufacturing technologies has significantly reduced the cost of a PV system, and PVs also have lower maintenance demands. Several PV power plants with capacities of 300 to 500 kW have been linked to power grids in Europe and the United States, and extensive research is now underway to achieve less expensive but more efficient PV cells.

D. Storage Batteries

Since both WTGs and PVs are intermittent sources of power, it is highly desirable to incorporate energy storage into such hybrid power systems. Energy storage can smooth out the fluctuations of wind and solar power and improve the load availability. In a certain sense, storage batteries can be deemed a buffer to balance the supply-and-demand relationship. When the power generated by WTGs and PVs exceeds the load demand, a certain amount of surplus power will be stored in the batteries within their total storage capacity for future use. On the contrary, when there is any deficiency in overall power generation, the stored power will be used to supply the load so as to enhance system reliability. Energy storage reduces the power dumped and thus helps to minimize the operational cost.

8

E.   Other Alternative Sources

1.   Tidal power

Tidal power is produced by capturing the energy contained in moving water mass due to strong waves or tides, and it has a fairly high efficiency rate. Like other renewable sources of energy, it requires a high capital cost but fairly low operation and maintenance costs. However, the installation of a barrage may significantly affect the water inside the basin as well as hamper fish activities. Among all kinds of intermittent renewable sources, tidal power is deemed capable of supplying relatively continuous and predictable power and is anticipated to increase considerably in the upcoming years.

2.   Biomass

In general, biomass refers to plant matter grown for use as biofuel as well as biodegradable wastes that can be combusted as fuel. It primarily includes solids, biofuels, biogas, landfill gas, and sewage treatment plant gas. Biomass is a type of sustainable energy but still contributes to global warming. If directly combusted without taking proper emissions filtering measures, it will cause environmental pollution problems as well. Based on the current technologies, production of liquid fuels from biomass is not sufficiently cost-effective due to the expenses caused by biomass production coupled with its conversion procedure to alcohols. By 2030, biomass-fueled electric power is expected to triple and meet 2% of the total world energy demand.

3.   Hydrogen and fuel cells

More recently, the fuel cell has been applauded as the "microchip of the energy industry" due to its great promise as an alternative for clean power generation. A

fuel cell is fundamentally an electrochemical device capable of converting hydrogen and oxygen into water, meanwhile producing electricity. Salient features of fuel cells are that they neither produce harmful emissions nor consume oil. Fuel cells are particularly useful in serving as power sources in remote locations or isolated areas such as spacecrafts and rural regions. They can also be applied to baseload power supply, combined heat and power generation, electric and hybrid electric vehicles, off-grid power generation, and so forth.

4. Geothermal energy

Geothermal can be interpreted as "earth heat" in plain text, and it can be used for clean power generation. Geothermal power is more competitive in countries that have restricted fossil-fuel resources. Geothermal energy for electricity generation has grown rapidly worldwide, reaching about 8,000 MW. Recent high and wildly fluctuating power prices have made geothermal energy more economically attractive.

Due to space restrictions, other alternative sources of energy such as hydropower and biofuels will not be discussed here. Corresponding literature may be referred to for more details. In this dissertation, the focus is put on the time-dependent energy sources such as wind power and solar power, which may have significant impacts on the power system reliability in grid integration.

CHAPTER III

RELIABILITY-CONSTRAINED POWER SYSTEM PLANNING AND

OPERATIONS INCLUDING TIME-DEPENDENT ENERGY SOURCES

System designers and planners always have concerns about system reliability. The term reliability relates to the ability of a system to perform its intended function for a given period of time under stated environmental conditions. The general approach has been, however, either intuitive or based on rule-of-thumb criteria derived from previous experience with similar systems. The intuitive approach has turned out to be inadequate due to the large scale and high complexity of modern industrial systems, where a composite of equipment and skills function as a unified entity. In the past two decades, more sophisticated quantitative techniques and indices have been developed to respond meaningfully to factors that affect system reliability. Quantitative assessment is achieved by building mathematical models that reasonably approximate the actual system and can be manipulated to derive suitable reliability measures. When quantitatively defined, reliability becomes a parameter that can be traded off with other parameters. The necessity of quantitative reliability springs from the ever increasing complexity of systems, cost competitiveness, alternative design evaluations, cost-benefit analysis, the need to study effects of operation and maintenance procedures, and so forth. Reliability modeling and evaluation is an important component in any reliability analysis program because the selected model provides the basis for predicting reliability measures [1], [2]. Various techniques of reliability modeling and evaluation can be classified into direct analytical modeling or simulation or a mixture of the two approaches. In the direct analytical modeling method, a model is built that reasonably approximates the physical system and is also amenable to calculation. The reliability measures are then attained by manipulating the model. Simulation also

deploys a mathematical model but proceeds by carrying out sampling experiments on this model. It is more flexible but is also more time-consuming and less accurate. Simulation can be used to provide estimates of the reliability measures. Monte Carlo simulation is a representative simulation method that is usually adopted to deal with reliability evaluation of large-scale or complex power systems [3]. Also, more recently, artificial intelligence based reliability evaluation has shown its promise in improving evaluation efficiency [4].

A.   Generation System Reliability Including Renewable Energy Sources

The objective of electric power systems is to supply electrical energy to consumers at low cost while simultaneously providing acceptable or economically justifiable service quality. Generation adequacy deals with the relative ability of the system to supply system load considering that generating units may be out of service when needed due to planned or unplanned outages or that the basic energy sources may be inadequate. Generation "adequacy" is distinct from the concept of "security," which deals with the relative ability of the system to survive sudden shocks or upsets such as faults or equipment failures without cascading failures or loss of stability. Generation adequacy is usually measured through the use of some adequacy index that quantifies system adequacy performance, and it is enforced through a criterion based on an acceptable value of this adequacy index. Some utilities rely on adequacy criteria whose values have been chosen based on engineering judgment to yield a reasonable balance between system cost and reliability performance and that have been validated by historical experience. However, if adequacy criteria are based on probabilistic indices that bear reasonable relationships to the actual reliability performance of the system, more pragmatic methods may be used to decide appropriate values of the

criteria. The reliability indices of generation capacity adequacy assessment can be broadly divided into two categories: deterministic and probabilistic. Deterministic indices normally include a percentage reserve margin as well as reserve margin in terms of the largest unit. Probabilistic indices usually comprise loss of load expectation (LOLE), frequency and duration (F&D) of capacity shortage events, and expected unserved energy (EUE). LOLE on an hourly basis is the expected number of hours per year when insufficient generating capacity is available to serve the load. It does not give information on a number of important system reliability attributes including magnitude of capacity shortages, duration of capacity shortage events, and expected amount of unserved energy. Frequency of generating capacity shortage events is defined as the expected number of such events per year. Duration is the expected length of capacity shortage periods when they occur. F&D indices use hourly load information and thus reflect the influences of daily load cycle shape. F&D methods model unit parameters more comprehensively than those models used in LOLE. F&D indices are conceptually superior with respect to LOLE. However, they have greater data requirements. The EUE index measures the expected amount of energy that will fail to be supplied per year due to generating capacity differences and/or shortages in basic energy supplies. Reliability analysis of power generation systems including time-dependent sources is aggravated by the volatile nature of wind resources, and thus the evaluation process unavoidably becomes more complex and challenging. The generating adequacy may be compromised provided that there is insufficient power available to fulfill the load due to intermittency of renewable sources of power. In the hybrid generation system design, besides the impact caused by generation volatility, the uncertainties including equipment failures coupled with random variations in both generation and load should all be considered. Usually time-series models can be used to accomplish generation and load forecasting by accounting for the randomness of

renewable sources of energy and load demands.

A system state depends on the combination of all component states and each component state can be characterized by the probability that the component appears in that state. Adequacy evaluation of power generation systems is usually concerned with assessing the capability of generation facilities to fulfill the system load requirements. In this assessment, the associated transmission and distribution facilities are deemed to be completely reliable and capable of transmitting and distributing the generated energy to the customer load points without failure possibility. Reliability indices of a generating system can be seen as the expected value of a test function applied to a system state, which is a vector representing the state of each component, in order to find out whether the specific generation combination corresponds to a feasible or infeasible solution. Thus, a fundamental parameter in reliability evaluation is the mathematical expectation of a given reliability index. Reliability evaluation is discussed from an expectation point of view in this study.

In this dissertation, four projects are concerned about the impacts of intermittent renewable energy sources on the power generation systems. They are reliability evaluation for hybrid generation systems including wind power penetration, economic power dispatch including wind power, optimum designs of hybrid power generation systems including multiple renewable energy sources, and reliability-based estimation of wind power capacity credit.

B.   Distribution System Reliability Including Renewable Energy Sources

Distributed generation (DG) is also known as embedded generation or dispersed generation, which is a hot topic in both academia and industry in recent years [5]. In the restructured power industry environment, distributed generation using renewable

energy sources is becoming increasingly important. Distributed generators are being directly connected to the power distribution networks, most often for enhancing the power system reliability in the presence of system faults and insufficient generation, or reducing the environmental impacts by avoiding use of fossil fuels.

However, interconnection of renewable energy sources to the existing distribution networks poses great challenges. The power flow in this type of power systems is bi-directional, which is significantly different from the traditional power distribution networks. The major concern of distribution network operators (DNOs) nowadays is the damaging impacts on power quality of the main power grid caused by the connected DGs. Thus, the coordination and control of protective devices should be redesigned. Moreover, the adverse impacts caused by the high degree penetration of alternative sources of energy should be taken care of.

As said earlier, when DGs are connected to the main power grid, one of the objectives is to enhance the system reliability. For instance, they can supply extra power to the power grid to minimize the loss of load probability; meanwhile, they can also be operated isolated from the main grid in the presence of system faults in the upstream network. Therefore, it is crucial to select the appropriate DG type, size, location, and priority in order to achieve the highest reliability of DG-enhanced distribution networks using the limited resources.

There are two industry-recognized indices for measuring reliability of power distribution networks:

- SAIDI (System Average Interruption Duration Index): Ratio between *total customer interruption durations* and *total number of customers served.*

- SAIFI (System Average Interruption Frequency Index): Ratio between *total number of customer interruptions* and *total number of customers served.*

In this dissertation, the optimum placement of both distributed generators and protective devices for distribution networks is discussed. The distributed generators can work in either islanding or grid-connected mode in order to optimize a composite reliability index made up of SAIDI and SAIFI.

In all the studies reported in this dissertation, we primarily address various system adequacy issues. It should be noted that in the context of system adequacy evaluation, the terms reliability and adequacy are usually interchangeable. This is because probabilistic methods are most often used to deal with system adequacy issues. Thus, throughout this dissertation, these two terms have the same meaning and can be substituted for one another.

CHAPTER IV

COMPUTATIONAL INTELLIGENCE BASED OPTIMIZATION METHODS

Optimization methods can be broadly classified into exact methods and heuristic techniques. Exact methods are usually based on the strict mathematical analysis, which may become less effective or even impractical for target problem when the system becomes large or complex. In these scenarios, heuristic methods may be a wise choice. There are two fundamental schemes for heuristics: "divide and conquer" and iterative improvement [6]. In the former scheme, the problem is first decomposed into a group of resolvable subproblems, and they are treated individually one by one. The solutions to the subproblems are then pieced together for achieving the final solution to the original problem. In this scheme, to yield adequate solutions the subproblems should essentially not be overlapping with one another, and they should be easy to patch back to recover the target problem. In the iterative improvement scheme, the design is started with a speculative configuration. Some reconfiguration operations are applied until a rearranged configuration able to improve the cost function is discovered. The reconfigured design then becomes the new configuration for subsequent rearrangement, and the reconfiguration process is iterated until no further improvements can be achieved for a certain number of iterations. We can see from the above procedure that iterative improvement composes a search process in the whole-solution space for achieving better designs. In the work reported in this dissertation, several meta-heuristic methods are used to accomplish different design and planning tasks for electric power systems.

The traditional approaches include linear programming, nonlinear programming, dynamic programming, network flows, and so on. These methods are usually rigorous in mathematical analysis but are weak in coping with high nonlinearity. They

even oftentimes suffer from the "curse of dimensionality". Due to the high complexity and high nonlinearity of many practical problems, meta-heuristics based on guided stochastic search have been proposed as an alternative to traditional analytical approaches. Computational Intelligence (CI) based search algorithms are a set of commonly used meta-heuristics, which can be further classified into population-based and non-population-based intelligent search. The former includes evolutionary algorithms, particle swarm optimization, ant colony optimization, bacteria foraging, artificial immune systems, and so forth; the latter includes simulated annealing, greedy randomized adaptive search procedures (GRASP), tabu search, and so forth.

In the following sections, four computational intelligence techniques used in this work will be introduced, which are genetic algorithms, particle swarm optimization, ant colony optimization, and artificial immune systems.

A.   Genetic Algorithms

Conventional derivative-based optimization methods are effective in resolving "smooth," i.e., continuous and differentiable problems, since they deploy derivatives to determine the direction of descent. However, derivative-based methods are often ineffective in dealing with problems lacking of smoothness, for instance, the problems with discontinuous, nondifferentiable, or stochastic objective functions. Genetic Algorithm (GA) is a population-based stochastic search procedure inspired by natural evolution [7]. GA has turned out to be an effective alternative for this kind of "nonsmooth" problems. Another reason for adopting GA is due to the large scale of solution space. The inherent directed search mechanism of GA helps to achieve outstanding convergence performance by truncating the solution space and avoiding inferior solutions.

In principle, GA is a simple iterative procedure that consists of a constant-size

population of individuals, each one represented by a finite string of symbols, known as the genome, encoding a possible solution in a given problem space. This space, referred to as the search space, comprises all possible solutions to the problem at hand. Generally, the genetic algorithm is applied to space which is too large to be exhaustively searched. The symbol alphabet used is often binary, though other representations have also been used, including character-based encodings, real-valued encodings, and – most notably – tree representations.

The standard genetic algorithm proceeds as follows: an initial population of individuals is generated at random or heuristically. In every evolutionary step, known as a generation, the individuals in the current population are decoded and evaluated according to some predefined quality criterion, referred to as the fitness, or fitness function. To form a new population (the next generation), individuals are selected according to their fitness. Many selection procedures are currently in use, one of the simplest being Holland's original fitness-proportionate selection, where individuals are selected with a probability proportional to their relative fitness. This ensures that the expected number of times an individual is chosen is approximately proportional to its relative performance in the population. Thus, the high-fitness individuals stand a better chance of "reproducing", while the low-fitness ones are more likely to disappear.

Selection alone cannot introduce any new individuals into the population, i.e., it cannot find new points in the search space. These are created by genetically inspired operators, of which the most well known are crossover and mutation. Crossover is performed with probability between two selected individuals, called parents, by exchanging parts of their genomes to form two new individuals, called offspring. In its simplest form, substrings are exchanged after a randomly selected crossover point. This operator tends to enable the evolutionary process to move toward "promising" regions of the search space. The mutation operator is introduced to prevent premature

convergence to local optima by randomly sampling new points in the search space. It is carried out by flipping bits at random, with some probability. Generally, genetic algorithms are stochastic iterative processes that are not guaranteed to converge. The termination condition may be specified as some fixed, maximal number of generations or as the attainment of an acceptable fitness level. The standard genetic algorithm can be presented in pseudo-code format as follows:

```
1  g:=0 {generation counter};
2  Initialize population P(g) ;
3  Evaluate population P(g) {i.e., compute fitness values};
4  while not done do
5      g:=g+1 ;
6      Select P(g) from P(g-1);
7      Crossover P(g) ;
8      Mutate P(g) ;
9      Evaluate P(g);
10 end
```

Algorithm 1: Pseudo-code of the standard genetic algorithm

B.   Particle Swarm Optimization

Particle Swarm Optimization (PSO) is a form of swarm intelligence, which was originally proposed by Kennedy and Eberhart [8]. It is motivated by social behavior of organisms such as bird flocking and fish schooling. In a flock of birds or a school of fish, if one individual finds a good way to move for the food or protection, other members in the swarm will be able to follow its movement promptly. This can be modeled by a swarm of particles moving in the multidimensional search space, each

of which has a position and a velocity. These particles fly across the hyperspace and record the best positions that they have ever encountered. Members of a swarm communicate desirable positions to one another and adjust their own velocities and positions accordingly. PSO can be used as an effective optimization tool to handle the optimization problems which are hard to resolve by the traditional analytical approaches. As an optimizer, PSO provides a population-based search procedure. Each single solution (i.e., a particle) can be deemed as a "bird" in the search space. Particles fly around in the multidimensional space and each particle adjusts its position based on both its own experience and that of its neighboring companions. In this way, PSO combines local search with global search for balancing the exploration and exploitation.

The procedure of a basic PSO algorithm can be illustrated as follows: For each particle, the particle parameters including both position and velocity are first initialized. Then its fitness value is calculated according to the fitness measure pre-specified. If the position is superior with respect to the best position *pbest* found so far, the current value is set as the new *pbest*. The particle with the best fitness value of all the particles is chosen as the *gbest*. Then, the particle velocity and the particle position are updated according to certain rules. Finally, the stopping criteria such as maximum iterations or minimum error are checked to see if the algorithm should halt or the above process should be repeated until the termination criteria are satisfied. During flight, each particle keeps track of its coordinates in the problem space which are associated with the best position it has achieved so far, whose fitness value is called *pbest*. Provided that a particle takes the whole population as its topological neighbors, the best value is a global best and is called *gbest*.

It is evident from the above procedure that PSO and GA share several common points. For instance, both of them begin with a randomly generated population; each

individual has a fitness value evaluated by the pre-specified criteria; both improve the solution quality through continuous adjustment of individual parameters. However, they also have distinctions in several aspects since their inner workings differ from one another. The philosophy of GA is "survival of the fittest" and that of PSO is "to follow the leader" and emergent behavior formation. For instance, PSO has no genetic operators such as crossover and mutation, and particles update their states with the internal velocities. The information sharing mechanism in PSO significantly differs from that in GAs. In GAs, the whole population moves like a group toward the promising region since individuals (i.e., chromosomes) share information with one another. However, in PSO, only local and global best positions are transparent to other individuals, which is in essence a form of one-way communication. Unlike GAs, PSO usually adopts the real-coded scheme. There are also less control parameters in PSO as compared to GA.

PSO algorithms are global optimization algorithms and do not need the operations for obtaining gradients of the cost function. Initially the particles are randomly generated to spread in the feasible search space. The update equation determines the position of each particle in the next iteration. Let $k \in \mathbb{N}$ denote the generation number, let $N \in \mathbb{N}$ denote the swarm population in each generation, let $x_i(k) \in \mathbb{R}^M$, $i \in \{1, \ldots, N\}$, denote the i-th particle of the k-th iteration, let $v_i(k) \in \mathbb{R}^M$ denote its velocity, let $c_1, c_2 \in \mathbb{R}_+$ and let $r_1(k), r_2(k) \sim U(0,1)$ be uniformly distributed random numbers between 0 and 1, let w be the inertia weight factor, and let $\chi \in [0,1]$ be the constriction factor for controlling the particle velocity magnitude. Then, the update equation is, for all $i \in \{1, \ldots, N\}$ and all $k \in \mathbb{N}$,

$$v_i(k+1) = \chi * (wv_i(k) + c_1 r_1(k)(pbest_i(k) - x_i(k)) + c_2 r_2(k)(gbest(k) - x_i(k))), \quad (4.1)$$

$$x_i(k+1) = x_i(k) + v_i(k+1), \quad (4.2)$$

where $v_i(0) \triangleq 0$ and

$$pbest_i(k) \triangleq \operatorname{argmin}_{x \in \{x_i(j)\}_{j=0}^{k}} f(x), \tag{4.3}$$

$$gbest(k) \triangleq \operatorname{argmin}_{x \in \{\{x_i(j)\}_{j=0}^{k}\}_{i=1}^{N}} f(x). \tag{4.4}$$

Hence, $pbest_i(k)$ is the position that for the i-th particle yields the lowest cost over all generations, and $gbest(k)$ is the location of the best particle in the entire population of all generations. The inertia weight w is considered to be crucial in determining the PSO convergence behavior. It regulates the effect of the past velocities on the current velocity. By doing so, it controls the wide-ranging and nearby search of the swarm. A large inertia weight facilitates searching unexplored areas, while a small one enables fine-tuning the current search region. The inertia is usually set to be a large value initially in order to achieve better global exploration, and gradually it is reduced for obtaining more refined solutions. The term $c_1 r_1(k)(pbest_i(k) - x_i(k))$ is relevant to cognition since it takes into account the particle's own flight experience, and the term $c_2 r_2(k)(gbest(k) - x_i(k))$ is associated with social interaction between the particles. Therefore, the learning factors c_1 and c_2 are also known as *cognitive acceleration constant* and *social acceleration constant*, respectively. The constriction factor χ should be chosen to enable appropriate particle movement steps.

In (4.1), the first term of its right hand side corresponds to the diversification mechanism while the latter two terms are relevant to the intensification mechanism in the search procedure. The first term is the velocity of the previous iteration. Without the latter two terms, the particle will keep on flying along the same direction until it reaches the boundary of the search space. It can be seen as a behavior which tries to explore new search areas. Thus, it facilitates the diversification in the search process. On the other hand, the latter two terms of (4.1) enable the intensification during the search. Without the first term, the particle velocity is only determined by the

best particle positions found so far (i.e., both personal and global best positions). The particle will try to move toward their *pbest* and *gbest*. As a result, PSO has a well-balanced mechanism to ensure both diversification and intensification in the search procedure.

C. Ant Colony Optimization

Ant Colony Optimization (ACO) is a metaheuristic algorithm which is particularly useful in dealing with highly complex discrete optimization problems [9]. It is inspired by the collective behaviors exhibited in the ant colony, which is capable of finding out the shortest path from its nest to the food source. Why are the ants so intelligent? This is because they use a chemical substance called pheromone which is deposited in the potential path. Each ant deposits a certain amount of pheromone in each path based on the path length, and the pheromone intensity indicates the relative length of each path. Based on this communication mechanism, most ants will follow the shortest path after some time. This phenomenon was observed and translated into mathematical model, which has turned out to be quite effective in handling certain applications such as telecommunication networks.

Here the Simple-ACO (S-ACO) algorithm is used to illustrate the inner working of ant colony algorithms. Although ACO has many variants, they do share some common procedures which will be listed in the following [9]. Here as an example, S-ACO is used to find out the minimum cost path on graphs. Each arc (i, j) in the graph $G = (N, A)$ is associated with a pheromone level τ_{ij}. The intensity of pheromone is sensed by the ants to determine their next movement. The highest pheromone intensity usually indicates a potentially shortest path.

- Path Searching: Initially, a constant amount of pheromone is assigned to each

arc. When an ant k locates in node i, the probability of choosing j as its next node can be calculated as follows:

$$p_{ij}^k = \begin{cases} \frac{\tau_{ij}^\alpha}{\sum_{l \in N_i^k} \tau_{il}^\alpha}, & j \in N_i^k; \\ 0, & \text{otherwise}; \end{cases} \quad (4.5)$$

where N_i^k is the neighborhood node of ant k when it is in node i.

- Pheromone Update: When the ant k is on its return travel to the source, it deposits a certain amount of pheromone $\Delta\tau^k$ in each path that it has traveled. For instance, when it traverses the arc (i, j), the pheromone intensity can be modified based on the following rule:

$$\tau_{ij} \leftarrow \tau_{ij} + \Delta\tau^k \quad (4.6)$$

where $\Delta\tau^k$ is usually a function of the path length. The shortest path is deposited with the most pheromone by this ant.

- Pheromone Evaporation: Pheromone evaporation can be regarded as a mechanism which encourages exploration of different paths. In doing so, the premature convergence of all the ants to the suboptimal solution may be avoided. The pheromone evaporation can be represented mathematically as follows:

$$\tau_{ij} \leftarrow (1 - \rho)\tau_{ij}, \forall(i, j) \in A, \quad (4.7)$$

where $\rho \in (0, 1]$ is a parameter.

After pheromone evaporation is applied to each arc, the pheromone intensity of each arc will be updated using $\Delta\tau^k$.

Although S-ACO is simple, it contains all the basic steps in an ACO cycle, including ants' movement, pheromone evaporation, and pheromone deposit. In this

dissertation, an improved ACO version termed Ant Colony System (ACS) is used. Its detailed description can be found in Chapter VI.

D.   Artificial Immune Systems

The biological immune system (BIS) is a complex adaptive pattern-recognition system which defends the mammalian body from foreign pathogens such as viruses and bacteria. From the computational viewpoint, it is a parallel and distributed adaptive system and it uses learning, memory, and associative retrieval mechanisms to handle challenging problems including pattern classification. Artificial immune system (AIS) is inspired from its natural counterpart BIS, and some computational models are built based on corresponding biological mechanisms [10]. Besides the machine learning and pattern recognition tasks, AIS can also be used for accomplishing complex optimization tasks. An optimization procedure called CLONALG is proposed to handle the optimization problems based on the clonal selection principle [11]. It is based on the idea that only the cells that recognize the antigens are selected to proliferate and the selected cells proceed with an affinity maturation process which increases their affinity to the selective antigens. Its major features include: 1) Selection and cloning of the most stimulated antibodies (Ab's); 2) Elimination of nonstimulated Ab's; 3) affinity maturation; 4) reselection of the clones proportionally to their antigenic affinity; 5) creation and maintenance of population diversity.

In AIS, an Ab repertoire (**Ab**) is exposed to an antigenic (Ag) stimulus (in our context **Ab** stands for the set of potential solutions and Ag refers to an objective function to be optimized) and those higher affinity Ab's will be chosen to create a population of clones. During proliferation, a few Ab's will experience somatic mutation proportional to their antigenic affinities. Low-affinity Ab's are placed through

simulating the process of receptor editing. The CLONALG carries out its search through somatic mutation and receptor editing, which is intended to balance the exploitation of the best solutions with the exploration of entire search space. It reproduces those individuals with higher affinity, performing blind variation and keeping improved maturated progenies. CLONALG conducts a kind of greedy search, where single members are optimized locally and newcomers perform a wider search in the whole solution space.

Assume the population size of Ab's is N and the length of each Ab is L. The nomenclature used in the computational iteration is listed in the following:

- $\mathbf{Ab}_{\{N\}}$: Available Ab repertoire $(\mathbf{Ab}_{\{N\}} \in S^{N \times L})$.

- $\mathbf{Ab}_{\{n\}}$: Ab's from $\mathbf{Ab}$ with the highest affinities to Ag $(\mathbf{Ab}_{\{n\}} \in S^{n \times L}, n \leq N)$.

- $\mathbf{Ab}_{\{d\}}$: Set of d new Ab's that will replace d lowest affinity Ab's from $\mathbf{Ab}_{\{N\}}$ $(\mathbf{Ab}_{\{d\}} \in S^{d \times L}, d \leq N)$.

- $\mathbf{f}$: Vector containing the affinity of all Ab's with respect to the antigen $(\mathbf{f} \in \Re^N)$.

- $\mathbf{C}$: Population of N_c clones generated from $\mathbf{Ab}_{\{n\}}$ $(\mathbf{C} \in S^{N_c \times L})$. After the maturation (i.e., hypermutation) process, the population $\mathbf{C}$ is termed as $\mathbf{C}^*$.

The basic computational iteration of CLONALG is laid out as follows [11]:

- The objective function and its associated constraints are treated as the antigen Ag, and its feasible solutions are deemed as N antibodies $\mathbf{Ab}_{\{N\}}$.

- Determine the vector $\mathbf{f}$ that contains the affinity of Ag to all the N Ab's in $\mathbf{Ab}$.

- Select the n highest affinity Ab's from $\mathbf{Ab}$ to constitute a new set $\mathbf{Ab}_{\{n\}}$ of high affinity Ab's with respect to Ag.

- The n selected Ab's are cloned independently and proportionally to their antigenic affinities, generating a repertoire $\mathbf{C}$ of clones: the higher the antigenic affinity, the higher the number of clones generated for each of the n selected Ab's.

- The repertoire $\mathbf{C}$ is continued with an affinity maturation process inversely proportional to the antigenic affinity, generating a population $\mathbf{C}^*$ of matured clones: the higher the affinity, the smaller the mutation rate.

- Determine the affinity $\mathbf{f}^*$ of the matured clones $\mathbf{C}^*$ with respect to antigen Ag.

- From this set of matured clone $\mathbf{C}^*$, reselect n Ab's to compose the set $(\mathbf{Ab})$.

- Replace the d lowest affinity Ab's from $\mathbf{Ab}_{\{N\}}$ with respect to Ag by new individuals in $\mathbf{Ab}_{\{d\}}$.

In running the algorithm, the stopping criterion is a predefined maximum number of iterations.

In the following chapters, five case studies will be discussed in detail, where aforediscussed computational intelligence based methods are proposed to resolve several important and challenging problems in planning and operations of electric power systems with renewable energy integration.

CHAPTER V

POPULATION-BASED INTELLIGENT SEARCH IN RELIABILITY
EVALUATION OF HYBRID GENERATION SYSTEMS WITH WIND POWER
PENETRATION

Adequacy assessment of power-generating systems provides a mechanism to ensure proper system operations in the face of various uncertainties including equipment failures. The integration of time-dependent sources such as wind turbine generators (WTGs) makes the reliability evaluation process more challenging. Due to the large number of system states involved in system operations, it is normally not feasible to enumerate all possible failure states to calculate the reliability indices. Monte Carlo simulation can be used for this purpose through iterative selection and evaluation of system states. However, due to its dependence on proportionate sampling, its efficiency in locating failure states may be low. The simulation may thus be time-consuming and take a long time to converge in some evaluation scenarios. In this chapter, as an alternative option, four representative Population-based Intelligent Search (PIS) procedures including genetic algorithm (GA), particle swarm optimization (PSO), artificial immune system (AIS), and ant colony system (ACS) are adopted to search the meaningful system states through their inherent convergence mechanisms. These most probable failure states contribute most significantly to the adequacy indices including loss of load expectation (LOLE), loss of load frequency (LOLF), and expected energy not supplied (EENS). The proposed solution methodology is also compared with the Monte Carlo simulation through conceptual analyses and numerical simulations. In this way, some qualitative and quantitative comparisons are conducted. A modified IEEE Reliability Test System (IEEE-RTS) is used in this investigation.

A. Introduction

Probabilistic methods are now being used more widely in power system planning and operations to deal with a variety of uncertainties involved. For instance, adequacy assessment is an important component to ensure the proper operations of power systems. Various adequacy indices are defined to evaluate the existence of sufficient facilities within the system to satisfy load demand as well as system operational constraints. Power generation adequacy relates to the facilities necessary to generate sufficient energy in the presence of different system uncertainties. More recently, wind power has attracted much attention as it does not consume depleting fossil fuels and is also environmentally friendly. However, due to the intermittency of wind power availability, the reliability issue should be readdressed when integrating wind power into the traditional power grid. The fluctuation of wind power during different time periods should be considered since it may compromise the power system reliability.

For most combinatorial optimization problems, as their dimension increases, the computational time needed by exact methods grows exponentially. Metaheuristics are approximate methods for resolving these challenging problems, and they can be applied to derive an adequate solution in a reasonable amount of time. In today's power-generating systems, the number of generating units has become very large. Inevitably, adequacy assessment of power systems becomes more challenging due to their larger scale and increasing complexity. Thus, in adequacy assessment, exhaustive enumeration is usually impractical due to an innumerable number of system states incurred. To solve the problem, recently Monte Carlo simulation (MCS) is more widely used as a useful computational method [12]. It has shown significant promise in accomplishing reliability evaluation of complex power systems.

In this study, as a potential alternative, Population-based Intelligent Search (PIS)

is used to find out a set of probable failure states, which contribute most significantly to the system adequacy indices. PIS is based on the guided stochastic search inspired by biological or social systems. Here, based on its optimization mechanism, PIS is used to scan and find out a set of most probable failure states which contribute significantly to system reliability indices. Rather than attempting to find a single optimal or near-optimal solution, PIS here is used as a scan and classification tool due to its intrinsic ability of population-based guided random search. Based on the system states derived by PIS, the adequacy indices including loss of load expectation (LOLE), loss of load frequency (LOLF), and expected energy not supplied (EENS) are subsequently calculated. An IEEE Reliability Test System (IEEE-RTS) is modified by incorporating multiple wind turbine generators (WTGs) in order to demonstrate the applicability and effectiveness of the proposed evaluation procedure.

The major improvements made in this study with respect to the previous work [13] can be summarized as follows:

- Instead of using only the genetic algorithm, the method has been generalized to all the population based stochastic search algorithms. All these algorithms have been unified under a single framework termed Population-based Intelligent Search (PIS) and all the discussions are based on the generic PIS method.

- The wind turbine generators have been incorporated into the generation system and in this proposed method, the reliability-evaluation procedure is revised to accommodate this change. The variability of wind power is accounted for in the reliability evaluation.

- Comparisons between Monte Carlo simulation and Population-based Intelligent Search are carried out both conceptually and numerically. For the first time in reliability evaluation, these two methods are compared in a systematic fashion.

The results achieved by different PIS algorithms are also compared.

The remainder of the chapter is organized as follows. Section B presents some fundamentals of adequacy evaluation for hybrid power-generating systems. Representative PIS algorithms and Monte Carlo simulation are discussed and compared in Section C. In Section D, the proposed PIS-based evaluation procedure is discussed in detail. Simulation results and analysis are presented and discussed in Section E. Finally, the chapter wraps up with some conclusions and future research suggestions.

B. Reliability Evaluation of Hybrid Generating Systems

The reliability analysis of hybrid generating systems including time-dependent sources has been investigated through different methods [14]–[19]. These proposed reliability evaluation techniques are usually intended to calculate the reliability indices including EENS, LOLE, and LOLF, which are three fundamental indices for adequacy assessment of power-generating systems.

The load is represented as a chronological sequence of N_T discrete values L_t for successive time steps $t = 1, 2, \ldots, N_T$. Each time step has equal duration $\Delta T = \frac{T}{N_T}$ where T is the entire period of observation. The general expressions for calculating the three indices are as follows:

$$EENS = \Delta T \sum_{t=1}^{N_T} U_t \tag{5.1}$$

where U_t is the unserved load during the time step t and it can be calculated by

$$U_t = \sum_{X_t > X_{cco_t}} (X_t - X_{cco_t}) P(X_t) \tag{5.2}$$

where X_t is the total capacity outage at time instant t, $P(X_t)$ is the probability that a system capacity outage occurs exactly equal to X_t, X_{cco_t} is the critical capacity

outage at time instant t:

$$X_{cco_t} = C_{g_t} + C_{w_t} - L_t \tag{5.3}$$

In the above definition, the term $C_{g_t} + C_{w_t}$ indicates the effective total system capacity (that is, the summation of conventional sources of power C_g and wind power C_w) at time instant t provided that all the units are available, L_t is the load demand in period t. When $X_t > X_{cco_t}$, capacity deficiency occurs. Expected number of hours of load loss is given by

$$LOLE = \frac{\Delta T}{T} \sum_{t=1}^{N_T} P_{f_t} \tag{5.4}$$

where P_{f_t} is the loss of load probability during hour t. Loss of load frequency is given by,

$$LOLF = \frac{\Delta T}{T} \sum_{t=1}^{N_T} (F_t^d + F_t^c + F_t^u) \tag{5.5}$$

where F_t^d is the frequency component caused by the load variation and fluctuation in the intermittent sources; and F_t^c and F_t^u are components of frequency due to interstate transitions in conventional and unconventional sources of power.

C.   Monte Carlo Simulation and Population-based Intelligent Search

The basic intent of power system reliability analysis is to determine some probabilistic measure of the undesirable events. Methods of power system reliability analysis have been considered to fall into two broad categories: analytical and simulation methods [20]. Basically, there are three stages inherent in any reliability method: state selection, state evaluation and index calculation. The analytical techniques and simulation techniques differ mostly in the process of state selection as the number of possible states is extremely large for most practical applications. The analytical techniques use some device to circumvent the problem of straightforward enumeration such as
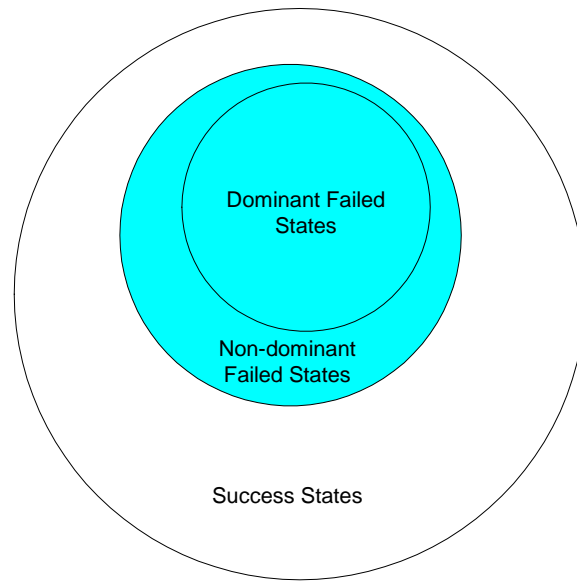
Fig. 1. Classification of system states in the whole state space

state merging, truncation, implicit enumeration and sequential model building. The simulation methods select system states based on their respective sampling mechanisms. For instance, Monte Carlo sampling techniques accomplish this by sampling states proportional to the probability of their occurrence. PIS-based algorithms are characterized as artificial intelligence techniques, and they choose system states based on their fitness values in relation to the target problem.

1. State space

Both Monte Carlo sampling and population-based intelligent search are examined in this chapter for their efficiencies in evaluating system reliability. The whole state space can be graphically illustrated in Figure 1 by classifying all system states into different sets.

Each system state is randomly scattered in the state space. The total state space can be broadly divided into two sets: success and failed system states. In MCS, these

two sets of system states are sampled proportional to their respective probabilities, and it is this stochasticity that makes the MCS work. Based on all the samples, the desired reliability indices are estimated. Even though a state is a repeated sample, it still counts for index calculation. On the contrary, in PIS, the success states are meaningless to reliability indices as they do not contribute to these indices. The painted region shown in Figure 1 includes all the failed system states, which can be further classified into dominant and non-dominant failed states. As the probability of non-dominant failed states is relatively low, their impact on reliability indices is very minor and thus in PIS they are ignored in the calculations. Only the dominant failed states are meaningful to index calculation in PIS. The major task of MCS and PIS is to calculate the reliability indices by sampling the search space based on their respective sampling mechanisms.

2.   Monte Carlo Simulation

Monte Carlo simulation methods, which treat the problem as a series of experiments, estimate reliability indices by simulating the actual process using probability distributions of state residence times. Non-sequential MCS and sequential MCS are two typical approaches. In non-sequential MCS, the state space is randomly sampled regardless of the system operation process chronology. In sequential MCS, the chronological representation is used, where the system states are sequentially sampled for certain periods. The duration of the states and the transitions between consecutive system states are represented in these synthetic sequences. The sequential MCS usually requires higher computational effort than non-sequential MCS. Some research has also been done combining analytical methods and simulation methods for power system reliability studies [21]–[23]. In this chapter non-sequential simulation or random sampling is used for comparison with the PIS based methods.

a. Computational procedure

Several reliability indices have been proposed in the literature. Perhaps loss of load probability (LOLP) is the most widely known power system reliability index. This section gives various steps of Monte Carlo simulation for the LOLP index but the same process can be used for other indices. Typical steps for LOLP calculation using simple Monte Carlo simulation can be described as follows.

- Step 1: Select the seed for the random number generator. Set the maximum iteration number and let the initial iteration number $K = 1$.

- Step 2: Sample the system state and classify it as loss-of-load or otherwise.

$$X_i = \begin{cases} 1, & \text{loss-of-load state;} \\ 0, & \text{otherwise.} \end{cases} \tag{5.6}$$

Note that the subsequent stopping criteria are not checked until sufficient system states are sampled and evaluated in order to ensure an unbiased calculation of these statistical criteria used for halting the program.

- Step 3: Calculate LOLP, variance of the estimated LOLP and the coefficient of variation.

$$\widehat{LOLP} = \frac{1}{K} \sum_{i=1}^{K} X_i \tag{5.7}$$

$$V(\widehat{LOLP}) = \frac{1}{K}(\widehat{LOLP} - \widehat{LOLP}^2) \tag{5.8}$$

$$\sigma = \frac{\sqrt{V(\widehat{LOLP})}}{\widehat{LOLP}} \tag{5.9}$$

where K is the total number of samples.

- Step 4: Check whether the coefficient of variation σ is less than a specified threshold δ . If $\sigma < \delta$ or $K > K_{max}$, stop; otherwise, $K = K + 1$, go to step 2.

b. Stopping criteria

MCS is a fluctuating convergence process [12]. The estimated indices gradually converge to their "real" values as the simulation goes on. MCS should be terminated when the estimates of reliability indices reach a stipulated degree of confidence. A stopping criterion is used to provide a compromise between the solution accuracy and computational effort. As indicated in the above steps, the coefficient of variation represented in (5.9) is quite often adopted as the convergence criterion, which is a measure of the uncertainty around the estimates. A number of experiments have demonstrated that the coefficient of variation for EENS takes the longest time to stabilize. Thus, when calculating multiple indices, the EENS coefficient of variation can be used as the stopping rule. Besides the coefficient of variation, the number of samples can also be used as the stopping criterion. The simulation pauses at a specified number of samples and the coefficient of variation is checked to see if it is acceptable. If yes, halt the MCS; or else, increase the number of samples [12].

c. Some remarks

From the steps of the straight Monte Carlo simulation, we can make two observations: 1. For each sampled state, determination needs to be made whether it is a loss of load state or not. This typically needs a flow calculation to be made. Depending on the method of flow calculation, this step could impose a significant computational burden. 2. Due to the random sampling nature, many similar states are sampled in simulation and their characteristics determined repeatedly. Therefore, the straight Monte Carlo simulation could be very computationally inefficient.

The main advantages of Monte Carlo simulation include: 1. the ability to model complex systems in more detail and accuracy than is possible in analytical methods;

2. the required number of samples for a given accuracy depends on the variance which tends to decrease with the system size; 3. the method can not only calculate the expected value of reliability indices but also their distributions. The primary disadvantage of Monte Carlo simulation is the lengthy computational time to achieve satisfactory statistical convergence of reliability index values. The time for convergence is inversely proportional to the loss of load probability.

3. Population-based Intelligent Search

More recently, some methods for intelligent search of state space using PIS algorithms such as genetic algorithms have been shown to have promise in reliability evaluation of power systems [13], [24]. Population-based search renders it possible to evaluate system states in parallel and in this way, a population of individuals is evaluated in each iteration. Since our problem is not trying to find out a single optimal solution, this characteristic is of particular benefit in enabling the optimizer to serve as a scan and classification tool. Distinguished from the random sampling in MCS, in PIS sampling can be interpreted as the "optimization process". The process of applying PIS optimization operators in deriving the next generation of individuals is the sampling mechanism of PIS algorithms. Here the individuals with higher fitness values have higher chances to be sampled in each iteration. In the problem under consideration, higher fitness means higher probability of failure.

a. Computational procedure

The general computational flow of any PIS algorithms can be described in the following:

- Step 1: A population of individuals is randomly created.

- Step 2: Each individual is evaluated based on the specified objective function, which is used to measure the "fitness" of each individual. Here the term "fitness" is slightly abused to generally indicate the "goodness" of each individual with respect to the specific problem, though it is usually used in genetic algorithms.

- Step 3: Determine if any stopping criterion is satisfied. If yes, halt the PIS algorithm; otherwise, go to next step.

- Step 4: Different PIS operations are applied to each individual in order to create the next generation of individuals.

- Return to Step 2 until a stopping criterion is satisfied.

b. Stopping criteria

In our problem, PIS is adopted as a scan tool, where a number of meaningful states are targeted instead of only the optimal or near-optimal one. Different from commonly seen optimization problems, here the stopping rule should be set to ensure that sufficient system states have been identified by the final iteration. Thus, the selection of stopping criterion may become somewhat trickier. Three stopping criteria may be used depending on the specific problem. The first one is to halt the algorithm when the maximum number of iterations is reached. This value is pre-specified and thus it requires careful tuning. The second stopping rule is the desired number of failure states. The proper setting of this number requires a very clear insight on the complex target problem beforehand, which is usually highly difficult or unrealistic to achieve. The third stopping criterion is to examine the difference between two consecutive objective values. If the differences keep being below a certain small value for a specified number of iterations, the algorithm is terminated.

c.   Some remarks

1. Due to their stochastic search based optimization mechanisms, PIS-based algorithms may become more efficient in handling highly complex and highly nonlinear large-scale practical systems with respect to other existing methods. 2. The stopping criteria are somewhat less mathematically strictly defined as compared with MCS, and in some sense they are more subjective and thus may demand considerable tuning effort for each specific task.

d.   Representative PIS algorithms

Four representative PIS algorithms adopted in this study are briefly introduced here, which include genetic algorithm (GA), particle swarm optimization (PSO), ant colony system (ACS), and artificial immune system (AIS). GA is inspired by the biological evolution with the philosophy of "survival of the fittest" [7]. An individual with the highest fitness value has the highest chance to be selected to reproduce its next generation. PSO is invented based on the social behavior of fish schooling and bird flocking with the philosophy of "following the leader" [8]. The swarm moves as a group in the search space guided by the best local and global individuals found so far. ACS is inspired from the collective behavior exhibited in an ant colony on how to find the shortest route from nest to the food [9]. The trail deposited with the highest level of pheromone has the highest fitness value. AIS model is built based on biological immune system by mimicking how the antibodies react to the antigen [11]. The most stimulated antibody has the highest probability to proliferate. All of these four algorithms are population-based search while featuring different optimization mechanisms. Due to space restrictions, the detailed discussion of each algorithm is referred to the respective aforementioned literature.

4. Conceptual comparison between MCS and PIS

As indicated previously, the most significant difference between MCS and PIS lies in their sampling mechanisms. In MCS, system states are sampled based on their occurrence probability, and both success and failure states sampled contribute to the estimation of reliability indices. In our scenarios, this means the failure states have much less probability to be sampled with respect to the success states, since the failure states have less occurrence probability in power systems. Also, as the system becomes more reliable, the probability to sample the failure states become less. This explains why the convergence will be a concern in the reliability assessment of highly reliable systems. Unlike MCS, PIS is rather problem-dependent, where system states with higher failure probabilities have higher chances to be selected and evaluated. Here in PIS the failure probability of system state is used to guide the search. In some sense, this characteristic enables PIS to have promise to outperform MCS for some type of problems due to its potentially higher algorithmic efficiency. The driving force behind each PIS renders the search more purposeful by avoiding problem-independent random sampling. Also, unlike MCS, in PIS only the failure states are useful in estimating reliability indices. Due to the difference of estimation philosophies between MCS and PIS, the deviations of estimation results in relation to the "real" values may be different between them. For instance, in MCS, the estimated values of indices may be larger or smaller than the actual values; however, in PIS, the estimated values are always somewhat smaller than the actual ones. Especially, in highly reliable systems, since failure states are scattered in the state space in an extremely sparse fashion, it is possible that the MCS method can not sample the failure states in their "real" ratio with respect to the total number of system states. This will inevitably lead to larger estimation errors of the intended reliability indices

or even cause convergence problem.

It should be noted that PIS-based algorithms can have a special advantage in cases where flow calculations using DC/AC load flow are needed to evaluate a sampled state. When a state is sampled, it can be identified to be loss of load only after the evaluation process. Since in MCS, majority of the states sampled are success states, this flow calculation will need be carried out more often. On the other hand, in PIS the states are sampled in a more directed fashion and thus the evaluation process will be used more efficiently.

The rigorous analysis of PIS algorithms is difficult [25]. In recent years, some investigations are being conducted attempting to combine these two methods [26] or interpret PIS under the well-established MCS framework [27]. Meanwhile, a considerable number of convergence proofs have also been carried out for some PIS-based algorithms [28].

D. PIS-based Adequacy Evaluation

In PIS algorithms, each individual is regarded as a potential solution and many individuals comprise a population. For a specific PIS algorithm, individual has different names. For instance, in GA, each chromosome is an individual, which is made up of a bunch of genes. In ACS, the tour traveled by each ant (referred to as "ant" for brevity) is deemed a potential solution. In PSO, each particle flying in the search space is thought of as a candidate solution. In AIS, each antibody is seen as a potential solution. In this investigation, binary coding scheme is used to represent each individual, where each bit takes one or zero to indicate the generator state. "One" and "zero" represent the working and failed status of each generator, respectively. Since there may be several groups of identical generators used in terms of generator

types (conventional or wind turbine generators), generator capacities, and reliability parameters, all of these generators are grouped accordingly to reduce computational cost. Assume the generators are divided into n groups, where each group is composed of states of single or multiple generators and they are represented by binary numbers. In this way, multiple binary bits representing an individual are used to indicate various generation combinations. The target problem is concerned with combinatorial optimization, and its objective is to find out the failure state array which can be used to calculate different adequacy indices. The configuration of each individual (i.e., system state) can be illustrated as in Figure 2. All the generators involved are divided into n groups and each bit indicates the corresponding generator condition (i.e., working or failure status).

G_1	G_2	....	G_{n-1}	G_n
$C_1........C_{G1}$	$C_{G1+1}........C_{G2}$	....	........C_{m_g}	$U_1........U_{m_w}$

Fig. 2. Individual (i.e., system-state) representation

There are two major stages in the proposed evaluation procedure: First the failure-state array with respect to the maximum load demand is derived using PIS, and then the reliability indices are calculated by convoluting the effective total capacity with the hourly load based on the state array achieved previously. The evaluation procedure is extended from that used in [13] by incorporating the variability of wind power. The computational flow of the proposed evaluation procedure is laid out in the following.

- Step 1: Generate a population of individuals randomly. The states of both conventional generators and wind turbine generators (WTGs) are initialized by

binary numbers.

- Step 2: Evaluate each individual i based on the defined objective function (probability of not satisfying load with respect to the maximum load demand L_{max}). If its value is less than the specified threshold (a small value below which the corresponding states are filtered out), it is assigned a very small fitness value in order to reduce its chance of participating in subsequent PIS operations. Based on the attained state array, the overall system probability of load loss against the maximum load demand is calculated.

The objective value of state i is calculated as follows:

- Calculate the effective generating capacity of state i including WTGs:

$$Cap_{i,max} = \sum_{j=1}^{m_g} c_j g_j + \sum_{j=1}^{m_w} u_j w_r \qquad (5.10)$$

where m_g is the number of conventional generators; c_j indicates the state of conventional generator j; g_j is the capacity of generator j; m_w is the number of WTGs; u_j indicates the state of WTG j, and in each hour period, it has only one state: 1 (working) or 0 (failed) for a specific WTG; w_r is the rated power capacity of WTG. Here if the capacity $Cap_{i,max}$ is larger than the maximum load demand L_{max}, the fitness of its corresponding individual is assigned a very small value so as to reduce its chance to contribute to the next generation, since it represents a success state. The rated WTG capacity is used here in order to ensure that all possible failure states are included for further evaluations.

- The failure probability of state i can be calculated as follows:

$$P_i = \prod_{j=1}^{m} p_j \qquad (5.11)$$

where $m = m_g + m_w$ is the total number of conventional and unconventional generators, p_j can take one of the following two values: for the conventional units, if $c_j = 1$, then $p_j = 1 - FOR_j$; and if $c_j = 0$, then $p_j = FOR_j$. In a similar manner, for WTGs, if $u_j = 1$, then $p_j = 1 - FOR_j$; and if $u_j = 0$, then $p_j = FOR_j$. FOR_j represents the forced outage rate (FOR) of generator j. The probability of each generator down equals its FOR. Also note that only full outages are considered in this investigation.

– Calculate the number of all possible permutations (i.e., equivalents) of the evaluated state i:

$$Copy_i = \begin{pmatrix} G_1 \\ O_1 \end{pmatrix} \cdots \begin{pmatrix} G_j \\ O_j \end{pmatrix} \cdots \begin{pmatrix} G_n \\ O_n \end{pmatrix} \qquad (5.12)$$

where O_j is the number of "ones" in group j of length G_j.

– The fitness of this state is

$$Fit_i = Copy_i * P_i \qquad (5.13)$$

It is the objective function to be maximized by the PIS-based optimizer. Its value (i.e., fitness) is determined by the state of each generator.

– Frequency of this state can be calculated as follows [29], [30]:

$$F_i = P_i * \left(\sum_{j=1}^{m} (1 - b_j)\mu_j - \sum_{j=1}^{m} b_j \lambda_j \right) \qquad (5.14)$$

where b_i indicates the generator state; μ_j and λ_j are repair rate and failure rate of generator j, respectively.

– Save information on eligible states including P_i, F_i, and $Copy_i$, which will be used in subsequent calculations.

   – Repeat the above procedure for the remaining individuals until all of them are evaluated. Before each evaluation, the individual under consideration will be checked to ensure it is not the equivalent of any previously evaluated ones. If it is a previously evaluated state, its fitness will be assigned a very small number in order to eliminate it very soon in the following optimization operations.

- Step 3: Increase the iteration number by one;

- Step 4: Check if any stopping criterion is met. If yes, halt the algorithm and output the state array derived. If no, go to the next step.

- Step 5: Different PIS operators are applied for producing the next generation, and then repeat the procedure from Step 2 to Step 4 until any stopping criterion is satisfied.

- Step 6: Calculate the adequacy indices based on the achieved state array. Due to the time-dependent nature of wind power, the total effective generating capacity of state i at hour t should be calculated as follows:

$$Cap_{i,t} = \sum_{j=1}^{m_g} c_j g_j + \sum_{j=1}^{m_w} u_j w_j \tag{5.15}$$

where w_j is the actual output of WTG j at hour t. It can be calculated by $w_j = \alpha_t * w_r$, where α_t is the ratio of WTG output at hour t with respect to the rated WTG power capacity, and this derating factor is used to calculate the effective WTG output during hour t. The derating factor is provided or derived using the wind speed forecasting procedure. It is usually modeled as a random variable by time series techniques such as the Autoregressive Moving Average (ARMA) model. In the ARMA model, the power output of WTG in each time

step can be represented as a random variable by accounting for its association with those in previous time steps. The derating factor varies over time, but for a given time interval, it is realized as a constant value (even though it is modeled as a stochastic variable) for reliability calculation. Thus, it can be deemed as a variable "constant", since it varies along the observation horizon and meanwhile, it is a fixed value for a given time step. No matter what kind of method is used to evaluate system reliability, the derating factor of fixed value in each time period (e.g., hour or smaller time step) is always needed, even if the derating factor is modeled as a stochastic variable. The time step used for reliability calculation is determined by the accuracy requirement. If $Cap_{i,t}$ is larger than or equal to the load demand L_t at hour t, it is in fact a success state and will not be accounted for in calculating reliability indices; Or else, it will be included in subsequent calculations.

$$P_{f_t} = \sum_{j=1}^{sn} S_j * P_j * Copy_j \tag{5.16}$$

where sn is the number of failure states attained previously. S_j is a flag indicating if the loss of load occurs at hour t for state j: it is zero when $Cap_{i,t} \geq L_t$; otherwise it is set as one. The value of sn may be smaller than the total number of states obtained at the first stage, since some of the states may become success ones at different time periods due to the variations of both loads and derating factors. Since duration of each time step is one hour, LOLE in hours within the observation horizon T can be calculated as follows:

$$LOLE = \sum_{t=1}^{N_T} P_{f_t} \tag{5.17}$$

The expected energy not supplied (EENS) in megawatts hour can be calculated

as follows:

$$EENS = \sum_{t=1}^{N_T} PNS_t \tag{5.18}$$

where PNS_t is the power not supplied for hour t:

$$PNS_t = \sum_{j=1}^{sn} S_j * P_j * Copy_j * (L_t - Cap_{j,t}). \tag{5.19}$$

LOLF includes two components: frequency of generating capacity "FG" and frequency due to load change "FL".

$$FG = \sum_{t=1}^{N_T} LOLF_t \tag{5.20}$$

where $LOLF_t$ is the loss of load frequency at hour t:

$$LOLF_t = \sum_{j=1}^{sn} S_j * F_j * Copy_j; \tag{5.21}$$

$$FL = \sum_{t=2}^{N_T} V_t * [P_{f_t} - P_{f_{t-1}}] \tag{5.22}$$

where V_t is zero if the value between brackets is negative, and otherwise it equals to one.

The LOLF in occurrences during the observation time span T is calculated as

$$LOLF = FG + FL. \tag{5.23}$$

Furthermore, based on the state array achieved, the contribution of each system state to the total system adequacy becomes clear and capacity outage table can be also built from it. Another major advantage of this approach is that as long as the actual peak load is not larger than the one used for deriving the state array, the state array achieved can always be used for calculating the actual adequacy indices for various scenarios with different peak loads.

The proposed procedure can also be used in reliability evaluation of composite systems, where the transmission failures can be seen as additional component states besides the generator failures. That is, in PIS, these component states can also be encoded into an individual in the same way as the generator failures. The objective function (5.13) indicating the system failure probability can be revised accordingly by including the transmission failures. In this scenario, power flow analysis is needed for state evaluation. Similar to the evaluation procedure for generation systems, here the proposed method can also be divided into two major stages. First, PIS searches intelligently for failure states through its fitness function, using the linear programming optimization model to determine if a load curtailment is needed for each sampled state. Sampled state data are then saved in state array. The sampling process and evaluation procedure can be linked by the power flow analysis solved by linear programming. Each time when a system state is sampled, the power flow analysis routine will be called to determine if a loss of load is caused. After the search process stops, the second step begins by using all of the saved states data to calculate the annualized indices for the whole system and at each load bus. Each power transmission line is assumed to have two states, up and down. Its failure probability can be calculated from its failure rate and repair rate.

E.   Simulations and Evaluation

A WTGs-augmented IEEE Reliability Test System (IEEE RTS-79) is used in simulations [31]. The original RTS has 24 buses (10 generation buses and 17 load buses), 38 lines and 32 conventional generating-units. The system annual peak load is 2850 MW. The total installed generating capacity is 3405 MW. In this study, one unconventional subsystem comprising of multiple identical WTGs is added to the RTS.

Each WTG has an installed capacity of 1 MW, a mean up time of 190 hours and a mean down time of 10 hours. The hourly derating factors for WTG output can be found in [15]. These hourly derating factors used in the simulation studies for reflecting hour-to-hour variations have included the stochastic nature of wind power and are stochastic variables. Reliability indices are calculated for a time span of one week and the load cycle for week 51 with peak load 2850 MW, low load 1368 MW and weekly energy demand 359.3 GWh. Different wind power penetration levels are examined by incorporating three installed wind power capacities of 100 MW, 200 MW, and 400 MW.

For peak load of 2850 MW with wind power penetration, the system adequacy indices obtained using the analytical method [15], MCS, and proposed PIS methods are listed from Table I to Table III. Distinguished from the negative margin method and clustering method, in the analytical method the mean capacity outage table is constructed to simultaneously compute EENS, LOLE, and LOLF with reduced computational cost. The overall system is divided into two subsystems including the conventional subsystem and the unconventional subsystem (i.e, WTGs). The computation procedure for these three indices is as follows:

- Build the capacity outage table, the cumulative outage probability and frequency tables for the conventional subsystem, using the unit addition algorithm.

- Build the capacity outage table, the cumulative outage probability and frequency tables for the unconventional subsystem considering the availability of intermittent sources, in a similar fashion.

- Build the capacity outage table for the overall system through combining capacity outage tables constructed in the above two steps.

- Build the mean capacity outage table for the conventional subsystem based on the recurrence approach.

- Calculate the hourly contributions to the indices.

- Calculate EENS, LOLE, and LOLF by summation over the whole period of observation.

The units of LOLE, EENS, and LOLF are h/week, MWh, and occ./week, respectively. The time is in seconds. Here all the four discrete PIS optimizers mentioned earlier are used to derive the meaningful system states. The population sizes for all PIS algorithms are set at 300. We can see that the performance of MCS is somehow the worst among all methods in all scenarios of our problem in terms of solution quality and computational cost. The solutions derived by all PIS algorithms are comparable to the ones derived by the analytical method. Among them, the solutions from ACS are slightly more accurate than those of others. GA is the most computationally expensive one primarily due to its time-consuming genetic operations. Binary PSO (BPSO) [32] has the shortest convergence time due to its simple operations. For comparison with another analytical approximation method, a clustering method is used to calculate the EENS [15]. It uses fixed margin increment of 10 MW and clustering with the nearest centroid sorting algorithm. The number of clusters is set as 80. The EENS's derived are 207.6943 MWh, 159.1898 MWh, and 98.8874 MWh for integrated wind power capacities of 100 MW, 200 MW, and 400 MW, respectively. We can see that the results obtained from all population-based intelligent search methods used slightly outperform the clustering method in terms of EENS accuracy in such settings. Furthermore, as the system complexity increases (in this context it means more WTGs are integrated), the computational efficiency advantage of the population-based stochastic search becomes more evident in relation

to the analytical method. We can also see that as the power system becomes more reliable, the effectiveness and efficiency of MCS method are decreased in terms of both solution quality and computational expense. That is, with more WTGs incorporated, the solutions become more inaccurate and higher computational costs are caused in relation to the four PIS-based algorithms. This observation matches the conceptual analyses presented earlier.

Table I. Reliability indices for unconventional capacity 100 MW

Method	LOLE	EENS	LOLF	Time
ACS	1.487890	207.761	0.310570	6.7
AIS	1.487879	207.740	0.310563	6.8
BPSO	1.487856	207.723	0.310559	5.7
GA	1.487820	207.702	0.310543	11.7
MCS	1.493332	208.989	0.311240	19.8
Analytical method	1.487951	207.902	0.310602	8.4

Table II. Reliability indices for unconventional capacity 200 MW

Method	LOLE	EENS	LOLF	Time
ACS	1.185620	159.243	0.258272	11.9
AIS	1.185601	159.223	0.258264	12.4
BPSO	1.185583	159.216	0.258256	9.8
GA	1.185560	159.203	0.258251	18.3
MCS	1.174901	157.001	0.256401	34.6
Analytical method	1.185692	159.402	0.258305	16.5

Since more system states are derived as the optimization process proceeds, the solutions will become more accurate with more iterations. Thus, there should be a

Table III. Reliability indices for unconventional capacity 400 MW.

Method	LOLE	EENS	LOLF	Time
ACS	0.789780	98.921	0.193233	21.6
AIS	0.789768	98.912	0.193229	22.7
BPSO	0.789760	98.909	0.193221	15.4
GA	0.789740	98.900	0.193213	29.3
MCS	0.771991	96.211	0.190632	59.4
Analytical method	0.789840	99.085	0.193275	29.9

tradeoff between the computational cost and solution accuracy. Here the stopping criterion set after careful tuning is the number of maximum iterations, which is 100 in this problem. It turns out to be a reasonable number since comparable results are attained by this generation. Furthermore, as an example, Table IV shows the growth of reliability indices with the increasing number of iterations by using ACS as the PIS algorithm in the third evaluation scenario.

Table IV. Growth of reliability indices with the increasing generations

Generations	LOLE	EENS	LOLF
25	0.248773	32.459	0.063098
50	0.503987	70.546	0.138953
75	0.655530	85.999	0.169908
100	0.789780	98.921	0.193233

The size of the entire search space is $2^{(32+N_{WTG})}$, where N_{WTG} is the number of WTGs taking 100, 200, and 400 in our problems. We can appreciate that all three cases involve a large number of system states. Despite the difference of sampling mechanisms between MCS and PIS, it is still viable to compare these two methods in

terms of number of total samples for deriving the comparable results. In MCS, every sample counts in index calculation, while in PIS only the sampled failure states are seen valid. The total samples of MCS in three different evaluation scenarios are around 46,000, 59,000, and 89,000 for deriving the results as shown in the above tables. In PIS, all calculations are based on the identical total sampling number of 30,000, since the size of search space is 300×100. Thus, in terms of sampling efficiency, PIS-based algorithms have exhibited a certain degree of superiority in this problem with respect to the MCS method, as they are capable of deriving more accurate results with less number of samples in a shorter time.

Here the commonly used convergence trajectory of PIS is not as illustrative as that used in optimization problems anymore. For a more informative indication, we define a ratio to measure the convergence performance (i.e. sampling efficiency) of different PIS algorithms for the scan and classification task.

$$\lambda = \frac{\text{Number of meaningful states sampled}}{\text{Number of total samples}} \tag{5.24}$$

This ratio can be used in each generation or across the whole optimization process. It varies depending on the algorithm efficiency and solution density in the search space. Table V illustrates the ratios of different PIS-based algorithms in the whole optimization process for the first scenario, where 100 WTGs are incorporated. ACS found out a bit larger number of meaningful states than others, which lead to slightly more accurate results. It should be noted that although this ratio is defined for measuring the convergence performance of PIS, it also has significance in the context of MCS which is virtually the estimate of LOLP as defined in (5.7), if the "meaningful states" are also interpreted as the "dominant failed states". In this evaluation scenario, the ratio equals to 0.889%. As compared with PIS, in MCS a smaller proportion of sampled system states turn out to be dominant failed states. Also, as more WTGs are incor-

porated, this ratio will become even smaller because of higher reliability. Further, in the proposed PIS method, all equivalents of the sampled state are sought out to avoid repeated sampling and evaluation; however in MCS, due to repeated sampling, equivalent samples may be evaluated repeatedly. Therefore, as mentioned earlier, in certain scenarios where flow calculation is required to evaluate each system state, PIS is promising to outperform MCS further through its directed search.

Table V. Comparison of sampling efficiency of different PIS algorithms in the entire optimization process.

Method	Sampled Meaningful States	Ratio λ
ACS	2,041	6.80%
AIS	2,021	6.74%
BPSO	2,016	6.72%
GA	2,002	6.67%

Moreover, the evolution of this ratio in terms of computational iterations is illustrated in Figure 3. Though for each PIS algorithm the trajectories differ with one another quantitatively, they do exhibit a similar pattern. We can see that as the optimization proceeds, first this ratio increases gradually because of the fitness-guided sampling mechanisms of these four PIS-based algorithms. This means that the proportion of meaningful individuals in the entire population becomes larger as the optimization proceeds. In particular, the ratio will reach its maximum value in a certain generation. For instance, in ACS this ratio reaches its maximum in the 70-th generation, which indicates that in this generation, about 14.4% individuals in the population of size 300 are useful for index calculation. Then, the ratio after the 70-th generation keeps declining since there are limited dominant states remaining after previous generations of search, and the search space becomes much

sparser. This differs from the traditional convergence trajectory used in optimization problems, which usually continuously approaches the optimal or sub-optimal value without such a turning point changing from rising to falling ratios. This is because in traditional optimization problems, the most recent optimal solution found will not be worse than its previous one, so its trajectory always keeps moving toward the same direction (i.e., rising or falling).
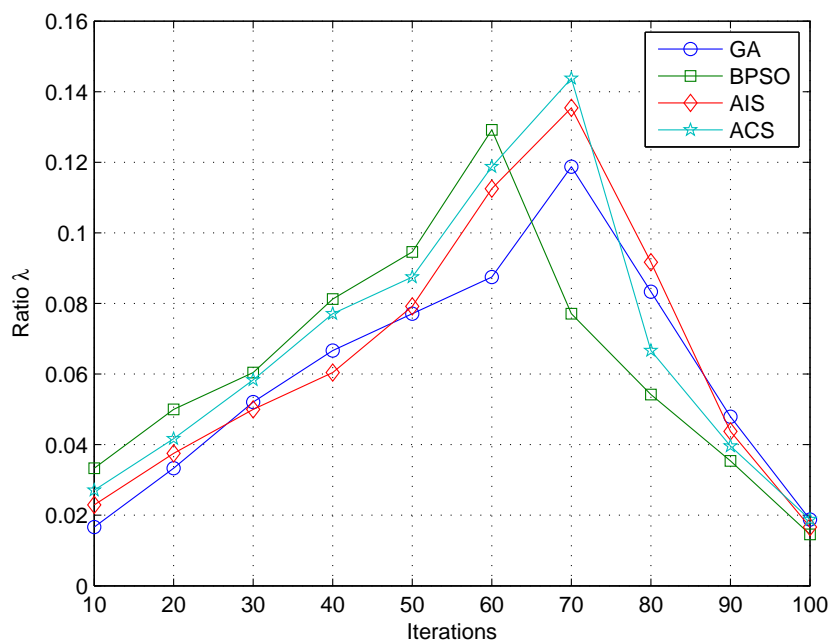
Fig. 3. Ratio of meaningful states and total sampled states

In some scenarios of reliability evaluation, PIS-based algorithms have promise to exhibit more effective and efficient performance with respect to the exact method and MCS method. The primary advantages of the proposed PIS method can be summarized in the following.

- The contribution of each system state to the overall adequacy indices can be easily calculated and identified. This feature is important when a sensitivity

study is desired to determine system states which have the most significant impact on the overall system reliability.

- The state array derived by the evaluation procedure may be reused for different load levels. As long as the actual peak load is smaller than the peak load used to derive the state array, the state array can be used to calculate reliability indices for different load demands. Moreover, the second-stage evaluation procedure can be generically used to calculate reliability indices for any set of failure states provided.

- In Monte Carlo simulations, system states are sampled dependent on their probabilities without consideration of their relevance to the problem being solved. However, in intelligent search methods, the system states most relevant to the target problem have higher chances to be sampled due to their higher fitness values, regardless of their occurrence probabilities. This fitness-guided search characteristic may be beneficial in adequacy assessment since it enables the search to avoid evaluating irrelevant system states, which do not contribute or contribute very trivially to the overall reliability indices. As a result, in some scenarios the time used for adequacy evaluation can be reduced and therefore the algorithmic efficiency is improved.

- The computational time is not considerably affected by the system reliability characteristics. In Monte Carlo simulations, longer computational time is needed to achieve simulation convergence with higher system reliability, and it is possible that larger approximation errors and sluggish convergence performance may be caused. In highly reliable systems, PIS exhibits more robust behavior than MCS due to their different sampling mechanisms.

- The computational time is reduced in evaluating scenarios where a large number of power sources with relatively small capacities are involved. For methods which need the construction of capacity outage table, it takes more time to build the outage table by incorporating the state of each WTG, which, however, has no significant impact on the entire system reliability if only one unit outage is considered each time. The optimization mechanism of PIS makes system states related to these small capacity additions die off or reproduce very fast and thus considerably reduces the computation expense required.

- The method can be generally used in adequacy evaluation of power-generating systems with and without time-dependent sources. Furthermore, it has no inherent limitations in dealing with larger-sized systems based on its convergence mechanism. This is in actuality one salient merit of this population-based stochastic search approach. On the contrary, most analytical methods become much less efficient or even unable to resolve the problem as the system complexity and size increase.

- The parallel or distributed computation can be accomplished simply using partitioning based on the probabilities or load demands [13]. This can considerably increase the computational efficiency of different PIS-based algorithms.

- Although the comparison between MCS and PIS in this chapter is based on generating systems, most of the understanding and insights presented are applicable to power system reliability in general, e.g., multi-area and composite system reliability analysis.

F.   Summary

Due to the penetration of time-dependent sources such as wind turbine generators, it becomes more complicated to evaluate the adequacy of power-generating systems which themselves have uncertainties such as equipment failures. In this chapter, we adopted a two-stage procedure to evaluate the system adequacy. First a set of dominant failure states is derived by a specific PIS algorithm based on its convergence mechanism. Then, three major reliability indices are calculated based on these failure states by also considering the intermittency of wind power. A numerical study is carried out to demonstrate the usefulness of the proposed method. As we can see, the effectiveness of the proposed evaluation procedure is largely determined by the efficiency of the search algorithm. PIS-based optimizers enable the search to avoid less meaningful system states and seek out the most significant states efficiently. Also some comparative studies are carried out conceptually and numerically in relation to the Monte Carlo simulation method. PIS has shown to be effective in searching out eligible system states within a reasonable time. The advantages of the proposed method are also evaluated with respect to other existing methods including the analytical method and Monte Carlo simulation. Our future work includes incorporating other system uncertainties such as stochastic generation/load variations as well as improving PIS-based algorithms in handling the target problem.

CHAPTER VI

RELIABILITY-CONSTRAINED OPTIMUM PLACEMENT OF RECLOSERS
AND DISTRIBUTED GENERATORS IN DISTRIBUTION NETWORKS USING
ANT COLONY SYSTEM ALGORITHM

Optimal placement of protection devices and distributed generators (DGs) in radial feeders is important to ensure power system reliability. Distributed generation is being adopted in distribution networks with reliability enhancement as one of the objectives. In this chapter, an ant colony system (ACS) algorithm is used to derive the optimal recloser and DG placement scheme for radial distribution networks. A composite reliability index is used as the objective function in the optimization procedure. Simulations are carried out based on two practical distribution systems to validate the effectiveness of the proposed method. Furthermore, comparative studies in relation to genetic algorithm are also conducted.

A.   Introduction

As said earlier, one of the objectives of incorporating distributed generation (DG) in the distribution networks is reliability enhancement [5], [33]–[36]. In a DG-enhanced feeder, power flow is not unidirectional and conventional protection logic needs to be modified accordingly. A faulted branch can be energized from both ends and the protection devices are desired to interrupt the fault current. There are primarily three scenarios [37] in the optimal design of a DG-enhanced distribution system:

- Optimal recloser placement for a given DG allocation;

- Optimal DG placement for a given recloser placement;

- Optimal recloser and DG placement.

In essence, such problems are highly combinatorial and the corresponding objective functions are usually nondifferentiable. Thus, traditional analytical approaches such as linear and nonlinear programming have difficulty in dealing with these problems. More recently, various computational intelligence techniques have been developed to find the optimum or near-optimum solutions based on guided stochastic search. Among them, swarm intelligence is a relatively novel technique which can be used for complex engineering design optimization [38], [39]. Especially, ant colony search based algorithms are a kind of outstanding discrete optimizers [40]–[45]. In this study, an ant colony system (ACS) algorithm is proposed to optimize the recloser (or DG) placement for a fixed DG (or recloser) allocation. The idea can be extended to the simultaneous placement of both reclosers and DGs.

The remainder of the chapter is organized as follows: In Section B, the problem is formulated, where the optimum replacement of reclosers and DGs in distribution networks is introduced and a composite reliability index is defined. The inner working of the ant colony search algorithm and its basic steps are discussed in Section C. In Section D, the proposed method for optimal recloser and DG placement in two practical distribution systems is detailed. Simulation results and analysis are given in Section E. Finally, conclusions are drawn and future research is suggested.

B. Problem Formulation

A DG-enhanced radial feeder is shown in Figure 4 [37]. It includes four reclosers and two generators. If there are no generators in the distribution network, the first recloser upstream the fault will operate in the presence of a fault anywhere on the line. This will make the customers located downstream the recloser lose service. When the distributed generators are incorporated, service can still be provided to some islands

with DG. For instance, if a fault occurs between recloser 1 and recloser 2 during system operations, only recloser 1 will operate if there is no DG in the feeder. Thus, loss of service will be caused to the customers downstream this recloser. However, if there are DGs incorporated as shown in the figure, both recloser 1 and recloser 2 will operate and thus an island is formed. The distributed generators may still be capable of providing satisfactory service to the islanded zone.
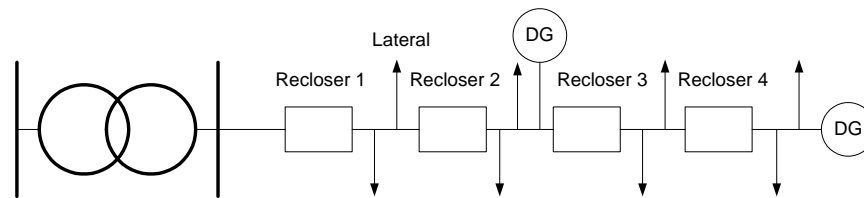
Fig. 4. Distributed generation-enhanced radial feeder

In the DG-enhanced distribution network, the sequence of events after a fault occurs is as follows: First DG is tripped, and the fault is detected and isolated by one or more protection devices, then the DG reconnects if it is not within the faulted zone. After the fault is cleared, recloser synchronizes its reclosing operation with the DG. As we can see, the locations of protection devices and distributed generators are highly dependent. Properly placed reclosers and distributed generators are crucial to achieve the optimal design of a DG-enhanced distribution network in terms of system reliability and investment costs.

The objective of protection devices and DGs placement in a radial feeder is to maximize the distribution network reliability under certain constraints. The system average interruption duration index (SAIDI) and the system average interruption frequency index (SAIFI) are typically used to measure the average accumulated duration and frequency of sustained interruptions per customer [37]. They are defined

as follows:

$$SAIDI = \frac{\sum u_i N_i}{\sum N_i} \qquad (6.1)$$

where N_i is the number of customers of load point i, and u_i is the outage time.

$$SAIFI = \frac{\sum r_i N_i}{\sum N_i} \qquad (6.2)$$

where r_i is the failure rate.

For the purpose of optimization, we define a composite reliability index through weighted aggregation of these two indices:

$$C = W_{SAIFI} * \frac{SAIFI}{SAIFI_T} + W_{SAIDI} * \frac{SAIDI}{SAIDI_T} \qquad (6.3)$$

where W_x indicates the weight for the corresponding reliability index, and the subscript T indicates the target value. This composite reliability index accounts for both SAIDI and SAIFI, which are the two most widely used indices for measuring the distribution system reliability. In this formulation, we incorporate the desired values of both indices which are empirically justified. The optimization algorithm is used to minimize the weighted composite index including interruption duration and frequency components. The smaller the value of the defined reliability index (i.e., objective function) is, the higher the system reliability becomes. The design constraints here are the number of reclosers or DGs available for this purpose coupled with the number of candidate locations determined by the system configuration.

C.   Ant Colony System Algorithms

This section describes the basic inner working as well as the basic steps in a typical ant colony system algorithm.

1. Basic principle

Ant colony algorithms are based on the behavior of social insects with an exceptional ability to find the shortest paths from the nest to the food sources using a chemical substance called pheromone [9]. Pheromone is used by the ants to communicate information with one another regarding the search path and to judge where to go. Ants deposit a certain amount of pheromone while walking, and each ant prefers to follow a direction rich in pheromone rather than a poorer one in a probabilistic fashion. Ant colony system (ACS) used in this study is extended from ant colony optimization (ACO), and it has a better performance than ACO in most engineering application scenarios. In ACS, the term "tour" is very often used to illustrate its mechanism. Each tour is a potential solution and it can be interpreted differently according to the nature of specific problems. For instance, in Traveling Salesman Problems (TSPs), it indicates a route connecting different cities, and in our problem, it represents a solution of recloser or DG locations.

2. Basic steps

The basic steps in the ant colony system (ACS) algorithm can be summarized as follows:

- Step 1: Initialization: In this phase, all ants are positioned on randomly generated starting nodes and initial values for trail intensity are set for each edge.

- Step 2: Tour construction: In this phase, each ant chooses the next node to move, considering the trail intensity and distance. Ants prefer to move to states which are connected by shorter edges or with higher pheromone intensity. This process is repeated until all ants finish their tours.

The state transition rule guiding the ant movement is as follows: an ant positioned in node r chooses the node s for its next step according to the following rule:

$$s = \begin{cases} \arg \max_{u \in J_k(r)} \{ [\tau(r,u), [\eta(r,u)]^\beta] \} & \text{if } q \leq q_0 \\ S & \text{otherwise.} \end{cases} \quad (6.4)$$

where q is a random number uniformly distributed in $[0, 1]$, q_0 is a parameter in $[0, 1]$, and S is a random variable chosen based on the probability distribution given in (6.5). The state transition rule gives the probability with which ant k at node r chooses to move to node s:

$$p_k(r, s) = \begin{cases} \frac{[\tau(r,s)][\eta(r,s)]^\beta}{\sum_{u \in J_k(r)} [\tau(r,u)][\eta(r,u)]^\beta} & \text{if } s \in J_k(r) \\ 0 & \text{otherwise.} \end{cases} \quad (6.5)$$

where τ is the pheromone level, $J_k(r)$ is the set of nodes to be visited by ant k positioned at node r, $\beta > 0$ is a parameter, which determines the relative importance of pheromone with respect to distance, and $\eta = \frac{1}{\delta}$ is a heuristic value equaling the inverse of the distance $\delta(r, s)$.

- Step 3: Fitness evaluation: After all ants have finished a tour, the fitness of each ant is evaluated. Usually, fitness function is defined to evaluate the performance of each ant. The pheromone intensity of edges between each stage is then updated according to these fitness values.

- Step 4: Trail intensity updating: The pheromone intensity of each edge will evaporate over time. For the edges that ants traveled in this iteration, their pheromone intensity can be updated by the state transition rule. Local pheromone updating rule and global pheromone updating rule are generally used to update the pheromone trail.

– Local updating rule: In deriving a solution, ants visit edges and alter their pheromone level based on the local updating rule:

$$\tau(r, s) \longleftarrow (1 - \rho)\tau(r, s) + \rho\tau_0 \tag{6.6}$$

where $0 < \rho < 1$ is a heuristically defined coefficient, and τ_0 is the initial pheromone level.

– Global updating rule: Global updating is carried out in the best tour found so far after all ants have finished their tours. The pheromone level is updated using the global updating rule:

$$\tau(r, s) \longleftarrow (1 - \alpha)\tau(r, s) + \alpha\Delta\tau(r, s) \tag{6.7}$$

where

$$\Delta\tau(r, s) = \begin{cases} (L_{gb})^{-1} & \text{if (r,s)} \in \text{Global-best-tour} \\ 0 & \text{otherwise.} \end{cases} \tag{6.8}$$

where $0 < \alpha < 1$ is the pheromone decay parameter, and L_{gb} is the length of the globally best tour.

• Stopping criteria: The above optimization process is terminated if the tour counter reaches the maximum prespecified number of iterations or all ants choose the same tour.

D. The Proposed Approach

In this study, two designs will be investigated: recloser placement for fixed DG locations and DG placement for fixed recloser locations. In this section, recloser placement will be used to illustrate the proposed method, which can also be applied to the optimum DG placement design in a similar fashion. In the DG-enhanced distribution

network, optimization becomes more complicated as compared with the traditional one. Quite often, it is difficult to locate the optimal recloser positions for supporting the normal power supply of isolated islands in the presence of faults. In this investigation, we propose an ant colony system algorithm to seek out the optimal recloser locations by minimizing the aforementioned composite reliability index. Since reclosers can only be placed on the feeder branches, this problem is concerned with discrete optimization. It appears natural to think of the ant colony system algorithm for this application considering its ability to handle discrete optimization problems.

1.   Search space

In the optimal recloser placement problem, the elements of the potential solution are positions of individual reclosers to be placed on the feeder. Figure 5 shows the search space of the recloser placement problem, where N is the number of available reclosers and M is the number of possible branches where reclosers may be placed. All possible candidate locations for recloser n are represented by the states in the search space corresponding to stage n. The number of stages equals to the number of reclosers. Each ant starts its tour at the home colony and stops at the destination. The ant opts for the state to move toward with a certain probability, which is a function of the amount of pheromone deposited on the connecting edges of each state. When an ant travels from one stage to the next, the state of each stage is recorded in the location list. In order to enable the ant to choose legal tours, transitions to the locations that have been occupied are prohibited until a tour is completed. After a tour is accomplished, the location list of each ant is used to calculate its current solution, i.e., the value of the objective function.
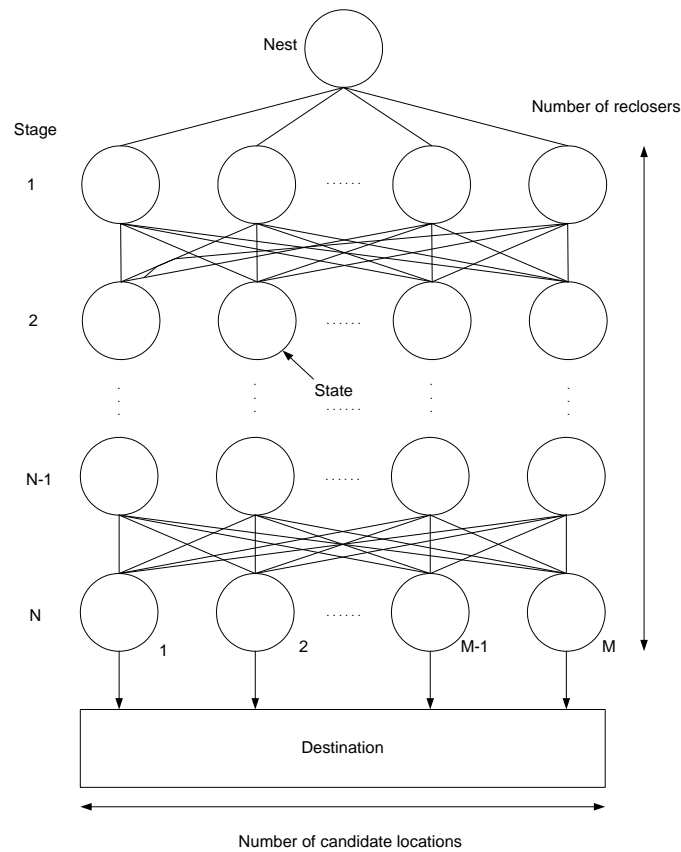
Fig. 5. Search space of the problem

2. Reliability evaluation

The procedure for calculating the system reliability is illustrated in Figure 6. For each recloser configuration (i.e., a potential solution), a composite reliability index is derived by determining the reliability zones that are bounded by the reclosers, simulating the faults in those zones, determining the online and offline loads, and finally calculating the value of the composite reliability index. For each reliability zone with DG, the maximum active power output of all generators in this zone is calculated after a fault occurs in other zones. The value is then compared with the load duration curve of this zone load. The number of faults is reduced by the

percentage of time that the zone generation is larger than the zone load.

3.   Solution construction and pheromone updating

Each ant updates the pheromone trails after it builds up a solution. Thus, ants can use different pheromone intensities to construct solutions in order to achieve diversification of solutions. On the other hand, the global updating is performed after all ants construct solutions by further adjusting the pheromone level of the best path achieved so far.

- Solution construction: Let τ_{ij}^{xy} be the pheromone intensity of trail on edge (i,j) between the consecutive stages x and y at iteration t. Each ant at state i of stage x opts for the next stage based on the state transition rules. For $q > q_0$, the transition rules are defined in the following:

$$p_{ij}^{xy}(t) = \frac{[\tau_{ij}^{xy}(t)][\eta_{ij}^{xy}]^{\beta}}{\sum_{j \in stagey}[\tau_{ij}^{xy}(t)][\eta_{ij}^{xy}]^{\beta}} \tag{6.9}$$

For $q \leq q_0$, the following state is selected:

$$\arg \max_{j \in stagey}\{[\tau_{ij}^{xy}(t)][\eta_{ij}^{xy}]^{\beta}\} \tag{6.10}$$

where η_{ij}^{xy} is the reduction of reliability index C values between stage x and y. β is the parameter that controls the relative importance of trail intensity versus the C reduction between the consecutive stages.

- Pheromone updating: After the solution is constructed, ant i has its location list $\Omega_i^{(t)}$ and fitness evaluation $C(\Omega_i^{(t)})$. All trail intensity can be updated based on the evaporation formula for local update:

$$\tau_{ij}^{xy}(t+1) = \rho \times \tau_{ij}^{xy}(t) + \tau_{ij}^{xy,(0)} \tag{6.11}$$

where $\tau_{ij}^{xy,(0)}$ is a small positive value. The ant with the highest fitness at each iteration will deposit the largest amount of pheromone to the edges of its location list. If ant k has the best solution in this tour, then the pheromone intensity of these edges in its location list can be further revised by the global updating rule

$$\tau_{ij}^{xy}(t+1) = \tau_{ij}^{xy}(t+1) + \frac{K_{pher}}{C(\Omega_k^{(t)})}, x, y \in \Omega_k^{(t)} \tag{6.12}$$

where K_{pher} is a constant relevant to the trail deposit. It can be appreciated that the smaller the value of the reliability index is, the larger the additional pheromone deposit will be.

4. Computational procedure

The computational procedure of the proposed optimization algorithm is shown in Figure 7, which is detailed in the following:

- Ant production initialization: The initial ant positions and the initial pheromone levels are created. Number of available reclosers and the capacity of each distributed generator are specified. The configuration of the radial feeder is represented to indicate all the candidate device locations.

- Fitness evaluation: The fitness of all ants is evaluated in terms of the objective function defined in (6.3). That is, the fitness value of each recloser placement scenario is assessed according to its resultant system reliability. With the evaluated fitness of all ants, the pheromone can be added to the particular direction that the ants have chosen.

- Ant dispatch: The ants are dispatched based on the level of pheromone and distance. As shown in (6.9) and (6.10), each ant chooses the next state to move

considering τ_{ij} and η_{ij} values. If an ant k positioned in state i chooses the next state j to move, then such a movement can be represented as follows:

- If $q > q_0$, select the next state randomly with the probability represented by (6.9):

- If $q \leq q_0$, select the next state with the best local pheromone-distance profile as indicated in (6.10).

Let K be the number of ants, then for each iteration, these K ants perform K movements during interval $(t, t+1)$. The pheromone of the visited path can be dynamically adjusted by (6.11). After all ants have completed their tours, the shortest path found by the ants is allowed to update its pheromone based on (6.12), which corresponds to the best recloser configuration found thus far.

- Termination conditions: The optimization process does not halt until the number of iterations reaches the pre-specified value, or the value of the objective function ceases improving for a certain number of iterations. The best path chosen among all iterations is the desired recloser placement scheme, i.e., the optimal solution to our problem.

E.   Simulation Results and Analysis

As mentioned earlier, two design cases will be investigated in the simulation studies. First, the proposed method is tested on a 69-segment, 8-lateral distribution feeder as shown in Figure 8 [37]. We assume that DG locations are fixed in the distribution system and all reclosers function identically. There are eight laterals, six of which are connected to a single DG at their ends. System parameters used in the simulations can be found in [46]. It is obvious that the enumeration method is not efficient, if

not impossible, for such a system. Here we assume that the fault incidence rate and the duration of faults are uniform over all feeder branches. Also, in the presence of a fault, only the minimum number of reclosers close to the fault are activated in order to isolate the fault. The total nominal feeder load is 3.8 MW. The reliability index weights are chosen as follows: $W_{SAIFI} = 0.33$, and $W_{SAIDI} = 0.67$. The target values of the reliability indices are set as follows: $SAIFI_T = 1.0$, and $SAIDI_T = 2.2$. They are empirically justified and indicate the satisfactory level of reliability.

The simulation program was coded using Visual C++ 6.0 and run in a 2.20 GHz Pentium-IV personal computer. Many parameters can impact the performance of the ACS algorithm. β reflects the relative importance of the reduction of objective function values between consecutive stages with respect to the trail intensity. ρ represents the trail persistence and $(1 - \rho)$ is the trail pheromone evaporation rate. K_{pher} is a large constant associated with the quantity of trail deposit. The proper tuning of ACS parameters is crucial to achieve an effective optimizer. After careful tuning, we selected the following parameter values: number of ants $= 200$, number of iterations $= 200$, $\beta = 1.0$, $\rho = 0.73$, and $K_{pher} = 60,000$. The update rule specified in (6.11) and (6.12) may cause the early stagnation during the stochastic search. In this situation, the trails on certain edges are so high that the ants will deposit more and more phoromone in this trail. This is undesirable since this kind of premature convergence usually leads to the local optimum. To avoid search stagnation, the allowed range of the pheromone trail intensity is specified as follows:

$$\gamma(r, s) = \begin{cases} \tau_{min} & \text{if } \gamma(r, s) \leq \tau_{min} \\ \tau_{max} & \text{if } \gamma(r, s) \geq \tau_{max}. \end{cases} \tag{6.13}$$

In this study, the upper and lower bounds are chosen as follows:

$$\tau_{max} = \frac{1}{C_{gbest}} \tag{6.14}$$

where C_{gbest} is the global best solution achieved so far, and

$$\tau_{min} = \frac{\tau_{max}}{K^2} \tag{6.15}$$

where K is the number of ants. As we can see, in Max-Min ACS, upper and lower bounds are added to impose explicit limits on pheromone trails during the optimization process. The bounds are selected based on empirical observations in some initial experiments, and during optimization they keep changing based on the global best solution obtained so far. This Max-Min ACS algorithm is capable of achieving a higher degree of exploration by trying more alternatives. The simulation results obtained based on different DG capacities and different numbers of reclosers are listed from Table VI to Table IX.

Table VI. No distributed generators in the distribution system (test system 1)

Number of reclosers	Reliability index value	Recloser locations
1	3.9560	8-9
2	2.8695	8-9, 30-31
3	1.9012	3-4, 30-31, 47-48
4	1.6042	3-4, 27e-28e 30-31, 47-48
5	0.9033	3-4, 11-12, 30-31, 47-48, 28e-65

Generally speaking, from the simulation results obtained, we can see that for a given capacity of distributed generators, the system reliability increases with more

Table VII. Maximum power of each distributed generator = 0.3 MW (test system 1)

Number of reclosers	Reliability index value	Recloser locations
1	3.8671	8-9
2	2.7005	8-9, 27-28
3	1.8109	3-4, 30-31, 47-48
4	1.3237	3-4, 27e-28e, 30-31, 47-48
5	0.8001	3-4, 10-11, 27e-28e, 30-31, 47-48

reclosers used. For the same number of reclosers used, the higher the maximum output of distributed generators, the higher the system reliability will become. When there is only one recloser, its optimal location complies with the traditional device placement rule, that is, the recloser should be put as near as possible to the central part of the entire radial feeder. Especially, provided that the loads are uniformly distributed, 25% reliability improvement can be achieved [37]. For the cases of the feeder with more reclosers, some branches turned out to be particularly important in improving the system reliability. For instance, in some cases, the branch between bus 47 and bus 48 is a crucial location for protective device placement since the addition of recloser in this position will considerably increase the system reliability. From the simulation results, we can see that the appropriate selection of DG capacity as well as the proper placement of protective devices are both very important in ensuring the system reliability.

For comparison purpose, genetic algorithm (GA) is also used to derive solutions for this problem, which has turned out to be very effective in various engineering optimization applications [7]. In GA, each candidate solution is deemed a chromosome

Table VIII. Maximum power of each distributed generator = 0.5 MW (test system 1)

Number of reclosers	Reliability index value	Recloser locations
1	3.5022	8-9
2	2.3341	8-9, 28-29
3	1.7432	8-9, 27-28, 50-51
4	1.1987	3-4, 30-31, 47-48, 66-67
5	0.7100	4-5, 10-11, 30-31, 47-48, 67-68

and the stochastic search is carried out based on a population of chromosomes. The defined composite reliability index is to be minimized and its value is seen as an indication of fitness for each chromosome. The higher the fitness value is, the higher the chromosome's chance to survive becomes. The computational procedure of GA for handling the target problem primarily includes the following steps:

- Step 1: Initially a set of chromosomes is created in a random fashion;

- Step 2: The fitness of each chromosome is evaluated based on the objective function defined;

- Step 3: Based on the fitness value of each chromosome, different genetic operators including reproduction, crossover, and mutation are applied in the entire population in order to produce the next generation of chromosomes.

- Step 4: Repeat Step 2 and Step 3 until any stopping criterion is satisfied. The chromosome with the highest fitness value is the final solution to the target problem.

Table IX. Maximum power of each distributed generator = 1.0 MW (test system 1)

Number of reclosers	Reliability index value	Recloser locations
1	3.3012	8-9
2	2.1455	8-9, 49-50
3	1.5066	4-5, 27e-28e, 47-48
4	1.0340	8-9, 28-29, 36-37, 49-50
5	0.5988	3-4, 10-11, 30-31, 49-50, 67-68

The simulation program was also coded in Visual C++ 6.0 and run in the same personal computer. In the simulations, the population size is 200, crossover rate is 0.65, and mutation rate is 0.05. Elitist strategy is used to preserve the best solutions found in each iteration, and the elite count is 2. The maximum number of iterations is 200, which is used as the stopping criterion.

The design scenarios where GA and ACS have different results are listed in Table X, and the different results are shown in Table XI.

As we can see from Table XI, the proposed ACS method outperforms the GA method in terms of solution quality, since in these design scenarios better locations are found for achieving higher system reliability by the proposed method. Furthermore, the computational time of ACS for deriving the solutions is about 14.4 seconds in different design scenarios, while that of GA is around 27.3 seconds. Thus, its computational efficiency is significantly higher than that of GA.

It should be noted that there are still some limitations which may lower the efficiency of the proposed method. For instance, ACS has some dependency on initial points, and the most effective combination of different parameters requires some time

Table X. Design scenarios where GA and ACS have different results (test system 1)

Design scenarios	DG capacity (MW)	Number of reclosers
DS 1	0.3	2
DS 2	0.5	3
DS 3	0.5	4
DS 4	0.5	5
DS 5	1	2
DS 6	1	3
DS 7	1	4

to tune. Also its final outputs have some stochastic characteristic. However, there are no inherent limitations for our proposed method to deal with larger-sized problems due to its guided stochastic search characteristic. It may take a longer time for the ACS to converge because more potential solutions are to be evaluated. But the extra time needed is not as significant as that in analytical methods, since its computational efficiency is relatively insensitive to system complexity and size. In actuality, with respect to analytical methods, one salient merit of the proposed method is its ability to deal with large-sized systems due to its outstanding convergence mechanism. Most analytical methods become much less efficient or even unable to resolve the problem when the system complexity and size increase.

Next, the design case of DG placement in fixed recloser locations is examined. The computational procedure is the same as presented in Section IV, except that here the DGs are to be placed. A larger-sized distribution system is used to demonstrate the effectiveness of the proposed method. The actual 394-bus and 1123-node radial distribution network [47] consists of 199 loads, 104 laterals/sub-laterals, and 44 normally closed reclosers. The total nominal load is 28.2 MW. Its one-line diagram is

Table XI. Comparison of different results obtained from GA and ACS (test system 1)

Scenarios	Schemes	Reliability value	Recloser locations
DS 1	GA	2.7407	8-9, 30-31
	ACS	2.7005	8-9, 27-28
DS 2	GA	1.7750	8-9, 28-29, 51-52
	ACS	1.7432	8-9, 27-28, 50-51
DS 3	GA	1.2089	4-5, 30-31, 47-48, 67-68
	ACS	1.1987	3-4, 30-31, 47-48, 66-67
DS 4	GA	0.7156	3-4, 10-11, 30-31, 47-48, 66-67
	ACS	0.7100	4-5, 10-11, 30-31, 47-48, 67-68
DS 5	GA	2.1698	8-9, 27-28
	ACS	2.1455	8-9, 49-50
DS 6	GA	1.5165	3-4, 28e-65, 47-48
	ACS	1.5066	4-5, 27e-28e, 47-48
DS 7	GA	1.0384	8-9, 27-28, 36-37, 48-49
	ACS	1.0340	8-9, 28-29, 36-37, 49-50

shown in Figure 9. Note that in this study each DG will be connected to a single bus, and the design objective is to connect DGs to the appropriate buses to enhance the overall system reliability. The reliability index weights are chosen as those in the first design, and the target values of the reliability indices are set as follows: $SAIFI_T = 1.2$, and $SAIDI_T = 2.7$. The results derived by the proposed method are listed from Table XII to Table XIV for different design scenarios. For comparison, GA is also used to place the DGs. The design scenarios where GA and ACS have different results are listed in Table XV, and the different results are shown in Table XVI.

Table XII. Maximum power of each distributed generator = 0.3 MW (test system 2)

Number of DGs	Reliability index value	DG locations
1	1.1976	157
2	1.1345	127, 157
3	1.0788	30, 127, 157
4	1.0464	30, 127, 157, 312
5	1.0207	30, 127, 157, 312, 336

Table XIII. Maximum power of each distributed generator = 0.5 MW (test system 2)

Number of DGs	Reliability index value	DG locations
1	1.1644	157
2	1.0907	70, 157
3	1.0245	70, 127, 157
4	0.9722	17, 70, 127, 157
5	0.9301	17, 70, 127, 157, 312

As we can see from Table XI, the proposed ACS method outperforms the GA method in terms of solution quality, since in these design scenarios better locations have been found which are capable of achieving higher system reliability. Furthermore, the computational time of ACS for deriving the solutions is about 43.7 seconds in different design scenarios, while that of GA is around 90.6 seconds. Thus, its computational efficiency is significantly higher than that of GA.

F. Summary

Distributed generation is being introduced into the traditional distribution network in order to enhance the power system reliability. The optimal placement of protection

Table XIV. Maximum power of each distributed generator = 0.7 MW (test system 2)

Number of DGs	Reliability index value	DG locations
1	1.1327	157
2	1.0521	70, 157
3	0.9850	70, 157, 336
4	0.9234	70, 157, 227, 336
5	0.8726	17, 70, 157, 227, 312

devices and DGs is crucial for achieving such an objective. In this chapter, an optimization procedure based on the ant colony system algorithm is developed to seek out the optimal recloser and DG locations by minimizing a composite reliability index. The simulation results from two test distribution systems validate the effectiveness of the proposed method. Furthermore, comparative studies with respect to genetic algorithm are also carried out. In future research, we will investigate the simultaneous placement of both reclosers and distributed generators, which are dependent on one another. More comprehensive reliability indices may be defined to guide the search process, and adaptive and automatic tuning can be introduced to further improve ACS efficiency. Also, the operational costs may be incorporated by minimizing the customer interruption costs.

Table XV. Design scenarios where GA and ACS have different results (test system 2)

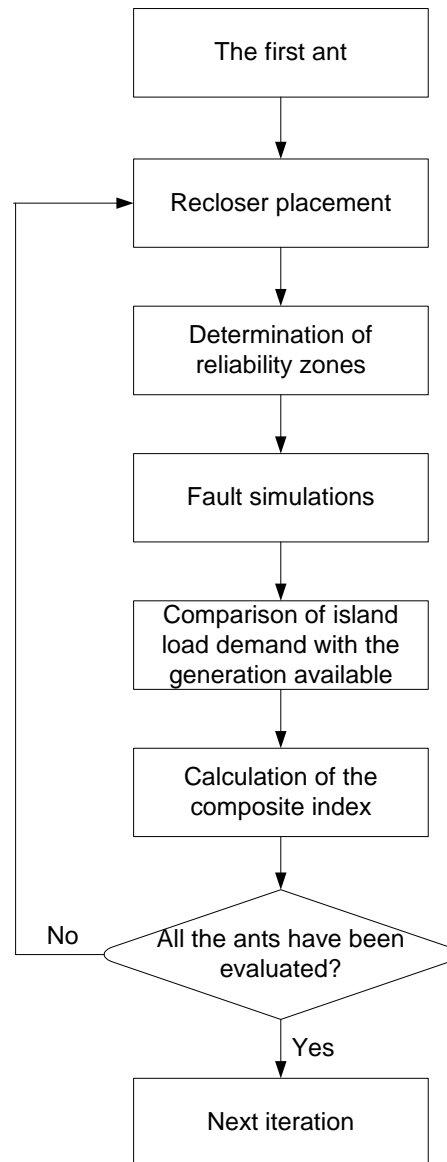| Design scenarios	DG capacity (MW)	Number of DGs
DS 1	0.3	2
DS 2	0.7	2
DS 3	0.5	3
DS 4	0.7	3
DS 5	0.3	4
DS 6	0.7	4
DS 7	0.3	5
DS 8	0.5	5
DS 9	0.7	5

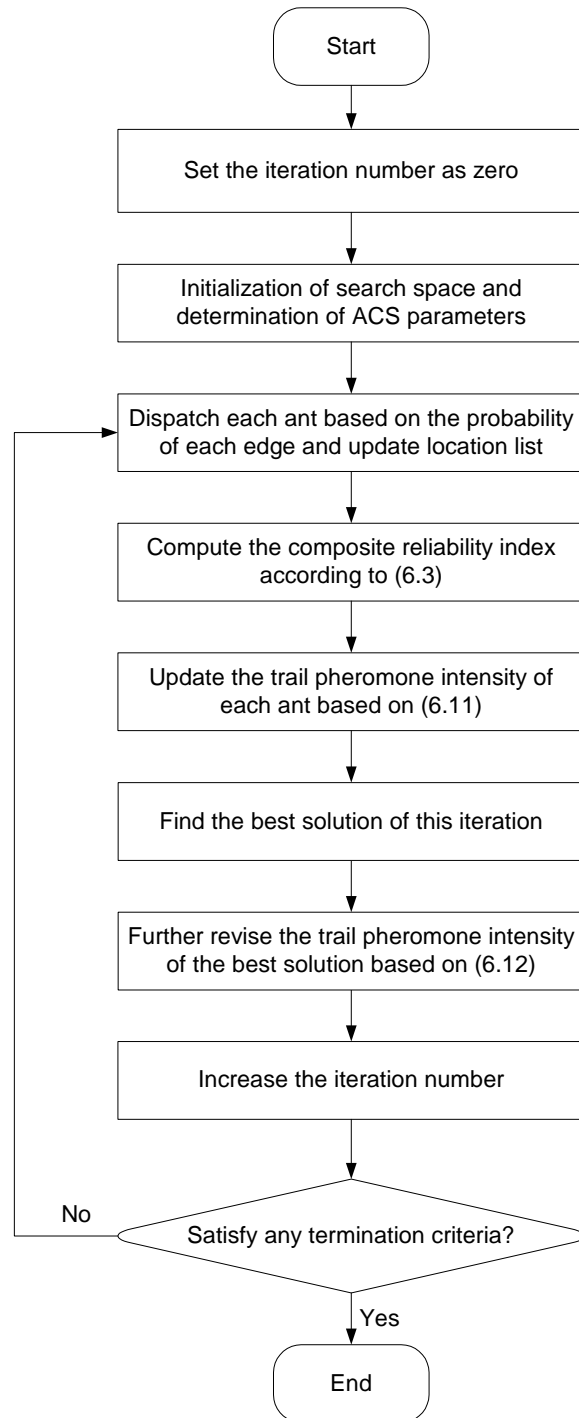Fig. 6. Flow chart for calculating system reliability of each recloser configuration

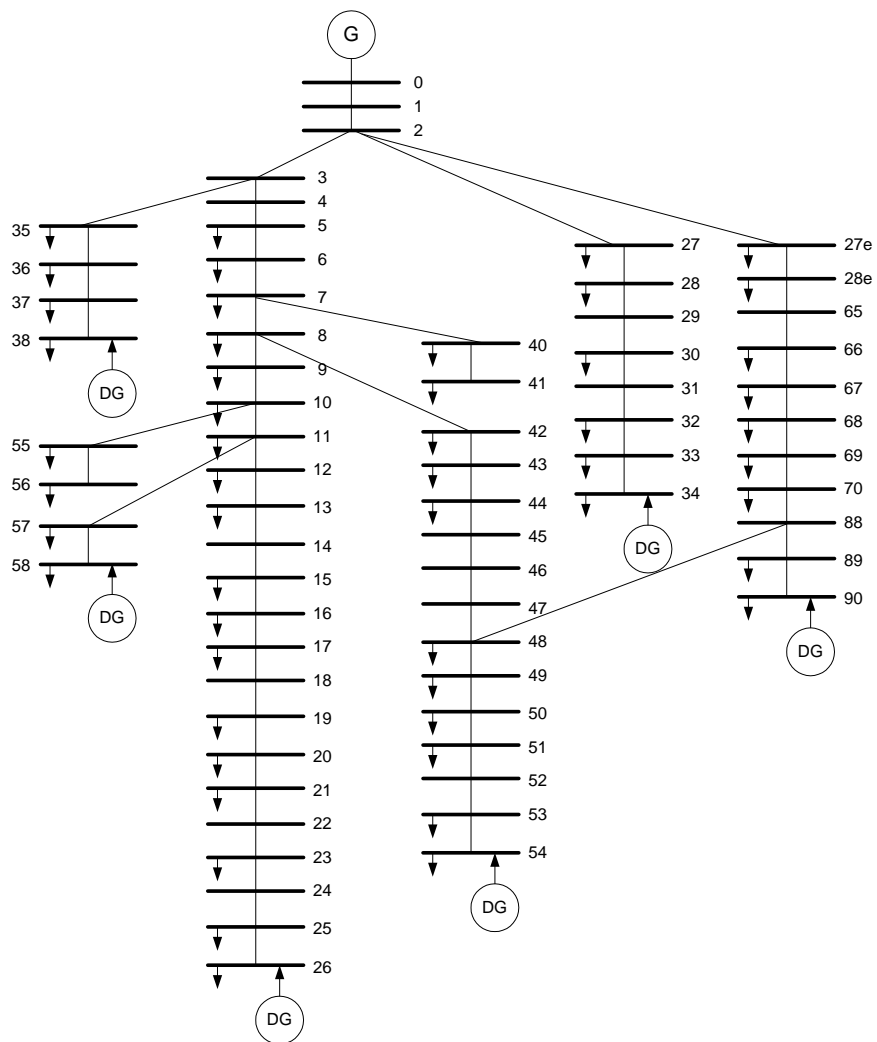Fig. 7. Computational procedure for the proposed algorithm.

Fig. 8. One-line diagram of the 69-bus test distribution system
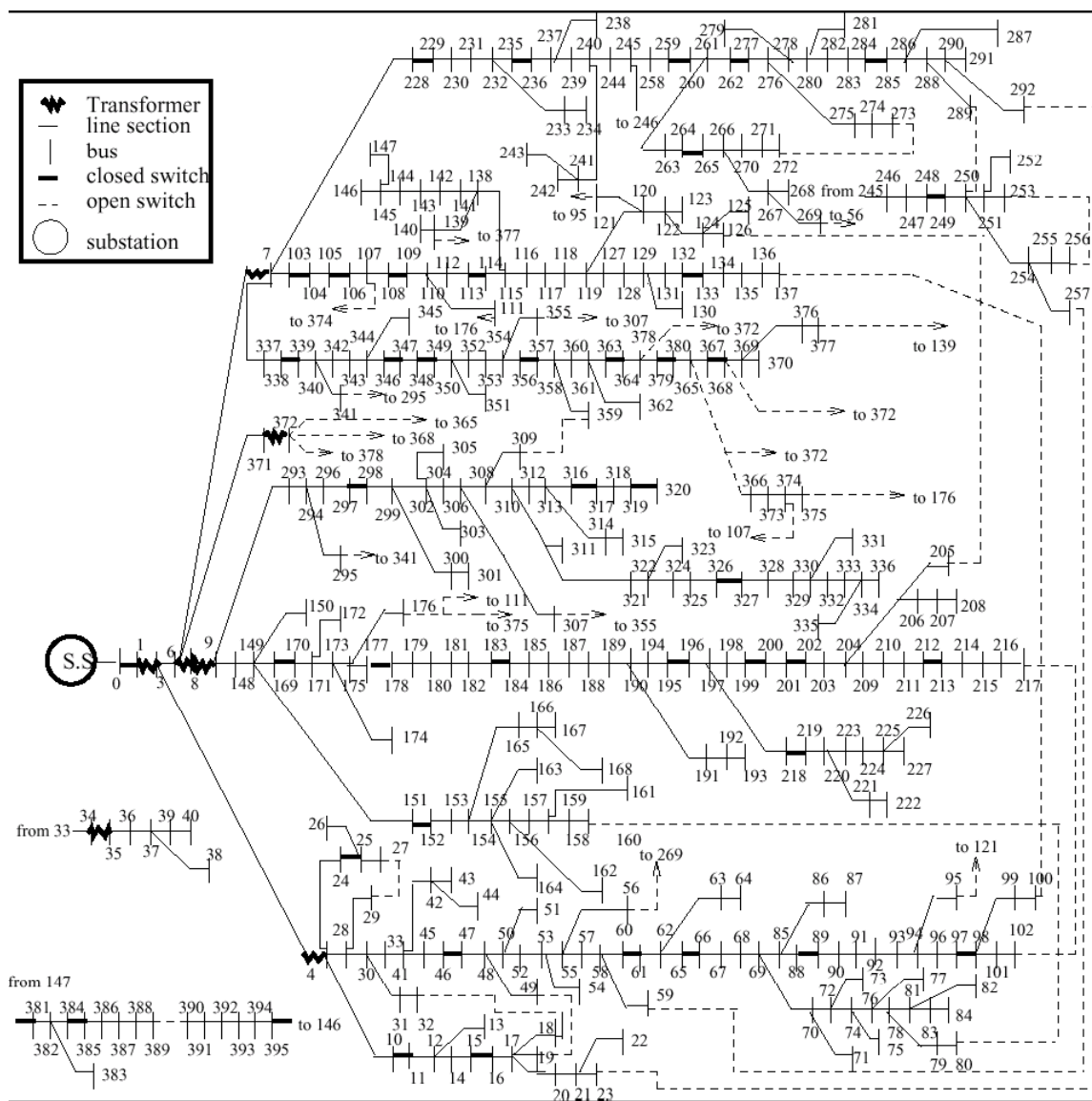
Fig. 9. One-line diagram of the 394-bus test distribution system [47]

Table XVI. Comparison of different results obtained from GA and ACS (test system
2)

Scenarios	Schemes	Reliability value	DG locations
DS 1	GA	1.1466	157, 193
	ACS	1.1345	127, 157
DS 2	GA	1.0589	157, 193
	ACS	1.0521	70, 157
DS 3	GA	1.0468	70, 157, 193
	ACS	1.0245	70, 127, 157
DS 4	GA	1.0029	127, 193, 336
	ACS	0.9850	70, 157, 336
DS 5	GA	1.0572	127, 193, 227, 360
	ACS	1.0464	30, 127, 157, 312
DS 6	GA	0.9421	70, 193, 227, 312
	ACS	0.9234	70, 157, 227, 336
DS 7	GA	1.0426	127, 157, 282, 312, 336
	ACS	1.0207	30, 127, 157, 312, 336
DS 8	GA	1.0106	70, 127, 157, 282, 312
	ACS	0.9301	17, 70, 127, 157, 312
DS 9	GA	0.9033	70, 157, 227, 282, 312
	ACS	0.8726	17, 70, 157, 227, 312

CHAPTER VII

RISK AND COST TRADEOFF IN ECONOMIC DISPATCH INCLUDING WIND
POWER PENETRATION BASED ON MULTI-OBJECTIVE MEMETIC
PARTICLE SWARM OPTIMIZATION*

Utilization of renewable energy resources such as wind energy for electric power generation has assumed great significance in recent years. Wind power is a source of clean energy and is able to spur the reductions of both consumption of depleting fuel reserves and emissions of pollutants. However, since the availability of wind power is highly dependent on the weather conditions, the penetration of wind power into traditional utility grids may incur certain security implications. Therefore, in economic power dispatch including wind power penetration, a reasonable tradeoff between system risk and operational cost is desired. In this chapter, a bi-objective economic dispatch problem considering wind penetration is first formulated, which treats operational costs and security impacts as conflicting objectives. Different fuzzy membership functions are used to reflect the dispatcher's attitude toward the wind power penetration. A multi-objective memetic particle swarm optimization (MOMPSO) algorithm is adopted to develop a power dispatch scheme which is able to achieve compromise between economic and security requirements. Numerical simulations including comparative studies are reported based on a typical IEEE test power system to show the validity and applicability of the proposed approach.

A.   Introduction

The major objective of Economic Dispatch (ED) is to schedule the power generation in an appropriate manner in order to satisfy the load demand while minimizing the total operational cost [48]–[51]. These ED problems are usually highly nonlinear and the metaheuristic methods have turned out to be more effective than the traditional analytical methods. In recent years, renewable energy resources such as wind power have shown great prospects in decreasing fuel consumption as well as reducing pollutants emission [52]–[58]. Unfortunately, the expected generation output from a wind park is difficult to predict accurately, primarily due to the intermittent nature of the wind coupled with the highly nonlinear wind energy conversion. This unpredictability may incur the security problems when the penetration of wind power in the traditional power system exceeds a certain level. For instance, the dynamic system stability may be lost due to excessive wind fluctuations. As a result, for achieving the tradeoff between system risk and total running cost, it is desirable to examine how to dispatch the power properly for the power system taking into account the impacts of wind power penetration. In this chapter, the ED model is first constructed as a bi-objective optimization problem through simultaneous minimization of both risk level and operational cost. For this purpose, an effective optimization prodecure is needed. Particle swarm optimization (PSO) is a salient meta-heuristics, which turns out to be capable of resolving a wide variety of highly nonlinear and complex engineering optimization problems with outstanding convergence performance. Meanwhile, it has strong ability to avoid premature convergence. In this study, a multi-objective memetic particle swarm optimization (MOMPSO) algorithm is proposed to derive the Pareto-optimal solutions for economic dispatch including wind power penetration. Moreover, considering the different attitudes of dispatchers towards wind power

penetration, we used several fuzzy membership functions to indicate the system security level in terms of wind power penetration and wind power cost. Different fuzzy representations including linear and quadratic functions can be used to reflect the dispatcher's optimistic, neutral, or pessimistic attitude toward wind power penetration. Furthermore, minimization of pollutant emissions is treated as the third design objective and the tradeoff surface among the three design objectives is also derived.

The remainder of the chapter is organized as follows. Section B presents the wind penetration model described by different fuzzy membership functions. Section C formulates the economic dispatch problem including its multiple objectives and a set of design constraints imposed. Section D introduces the inner workings of particle swarm optimization algorithms. The MOMPSO algorithm adopted is discussed in Section E. Simulation results and analysis are presented in Section F. Finally, conclusions are drawn and future research is suggested.

B.   Wind Power Penetration Model

Wind power integration is an important issue to address for achieving a reliable power system including wind power source. Because of the unpredictable and variable characteristics of wind power, its integration into the traditional thermal generation systems will incur the operator's concern on system security. Fuzzy definition regarding wind penetration is a viable way to represent the penetration level of the wind power, since it is usually difficult to determine the optimal wind power that should be integrated into the conventional power grids [58].

As shown in Figure 10, a fuzzy membership function μ regarding the wind penetration is defined to indicate the system security level. It can be mathematically
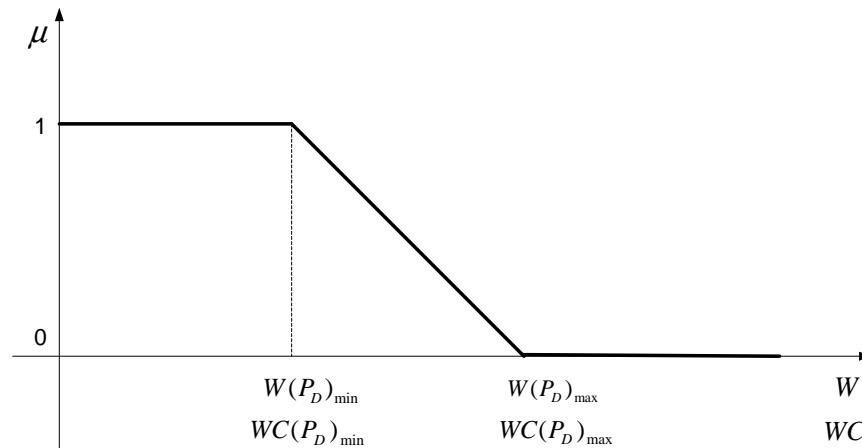
Fig. 10. Fuzzy linear representation of the security level in terms of wind penetration and wind power cost.

expressed in the following form [58]:

$$
\mu = \begin{cases}
1, & W \leq W(P_D)_{min} \\
\frac{W(P_D)_{max}-W}{W(P_D)_{max}-W(P_D)_{min}}, & W_{min} \leq W \leq W_{max} \\
0, & W \geq W(P_D)_{max}
\end{cases}
\tag{7.1}
$$

where W is the wind power incorporated in economic dispatch; $W(P_D)_{min}$ is the lower bound of wind power penetration, below which the system is deemed secure; $W(P_D)_{max}$ is the upper bound of wind power penetration, above which the system is considered as insecure due to the wind perturbations. Both $W(P_D)_{min}$ and $W(P_D)_{max}$ are dependent on the total load demand in the power dispatch.

The above defined membership function can also be represented in terms of the operational cost for incorporating wind power:

$$
\mu = \begin{cases}
1, & WC \leq WC(P_D)_{min} \\
\frac{WC_{max}-WC}{WC_{max}-WC_{min}}, & WC_{min} \leq WC \leq WC_{max} \\
0, & WC \geq WC(P_D)_{max}
\end{cases}
\tag{7.2}
$$

where WC is the running cost of wind power in the power dispatch; $WC(P_D)_{min}$ is the lower bound cost for producing wind power, below which the system is seen as secure; $W(P_D)_{max}$ is the upper bound cost for including wind power, above which the system is considered as insecure due to the wind intermittency. In a similar fashion, both $WC(P_D)_{min}$ and $WC(P_D)_{max}$ are dependent on the total load demand in the power dispatch. In this study, sensitivity studies are also carried out to illustrate the impact of different allowable ranges of wind power penetration as well as different running costs of wind power on the final solutions obtained.

To reflect dispatcher's differing attitudes toward wind power penetration, a quadratic membership function can be defined as follows [58]:

$$\mu = \begin{cases} 1, & W \leq W(P_D)_{min} \\ a_w W^2 + b_w W + c_w, & W_{min} \leq W \leq W_{max} \\ 0, & W \geq W(P_D)_{max} \end{cases} \tag{7.3}$$

where a_w, b_w, and c_w are the coefficients of the quadratic function, which determine its shape reflecting the dispatcher's attitude toward wind power. As shown in Figure 11, by selecting different coefficients a_w, b_w, and c_w, different shapes of the quadratic function can be defined. For the identical security level μ_0, the penetration levels of wind power differ for different defined functions $w_1 < w_2 < w_3$. The curves corresponding to these three values reflect the pessimistic, neutral, and optimistic attitudes of the dispatcher toward the wind power integration, respectively.

In a similar fashion, the security level can also be defined in terms of the operational cost of wind power. Its function shape is shown in Figure 12.

$$\mu = \begin{cases} 1, & WC \leq WC(P_D)_{min} \\ a_c WC^2 + b_c WC + c_c, & WC_{min} \leq WC \leq WC_{max} \\ 0, & WC \geq WC(P_D)_{max} \end{cases} \tag{7.4}$$
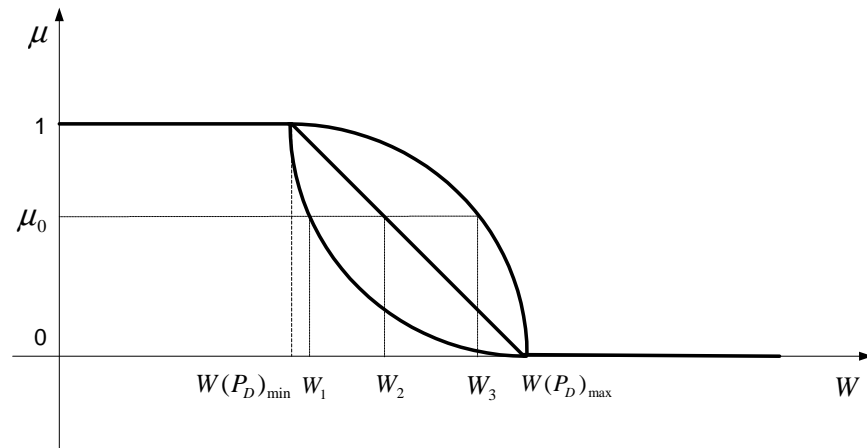
Fig. 11. Fuzzy quadratic representation of the security level in terms of wind power penetration

where a_c, b_c, and c_c determine the curve shape of the quadratic function defined in terms of the running cost of wind power.
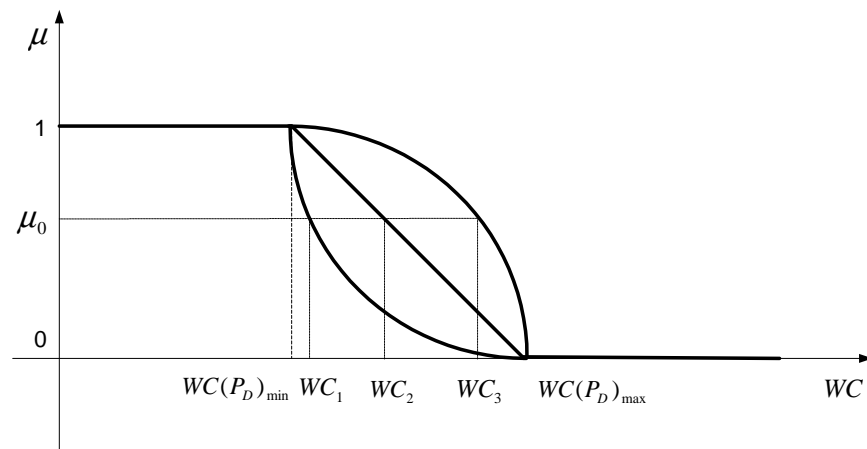
Fig. 12. Fuzzy quadratic representation of the security level in terms of wind power cost

C.   Problem Formulation

The problem of economic power dispatch with wind penetration consideration can be formulated as a bi-criteria optimization model. The two conflicting objectives, i.e., total operational cost and system risk level, should be minimized simultaneously while fulfilling certain system constraints. This bi-objective optimization problem is formulated mathematically in this section.

1.   Problem objectives

There are two objectives that should be minimized simultaneously, that is, system risk level and the total operational cost.

- Objective 1: Minimization of system risk level

  From the security level function defined in (7.1) and (7.2), we know that the larger the value of membership function μ is, the more secure the system will become. If the wind penetration is restricted under a certain level, the system can be considered as secure. On the contrary, if excessive wind penetration is introduced into the power dispatch, the system may become insecure. Here we define an objective function which should be minimized in order to ensure system security:

$$R(\mu) = \frac{1}{\mu} \tag{7.5}$$

- Objective 2: Minimization of operational cost

  The cost curves of different generators are represented by quadratic functions with sine components. The superimposed sine components represent the rippling effects produced by the steam admission valve openings. The total $/h

fuel cost $FC(P_G)$ can be represented as follows:

$$FC(P_G) = \sum_{i=1}^{M} a_i + b_i P_{Gi} + c_i P_{Gi}^2 + |d_i \sin[e_i(P_{Gi}^{min} - P_{Gi})]| \qquad (7.6)$$

where M is the number of generators committed to the operating system, a_i, b_i, c_i, d_i, e_i are the cost coefficients of the i-th generator, and P_{Gi} is the real power output of the ith generator. P_G is the vector of real power outputs of generators and defined as

$$P_G = [P_{G1}, P_{G2}, \ldots, P_{GM}] \qquad (7.7)$$

The running cost of wind power can be represented in terms of the value of membership function μ which indicates the system security level. For the linear membership function case,

$$WC(P_G, \mu) = C_w(W_{av} - (P_D + P_L - \sum_{i}^{M} P_{Gi})) - \mu * \Delta WC + WC_{max} \qquad (7.8)$$

where W_{av} is the available wind power from the wind farm, C_w is the coefficient of penalty cost for not using all the available wind power, P_D is the load demand, P_L is the transmission loss, and

$$\Delta WC = WC_{max} - WC_{min}. \qquad (7.9)$$

For the quadratic membership function case,

$$WC(P_G, \mu) = C_w(W_{av} - (P_D + P_L - \sum_{i}^{M} P_{Gi})) - \frac{b_c}{2a_c} \pm \sqrt{\frac{\mu - (c_c - \frac{b_c^2}{4a_c})}{a_c}} \qquad (7.10)$$

The sign of the last term in (7.10) is determined by the curve shape of the defined

quadratic function. Thus, the total operational cost TOC can be calculated as

$$TOC(P_G, \mu) = FC(P_G) + WC(P_G, \mu) \tag{7.11}$$

2. Problem constraints

Due to the physical or operational limits in practical systems, there is a set of constraints that should be satisfied throughout the system operations for a feasible solution.

- Constraint 1: Generation capacity constraint

  For normal system operations, real power output of each generator is restricted by lower and upper bounds as follows:

  $$P_{Gi}^{min} \leq P_{Gi} \leq P_{Gi}^{max} \tag{7.12}$$

  where P_{Gi}^{min} and P_{Gi}^{max} are the minimum and maximum power from generator i, respectively.

- Constraint 2: Power balance constraint

  The total power generation and the wind power must cover the total demand P_D and the real power loss in transmission lines P_L. For the linear membership function, this relation can be represented by

  $$\sum_{i=1}^{M} P_{Gi} + W_{max} - \mu * \Delta W = P_D + P_L \tag{7.13}$$

  For the quadratic membership function, the relation can be expressed by

  $$\sum_{i=1}^{M} P_{Gi} - \frac{b_w}{2a_w} \pm \sqrt{\frac{\mu - (c_w - \frac{b_w^2}{4a_w})}{a_w}} = P_D + P_L \tag{7.14}$$

  The sign of the last term of the left-hand side in (7.14) is determined by the

curve shape of the defined quadratic function. The transmission losses can be calculated based on the Kron's loss formula as follows:

$$P_L = \sum_{i=1}^{M} \sum_{j=1}^{M} P_{Gi} B_{ij} P_{Gj} + \sum_{i=1}^{M} B_{0i} P_{Gi} + B_{00} \tag{7.15}$$

where B_{ij}, B_{0i}, B_{00} are the transmission network power loss **B**-coefficients. It should be noted that the transfer loss of the wind power is not considered in this study.

- Constraint 3: Available wind power constraint

  The wind power used for dispatch should not exceed the available wind power from the wind park:

$$0 \leq P_D + P_L - \sum_{i}^{M} P_{Gi} \leq W_{av} \tag{7.16}$$

- Constraint 4: Security level constraint

  From the definition of membership function shown from (7.1) to (7.4), the values of μ should be within the interval of $[0, 1]$:

$$0 \leq \mu \leq 1. \tag{7.17}$$

3. Problem statement

In summary, the objective of economic power dispatch optimization considering wind penetration is to minimize $R(\mu)$ and $TOC(P_G, \mu)$ simultaneously subject to the constraints (7.12)–(7.17).

D. The Proposed Approach

Usually, traditional gradient-based optimization methods deal with multi-objective optimization problems by allocating weights to each of the objectives, which indicate their importance in the overall problem. However, it is often hard to find weights which can accurately reflect the real-life situation. Moreover, it is highly possible that these methods are not capable of detecting solutions lying in concave regions of the Pareto front [60]. Meta-heuristics such as evolutionary optimization techniques are especially suited to handle the multi-objective optimization problems since they are able to search simultaneously for multiple Pareto-optimal solutions. A set of Pareto-optimal solutions is derived during the optimization, in which each cost is found so that the whole set is no worse than any other set of solutions. In this research, an enhanced multi-objective optimization particle swarm optimization algorithm is designed to resolve the target power dispatch problem.

The standard PSO algorithm [8], [59] is not suited to resolve multi-objective optimization problems in that no absolute global optimum exists there, but rather a set of non-dominated solutions. Thus, to render the PSO algorithm capable of dealing with MO problems, some modifications become necessary. Parsopoulos and Vrahatis [60] used the weighted aggregation approach to handle MO problems by converting multiple objectives into a single one. The weights can be fixed or adaptive in the optimization. To approximate the Pareto front, the algorithm needs to run multiple times. Hu and Eberhart [61] proposed a dynamic neighborhood strategy which uses one-dimension optimization to cope with multiple objectives. Later, Hu, Eberhart, and Shi [62] modified this method by introducing an extended memory which stores the global Paerto-optimal solutions in order to reduce the computational cost. Coello Coello and Lechuga [63] present an MOPSO which maintains the previously found

non-dominated solutions. These solutions serve as the guides for the flight of particles. Mostaghim and Teich [64] proposed a sigma method, which adopts the best local guides for each particle to promote the convergence and diversity of the MOPSO approach.

When using stochastic search based algorithms to optimize multi-objective problems, two key issues usually arise in the algorithm design. First, the fitness evaluation should be suitably designed to guide the search toward the set of Pareto-optimal solutions. Second, the diversity of the population should be maintained by refraining the search from premature convergence. In this study, the classic PSO algorithm is revised accordingly to facilitate a multi-objective optimization approach. Meanwhile, local search and other mechanisms are incorporated to improve its performance which leads to a memetic algorithm termed multi-objective memetic particle swarm optimization (MOMPSO) [65]. A "meme" refers to a unit of cultural evolution capable of conducting local refinements. That is, individual could improve itself prior to communicating with the population it is in. Combining local search into traditional heuristic optimization methods has turned out to be able to achieve orders of magnitude faster search for some problem domains.

1. Multi-objective PSO framework

Most practical engineering optimization problems are concerned with several criteria or design objectives. Very often, these objectives are conflicting with each other. Thus, for such problems, the optimization design is essentially to find the best feasible design which optimizes the opposing objectives simultaneously while satisfying the constraints imposed. This type of problem is known as a multi-objective (or multi-criteria, or vector) optimization problem. In Multi-Objective (MO) optimization problems, the solution is called a Pareto-optimal set. A set of points is said to be

Pareto-optimal if any improvement in one of the objectives inevitably leads to the deterioration of at least one of the other objectives. In most situations, the Pareto-optimal set is on the boundary of the feasible region.

Let's assume that a set of variables $x_i, i = 1, ..., M$, is the decision variables for an optimization problem. In order to measure the goodness of a certain solution, some criteria for evaluating the solution quality should be defined. These criteria are expressed as a set of functions $f_1(x), \ldots, f_j(x), \ldots, f_P(x)$ of the decision variables, which are called objective functions. Oftentimes, some of them are contradicting with others. The constraints specify the feasible region X and any point x in X defines a feasible solution. It is impossible that all the $f_j(x), j = 1, \ldots, P$ values have an optimum in X at a common point x. Certain criteria should be developed to determine an optimal solution in this circumstance. One interpretation of the term optimum in the multi-objective optimization scenarios is the Pareto-optimum, which are highly associated with the concept of *dominance*. A solution x_1 dominates a solution x_2 if and only if the two following conditions are satisfied at the same time: Firstly, x_1 is no worse than x_2 in all objective evaluations, i.e., $f_j(x_1) \leq f_j(x_2)$ for all $j = 1, \ldots, P$. Secondly, x_1 is strictly better than x_2 in at least one objective, i.e., $f_j(x_1) < f_j(x_2)$ for at least one $j \in \{1, \ldots, P\}$. As a result, in a set of Pareto-optimal solutions, there is no solution which dominates another with respect to all the design objectives involved. It should be noted that multi-objective optimization needs a decision-making process as there is not a single solution but a set of non-dominated solutions from which the best should be chosen. That is, the major two tasks of MO optimization are to obtain a representative set of non-dominated solutions and then select a suitable solution from this set based on the specific criterion. In this study, the standard PSO algorithm is improved and extended to handle the stochastic EED application, which is essentially an MO problem. The framework of the whole PSO

algorithm can be illustrated as follows:

---

1 $A := \emptyset$;

2   **for** $i=1$ **to** N **do**

3 $\{x_i, v_i, gbest_i, pbest_i\} :=$ *Initialization()*;

4   **end**

5   **for** $t=1$ **to** $iter$ **do**

6   **for** $i=1$ **to** N **do**

7   **for** $d=1$ **to** M **do**

8 $v_{id} := wv_{id} + c_1 r_1 (P_{id} - x_{id}) + c_2 r_2 (G_{id} - x_{id})$;

9 $x_{id} := x_{id} + \chi v_{id}$;

10   **end**

11 $x_i :=$ *CheckConstraints* (x_i);

12   **if** $x_i \not\preceq a \; \forall a \in A$ **then**

13 $A := \{a \in A | a \not\prec x_i\}$;

14 $A := A \cup x_i$;

15   **end**

16   **end**

17   **if** $x_i \preceq pbest_i \vee (x_i \not\prec pbest_i \wedge pbest_i \not\prec x_i)$ **then**

18 $pbest_i := x_i$;

19   **end**

20 $gbest_i :=$ *GlobalGuide* $(x_i; A)$;

21   **end**

Algorithm 2: An archive-based MOPSO algorithm

As we can see, the MOPSO algorithm is constructed based on the archiving mechanism. "A" in the above algorithm represents the archive used in the optimiza-

tion process, which stores the updated non-dominated solutions found so far. At the start of PSO, the archive is set to be empty and its contents keep being modified as the optimization proceeds by absorbing superior solutions and dumping inferior ones. In each PSO cycle, it will be updated. The archiving mechanism will be elaborated a bit later. First in Initialization(), the initialization operations are conducted. The velocity, position, and search guides are randomly set while ensuring the feasibility of the resulting solutions. The archive is also initiated to be empty. In PSO operations, the procedure CheckConstraints() is added to guarantee the feasibility of the intended solutions. GlobalGuide() is built to choose the global search guides based on the fuzzification mechanism during the optimization run. The algorithm does not terminate until the acceptable set of non-dominated solutions is found.

2.   Archiving

The Pareto-dominance concept is used to evaluate the fitness of each particle and thus determine which particles should be selected to store in the archive of non-dominated solutions. Similar to the elitism used in evolutionary algorithms and the tabu list used in tabu searches, the best historical solutions found by the population are recorded continuously in the archive in order to serve as the non-dominated solutions generated in the past. The major function of the archive is to store a historical record of the non-dominated solutions found along the heuristic search process. The archive interacts with the generational population in each iteration so as to absorb superior current non-dominated solutions and eliminate inferior solutions currently stored in the archive. The non-dominated solutions obtained at every iteration in the generational population (swarm) are compared with the contents of archive on a one-per-one basis. A candidate solution can be added to the archive if it meets any of the following conditions:

- The archive is empty;

- The archive is not full and the candidate solution is not dominated by or equal to any solution currently stored in the archive;

- The candidate solution dominates any existing solution in the archive;

- The archive is full but the candidate solution is non-dominated and is in a less crowded region than at least one solution.

Furthermore, due to the global attraction mechanism in PSO, the historical archive of previously found non-dominated solutions would make the search converge toward globally non-dominated solutions highly possible.

3. Global best selection

In MOPSO, gbest plays an important role in directing the whole swarm move toward the Pareto front. Very often, the rapid swarm converges within the intermediate vicinity of the gbest may lead to the diversity loss and premature convergence. To resolve this, Fuzzy Global Best (f-gbest) scheme [65] is adopted in this study, which is based on the concept of possibility measure to model the lack of information about the true optimality of the gbest. In this scheme, the gbest refers to the possibility of a particle at a certain location, rather than a sharp location as defined in traditional PSO algorithms. In this way, the particle velocity can be calculated as follows:

$$p_{c,d}^k = N(g_{g,d}^k, \delta) \tag{7.18}$$

$$\delta = f(k) \tag{7.19}$$

$$v_{i,d}^{k+1} = w * v_{i,d}^k + c_1 * r_1^k * (p_{i,d}^k - x_{i,d}^k) + c_2 * r_2^k * (p_{c,d}^k - x_{i,d}^k) \tag{7.20}$$

where $p_{c,d}^k$ is the dth dimension of f-gbest in cycle k. The f-gbest is represented by a normal distribution $N(p_{g,d}^k, \delta)$, where δ indicates the degree of uncertainty regarding the optimality of the gbest position. To reflect the reduction of this uncertainty as the search proceeds, δ can be defined as a nonincreasing function of the number of iterations. For instance, here $f(k)$ is defined as a simple function

$$f(k) = \begin{cases} \delta_{max}, & \text{cycles} < \xi * \text{max\_cycles} \\ \delta_{min}, & \text{otherwise} \end{cases} \tag{7.21}$$

where ξ is a user-specified parameter which affects the change of δ. We can see that the f-gbest function is designed to enable the particles to explore a region beyond that defined by the search trajectory of original PSO. f-gbest encourages global exploration at the early search stage when δ is large, and facilitates local fine-tuning at the late stage when δ decreases. Thus, this scheme tends to reduce the possibility of premature convergence as well as enhance the population diversity.

4. Local search

During the heuristic multi-objective optimization process, since the MO optimization algorithm is attempting to build up a discrete picture of a possibly continuous Pareto front, it is often desired to distribute the solutions as diversely as possible on the discovered tradeoff curve. Furthermore, the uniformity among the distributed solutions is also crucial so as to achieve consistent and smooth transition among the solution points when searching for the best compromise solution based on the particular requirements of the target problem. Therefore, to accomplish these challenges, it is highly necessary to preserve the diversity of solutions distribution during the optimization process. In this investigation, the combination of a local search termed Synchronous Particle Local Search (SPLS) [65] into MOPSO can be regarded

as an effective measure for preserving distribution diversity and uniformity as well as speeding up the search process.

SPLS carries out guided local fine-tuning so as to promote the distribution of nondominated solutions, whose computational procedure is laid out in the following [65]:

- Choose S_{LS} individuals randomly from the population.

- Choose N_{LS} non-dominated individuals with the best niche count from the archive and store them in the selection pool.

- Allocate an arbitrary non-dominated individual from the selection pool to each of the S_{LS} individuals as *gbest*.

- Allocate an arbitrary search space dimension for each of the S_{LS} individuals.

- Assimilation operation: With the exception of the assigned dimension, update the position of S_{LS} individuals in the search space with the selected *gbest* position.

- Update the position of all S_{LS} assimilated individuals using (7.18)-(7.20) along the preassigned dimension only.

5. Constraints handling

Because the standard PSO does not take into account how to deal with the constraints, the constraints handling mechanism should be added to ensure the solution feasibility in constrained optimization problems such as power dispatch. In the proposed MOMPSO, a simple constraint checking procedure called rejecting strategy is incorporated. When an individual is evaluated, the constraints are first checked to

determine if it is a feasible candidate solution. If it satisfies all of the constraints, it is then compared with the non-dominated solutions in the archive. Or else, it is dumped. The dumped individual is then replaced by a randomly created one. Here the concept of Pareto dominance is applied to determine if it is eligible to be chosen to store in the archive of non-dominated solutions. The constraint satisfaction checking scheme used in the proposed algorithm proves to be quite effective in ensuring the feasibility of the non-dominated solutions.

6. Individual (particle) representation

It is crucial to appropriately encode the individuals of the population in PSO for handling the economic dispatch application. The power output of each generating unit and the value of membership function are chosen to represent the particle position in each dimension, and positions in different dimensions constitute an individual (particle), which is a candidate solution for the target problem. The position in each dimension is real-coded. The i-th individual P_{Gi} can be represented as follows:

$$P_{Gi} = [P_{Gi1}, P_{Gi2}, \ldots, P_{Gid}, \ldots, P_{GiM}, \mu_i], i = 1, 2, \ldots, N \qquad (7.22)$$

where M is the number of generators and N is the population size; P_{Gid} is the power generated by the d-th unit in i-th individual; and μ_i is the value of the membership function in i-th individual. Thus, the dimension of a population is $N \times (M + 1)$.

7. Algorithm steps

In principle, an archive-based MOPSO algorithm can be illustrated in Figure 13. As seen from the figure, initially the population is randomly created, and then the selection pressure from the PSO algorithm drives the population move towards the better positions. At each iteration, the generational population is updated and certain elite

individuals from it are chosen to store in the elite population (archive) based on the Pareto dominance concept. It should be noted that each individual also maintains a memory which records the best positions the individual has encountered so far. The personal best for each particle is selected from this memory. Meanwhile, among the individuals stored in the archive, the global best is singled out according to our fuzzified global guide selection strategy. Both guides are then used by the PSO to steer the search to promising regions. The procedure is repeated until the maximum number of iterations is reached or the solutions cease improving for a certain number of generations. Under this framework, other multi-objective optimization algorithms can also be developed based on different meta-heuristics such as evolutionary computation, simulated annealing, and tabu search.
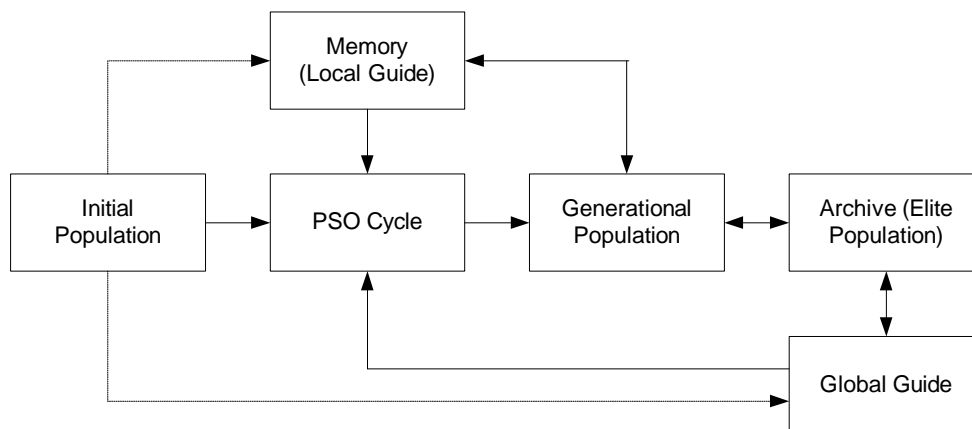

Fig. 13. Data flow diagram of the proposed algorithm

The proposed MOMPSO is applied to the constrained power dispatch problem in order to derive the optimal or near-optimal solutions. Its computational steps include:

- Step 1: Specify the lower and upper bounds of generation power of each unit as well as the range of security level.

- Step 2: Randomly initialize the individuals of the population. Note that the speed and position of each particle should be initialized such that each candidate solution (particle) locates within the feasible search space.

- Step 3: For each individual P_{Gi} of the population, the transmission loss P_{Li} is calculated based on **B**-coefficient loss formula.

- Step 4: Evaluate each individual P_{Gi} in the population based on the concept of Pareto-dominance.

- Step 5: Store the non-dominated members found thus far in the archive.

- Step 6: Initialize the memory of each particle in which a single local best *pbest* is stored. The memory is contained in another archive.

- Step 7: Increment iteration counter.

- Step 8: Choose the personal best position *pbest* for each particle based on the memory record; Choose the global best *gbest* according to the aforementioned f-gbest selection mechanism. Meanwhile, local search based on SPLS is carried out. The niching and fitness sharing mechanism is also applied throughout this process for enhancing the diversity of solutions.

- Step 9: Update the member velocity v of each individual P_{Gi}. For the output of each generator,

$$
\begin{aligned}
v_{id}^{(t+1)} &= \chi * (w * v_i^{(t)} + c_1 * \mathrm{rand}() * (pbest_{id} - P_{Gid}^{(t)}) \\
&+ c_2 * \mathrm{Rand}() * (gbest_d - P_{Gid}^{(t)})), \\
& i = 1, \ldots, N; d = 1, \ldots, M
\end{aligned}
\tag{7.23}
$$

where N is the population size, and M is the number of generating units. For the value of membership function μ,

$$
\begin{aligned}
v_{i,M+1}^{(t+1)} &= \chi * (w * v_i^{(t)} + c_1 * \text{rand}() * (pbest_{i,M+1} - \mu_i^{(t)}) \\
&+ c_2 * \text{Rand}() * (gbest_{M+1} - \mu_i^{(t)})),
\end{aligned}
\tag{7.24}
$$

- Step 10: Modify the member position of each individual P_{Gi}. For the output of each generator,

$$
P_{Gid}^{(t+1)} = P_{Gid}^{(t)} + v_{id}^{(t+1)}
\tag{7.25}
$$

For the value of membership function μ,

$$
\mu_i^{(t+1)} = \mu_i^{(t)} + v_{i,M+1}^{(t+1)}
\tag{7.26}
$$

Following this, add the turbulence factor into the current position. For the output of each generator,

$$
P_{Gid}^{(t+1)} = P_{Gid}^{(t+1)} + R_T P_{Gid}^{(t+1)}
\tag{7.27}
$$

For the value of membership function μ,

$$
\mu_i^{(t+1)} = \mu_i^{(t+1)} + R_T \mu_i^{(t+1)}
\tag{7.28}
$$

where R_T is the turbulence factor. The turbulence term is used here to enhance the diversity of solutions.

- Step 11: Update the archive which stores non-dominated solutions according to the aforementioned four Pareto-optimality based selection criteria.

- Step 12: If the current individual is dominated by the *pbest* in the memory, then keep the *pbest* in the memory; Otherwise, replace the *pbest* in the memory
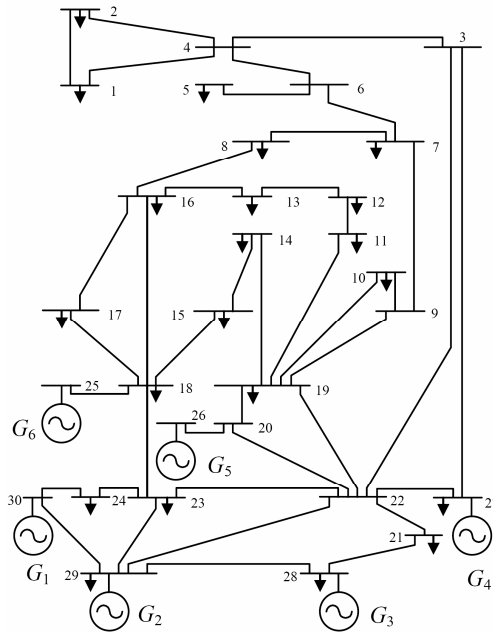
Fig. 14. IEEE 30-bus test power system

with the current individual.

- Step 13: If the maximum iterations are reached, then go to Step 14. Otherwise, go to Step 7.

- Step 14: Output a set of Pareto-optimal solutions from the archive as the final solutions.

E. Simulation and Evaluation of the Proposed Approach

In this study, a typical IEEE 30-bus test system with 6-generators is used to investigate the effectiveness of the proposed MOMPSO approach. The system configuration is shown in Figure 14. The system parameters including fuel cost coefficients and generator capacities are listed in Table XVII. The sinusoidal term in (7.6) is not considered in this study due to its relatively minor impact on the total fuel costs. The

B-coefficients are shown in (7.29). The load demand P_D used in the simulations is 2.834 p.u., the available wind power W_{av} is 0.5668 p.u., and the coefficient of penalty cost C_w is set 20 \$/p.u.

Table XVII. Fuel cost coefficients and generator capacities

Generator i	a_i	b_i	c_i	P_{Gi}^{min}	P_{Gi}^{max}
G_1	10	200	100	0.05	0.50
G_2	10	150	120	0.05	0.60
G_3	20	180	40	0.05	1.00
G_4	10	100	60	0.05	1.20
G_5	20	180	40	0.05	1.00
G_6	10	150	100	0.05	0.60

$$B_{ij} = \begin{bmatrix} 0.1382 & -0.0299 & 0.0044 & -0.0022 & -0.0010 & -0.0008 \\ -0.0299 & 0.0487 & -0.0025 & 0.0004 & 0.0016 & 0.0041 \\ 0.0044 & -0.0025 & 0.0182 & -0.0070 & -0.0066 & -0.0066 \\ -0.0022 & 0.0004 & -0.0070 & 0.0137 & 0.0050 & 0.0033 \\ -0.0010 & 0.0016 & -0.0066 & 0.0050 & 0.0109 & 0.0005 \\ -0.0008 & 0.0041 & -0.0066 & 0.0033 & 0.0005 & 0.0244 \end{bmatrix} \tag{7.29}$$

1.   Comparison of different design scenarios

Since PSO algorithms are sometimes quite sensitive to certain parameters, the simulation parameters should be appropriately chosen. In the simulations, both the population size and archive size are set to 100, and the number of generations is set

to 500. The acceleration constants c_1 and c_2 are chosen as 1. Both turbulence factor and niche radius are set to 0.02. The inertia weight factor w decreases when the number of generations increases:

$$w = w_{max} - \frac{w_{max} - w_{min}}{iter_{max}} \times iter \tag{7.30}$$

where $iter_{max}$ is the number of generations and $iter$ is the current number of iterations. From the above equation, we can appreciate that the value of w will decrease as the iteration number increases. In the search process, the most efficient way to locate the optimal or near-optimal solutions in a complex large search space is first to move to the smaller solution space as promptly as possible, and then seek out the desired solution in this space via thorough search. The parameter w is defined to regulate the size of search step of each particle. At first, the value of w is set relatively large in order to drive the particle to the solution area quickly. Then, when the particle approaches the desired solution, the size of each search step becomes smaller in order to prevent the particle from flying past the target position during the flight. In this way, the desired solutions can be sought through gradual refinement. For the f-gbest parameters, δ_{max}, δ_{min}, and ξ are chosen as 0.15, 0.0001, and 0.4, respectively. The simulation program is coded using C++ and executed in a 2.20 GHz Pentium-4 processor with 512 MB of RAM. In simulations, the minimum and maximum allowable wind power penetrations are set as 10% and 20% of the total load demand, respectively. The running cost of wind power is calculated based on its linear relationship with the amount of wind power integrated, i.e., $WC = \sigma W$. The coefficient σ indicating the running cost of wind power is set 50 \$/p.u. in the simulation. The parameters used in the simulations are listed below and different function curves are shown in Figure 15.

- Quadratic representation (optimistic design): $a_w = -9.9607$, $b_w = 4.94$, $c_w = $

0.4;

- Linear representation (neutral design): W_{min}=0.2834, W_{max}=0.5668;

- Quadratic representation (pessimistic design): $a_w = 4.9803$, $b_w = -7.7629$, $c_w = 2.8$.
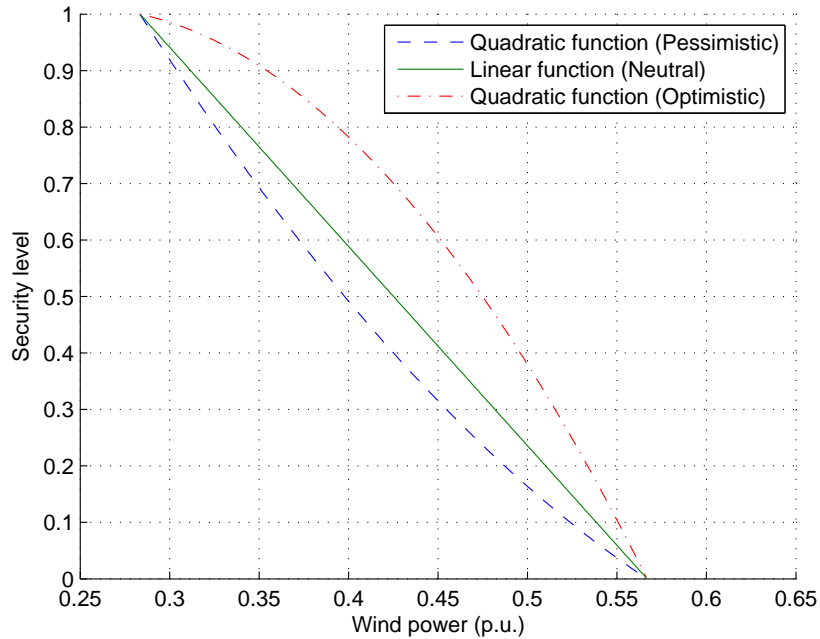
Fig. 15. Different curve shapes of membership functions

The illustrative non-dominated solutions derived in different design scenarios are listed in Table XVIII, and the Pareto-optimal fronts evolved using the proposed MOMPSO are shown in Figure 16.

As shown in the figure, the Pareto-optimal solutions are widely distributed on the tradeoff surface due to the diversity preserving mechanisms used in the proposed MOMPSO algorithm. Unlike the single-objective optimization, in multi-objective optimization the decision maker can choose a suitable solution based on his/her pref-

Table XVIII. Example solutions for different design scenarios.

Generators/objectives	Pessimistic	Linear	Optimistic
P_{G1}	0.0678	0.0500	0.0605
P_{G2}	0.2463	0.2430	0.2425
P_{G3}	0.3863	0.4029	0.4221
P_{G4}	0.9164	0.9300	0.9354
P_{G5}	0.4034	0.3990	0.3490
P_{G6}	0.3166	0.2929	0.2897
W	0.5043	0.5232	0.5408
Cost (\$/hour)	518.893	515.436	512.147
Risk level	6.5864	6.49894	6.31094

erence from a pool of non-dominated solutions. We can also appreciate that for the same risk level calculated from different membership functions, the optimistic design has the lowest operational cost since it includes the largest amount of wind power among all of the three designs. Wind power has the lowest operational cost as compared with the same amount of electric power from fuel-based generation.

2. Sensitivity analysis

Sensitivity analysis has been carried out in order to illustrate the impacts of different allowable ranges of wind power penetration as well as different running costs of wind power on the final non-dominated solutions derived. Here the linear membership function is used. We herein quantify the impact of wind penetration through numerical simulations by changing the permissible ranges of wind power penetration $[W(P_D)_{min}, W(P_D)_{max}]$. In the simulations for determining the impact of different allowable wind penetration ranges, the running cost of wind power is kept unchanged,
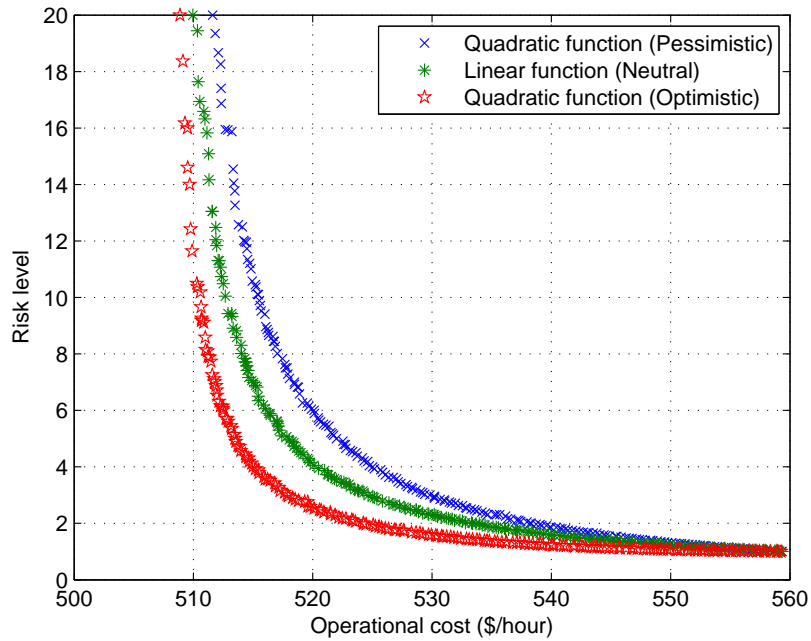
Fig. 16. Pareto fronts obtained based on different membership functions

i.e., $\sigma = 50\$/p.u.$ In a similar fashion, in the simulations for examining the impact of running costs of wind power, the penetration range of wind power is fixed, i.e., $[W(P_D)_{min}, W(P_D)_{max}] = [10\% * P_D, 20\% * P_D]$. The derived Pareto fronts are shown in Figure 17 and Figure 18, respectively. From the figures, we can appreciate that the non-dominated solutions vary with the different ranges of allowable wind penetration as well as the running costs of wind power. In Figure 17, at the same risk level, the design scenario with the largest value of maximum allowable wind penetration W_{max} has the lowest cost since the most portion of wind power is integrated. In Figure 18, at the identical risk level, the scenario with the lowest running cost of wind power results in the lowest overall cost since the same amount of wind power is integrated with the lowest cost.
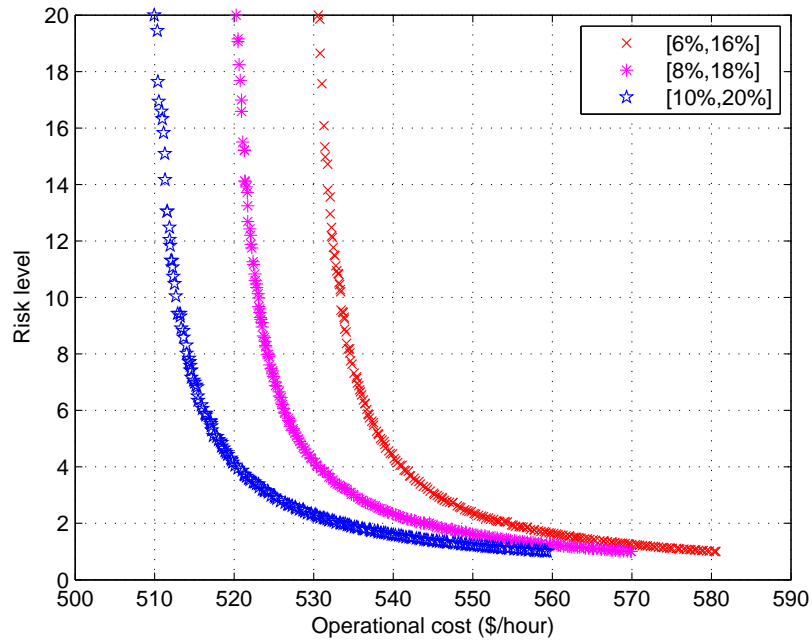
Fig. 17. Pareto fronts obtained for different wind penetration ranges

3. Comparative studies

In order to conduct a quantitative assessment of the performance of a multi-objective optimization algorithm, normally four major issues should be considered:

- Minimize the distance of the approximated Pareto front obtained from the target algorithm with respect to the true Pareto front. Since the true Pareto front is unknown in most practical problems, this requirement can be interpreted as increasing the accuracy of the obtained final solutions (i.e., to render the obtained Pareto front as close to the true one as possible).

- Maximize the spread of the obtained solutions. It means that the diversity of the solutions should be maximized in the optimization run by rendering the distribution of the solutions as smooth and even as possible. Thus, the decision-
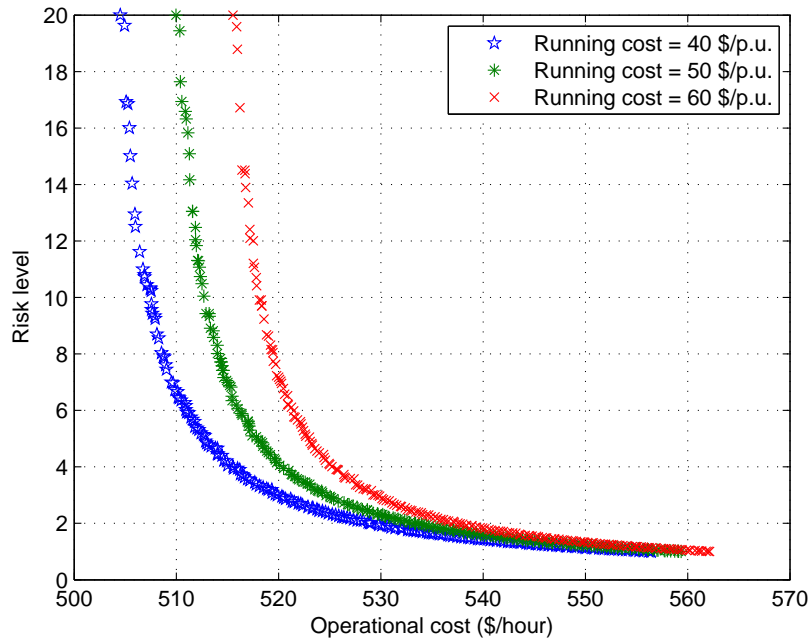
Fig. 18. Pareto fronts obtained for different running costs of wind power

maker will have more choices for different demands on decision.

- Maximize the number of elements of the Pareto-optimal set. The extent of the estimated Pareto front should be increased, i.e., a wide range of non-dominated solutions in objective space should be derived by the optimizer. For each objective, a sufficiently wide range of values should be covered by the non-dominated solutions.

- Minimize the computational cost. Most of the MO optimization algorithms are computationally expensive, thus the computational time is an important criterion for measuring the efficacy of an algorithm in dealing with such problems.

Thus, certain quantitative metrics need to be defined in order to compare the performance of different MO algorithms in a more objective fashion. A comparative

study is conducted to examine how competitive the proposed approach is in dealing with the target problem. Comparison of Pareto front estimates is not a easy task since it is unlikely to evaluate the quality of a Pareto front using any single measure. Here, we use four measures to comprehensively assess the performance of different optimizers in terms of accuracy, diversity, extent, and computational economy. Note that all the following comparisons are conducted based on the neutral design scenario with the original design parameters.

- **C-metric**: C-metric is quite often used to examine the quality of the Pareto fronts obtained [66]. Let $S_1, S_2 \subseteq S$ be two sets of decision solutions. The C-metric is defined as the mapping between the ordered pair (S_1, S_2) and the interval $[0, 1]$:

$$C(S_1, S_2) = \frac{|\{a_2 \in S_2; \exists a_1 \in S_1 : a_1 \preceq a_2\}|}{|S_2|} \tag{7.31}$$

  Provided that $C(S_1, S_2) = 1$, all solutions in S_2 are dominated by or equal to solutions in S_1. If $C(S_1, S_2) = 0$, then none of the solutions in S_2 are covered by S_1. Both $C(S_1, S_2)$ and $C(S_2, S_1)$ should be checked in the comparison since C-metric is not symmetrical in its arguments, i.e., the equation $C(S_1, S_2) = 1 - C(S_2, S_1)$ does not necessarily always hold. Table XIX illustrates the comparison of C-metric for different algorithms, where "O", "F", "S", and "M" indicate the original MOPSO, MOPSO only with f-gbest selection, MOPSO only with SPLS, and MOMPSO, respectively.

- **Spacing**: The spacing metric is defined to measure the spread of the non-dominated solutions. For instance, one of such metrics is to measure the range variance of neighboring individuals in the set of non-dominated solutions [67].

Table XIX. Comparison of C-metric for different algorithms

	C(M, O)	C(O, M)	C(M, F)	C(F, M)	C(M, S)	C(S, M)
Best	1.0	0.1001	1.0	0.1427	1.0	0.1503
Worst	0.9899	0.0	0.9890	0.0	0.9811	0.0
Average	0.9993	0.0001	0.9905	0.0002	0.9880	0.0005
Median	0.9995	0.0001	0.9928	0.0002	0.9882	0.0005
Std. Dev.	0.0001	0.0001	0.0009	0.0001	0.0010	0.0002

It is defined as

$$SP = \sqrt{\frac{1}{n-1}\sum_{i=1}^{n}(\overline{d} - d_i)^2} \tag{7.32}$$

where $d_i = \min_j(|f_1^i(\overrightarrow{x}) - f_1^j(\overrightarrow{x})| + |f_2^i(\overrightarrow{x}) - f_2^j(\overrightarrow{x})|)$, $i, j = 1, \ldots, n$, $\overline{d}$ is the mean of all d_i, and n is the number of non-dominated solutions found so far. The larger the value is, the more unevenly the solution members are spaced. If the value of SP is zero, all members in the Pareto front are equidistantly distributed. Table XX illustrates the comparison of the spacing metric for different algorithms. For simplicity of notation, here f-gbest is used to denote the MOPSO only with f-gbest and SPLS represents the MOPSO only with SPLS.

Table XX. Comparison of the spacing metric for different algorithms

Spacing	MOPSO	f-gbest	SPLS	MOMPSO
Best	0.0489	0.0403	0.0397	0.0389
Worst	0.1077	0.0996	0.0988	0.0767
Average	0.0526	0.0422	0.0418	0.0402
Median	0.0521	0.0412	0.0410	0.0375
Std. Dev.	0.2562	0.1131	0.0988	0.0612

- **Error ratio**: The metric termed error ratio was proposed by Van Veldhuizen [68] to indicate the percentage of solutions that are not members of the Pareto-optimal set. It is given as

$$ER = \frac{\sum_{i=1}^{n} e_i}{n} \tag{7.33}$$

where n is the number of solutions in the current set of non-dominated solutions. If vector i belongs to the Pareto-optimal set, then $e_i = 0$; or else $e_i = 1$. It is evident that if $ER = 0$, all the solutions derived from the optimizer are members of the Pareto-optimal set. Table XXI illustrates the comparison of the error ratio metric for different algorithms.

Table XXI. Comparison of the error ratio metric for different algorithms

Error ratio	MOPSO	f-gbest	SPLS	MOMPSO
Best	0.0051	0.0	0.0	0.0
Worst	0.3698	0.2899	0.2640	0.2486
Average	0.2305	0.1196	0.1181	0.1030
Median	0.2209	0.1090	0.1086	0.0980
Std. Dev.	0.2253	0.1643	0.1904	0.1088

- **Computational time**: Under the exactly identical environments including both hardware and software platforms, different algorithms are compared in terms of the CPU time consumed in obtaining their corresponding Pareto fronts. Table XXII illustrates the time needed for obtaining 100 mutually non-dominated solutions for different algorithms.

From the above comparative studies, we can find the following three major advantages of the solutions obtained by MOMPSO with respect to those derived from the other three algorithms:

Table XXII. Comparison of computational time for different algorithms (in seconds)

CPU time	MOPSO	f-gbest	SPLS	MOMPSO
Best	15.2	14.9	12.8	11.2
Worst	19.9	17.9	16.4	12.5
Average	17.5	16.0	13.1	11.7
Median	17.9	16.4	13.4	11.6
Std. Dev.	0.1024	0.0549	0.0602	0.0121

- Higher quality solutions are obtained using the MOMPSO. In the set of solutions obtained using MOMPSO, most of them have better objective function values than those derived from other approaches.

- The solutions of MOMPSO have better diversity characteristics. This is primarily due to the several diversity retention mechanisms used:

  - A useful distribution preservation measure adopted in this study is the fuzzification mechanism used during the selection of global guide for each particle in every generation;

  - A local search scheme termed Synchronous Particle Local Search (SPLS) is integrated into the original MOPSO in order to enhance the population diversity and expedite the convergence speed;

  - Niching and fitness sharing is used to preserve the population diversity by preventing the population from falling into the detrimental genetic drift;

  - In the archiving process, the individuals lying in less populated regions of the objective have higher chance to be chosen than those in the highly populated areas;

– A turbulence factor is added to the PSO operations, which may increase the solution diversity by enhancing the randomness in a particle's movements.

The diversity is preserved by MOMPSO while there is no guarantee that the solutions obtained by objective aggregation approach will span over the entire tradeoff surface.

- The computational time of MOMPSO is less than the other methods. The SPLS mechanism incorporated reduces the computational expense due to its capability of facilitating convergence speedup.

F. Summary

This chapter investigates the integration of wind power into conventional power networks and its impact on generation resource management. Wind power is environmentally friendly since it is able to reduce the fossil fuel and natural gas consumption. Also, wind power needs less operational cost since it does not consume fossil fuels and natural gases. However, due to the intermittent and variable nature of the wind power, it is usually quite difficult to determine how much wind power should be integrated to ensure both power system security and operational cost reduction. In this chapter, fuzzy representations of system security in terms of wind power penetration level and operational costs are adopted in constructing economic dispatch models. A multi-objective memetic particle swarm optimization (MOMPSO) algorithm is developed to derive the non-dominated Pareto-optimal solutions in terms of the specified multiple design objectives. Different design scenarios can be formulated according to dispatcher's attitudes toward wind power integration with respect to risk and cost. A numerical application example is used to illustrate the validity and applicability of the developed optimization procedure. In the further investigations, probabilis-

tic methods may also be adopted to handle various uncertainties in power systems including wind power penetration.

CHAPTER VIII

MULTI-CRITERIA DESIGN OF HYBRID POWER GENERATION SYSTEMS

BASED ON A MODIFIED PARTICLE SWARM OPTIMIZATION ALGORITHM

Multi-source hybrid power generation systems are a type of representative applications of the renewables' technology. In this investigation, wind turbine generators, photovoltaic panels, and storage batteries are used to build hybrid generation systems which are optimal in terms of multiple criteria including cost, reliability, and emissions. Multi-criteria design facilitates the decision-maker to make more rational evaluations. In this study, an improved particle swarm optimization algorithm is developed to derive these non-dominated solutions. Hybrid generation systems under different design scenarios are designed based on the proposed approach. First, a grid-linked hybrid system is designed without incorporating system uncertainties. Then, adequacy evaluation is conducted based on probabilistic methods by accounting for equipment failures, time-dependent sources of energy, and stochastic generation/load variations. In particular, due to the unpredictability of wind speed and solar insolation as well as the random load variation, time-series models are adopted to reflect their stochastic characteristics. An adequacy evaluation procedure including time-dependent sources is adopted. Sensitivity studies are also carried out to examine the impacts of different system parameters on the overall design performance.

A. Introduction

With the increasing concerns on air pollution and global warming, the clean green renewable sources of energy are expected to play more significant role in the global energy future [5], [36], [77]. Most of them are environmentally benign and do not contribute to the atmospheric pollution, acid rain, and global climate warming. Fur-

thermore, due to public support and government incentives over recent decades, they are growing rapidly, not only in technical performance, but also in the breadth of applications. The public attention has remained focused on these renewable technologies as environmentally sustainable and convenient alternatives. Among them, wind power and solar power are the two most widely used renewable sources of energy since they feature certain merits as compared with the conventional fossil-fuel-fired generation. For instance, wind turbine generators (WTGs) generate no pollution and they do not consume depleting fossil-fuels. Photovoltaic (PV) systems produce no emissions, are durable, and demand minimal maintenance to operate. Unfortunately, these renewable sources of energy are essentially intermittent and quite variable in their output. Also, they require high capital costs. Thus, it is possible that power fluctuations will be incurred since both power sources are highly dependent on the weather conditions [76]. To mitigate or even cancel out the fluctuations, energy storage technologies such as storage batteries (SBs) can be employed. SBs may absorb the surplus power and provide the deficit power in different operating situations [71], [72]. As a result, hybrid generation systems have attracted much attention [74], [75], [78]–[81]. However, besides the fluctuations of time-dependent sources, there are various uncertainties existing in operations of such hybrid systems, e.g., possible equipment failures and stochastic generation/load variations. Therefore, reliability evaluation for the intended system using probabilistic methods is highly desired. In this investigation, adequacy evaluation theory is used in the design to ensure the system reliability in the presence of generating-unit malfunctions. To reflect the stochastic characteristics of wind and solar power, an autoregressive moving average (ARMA) time series is used to model the wind speed and solar insolation in different time instants. Furthermore, autoregressive integrated moving average (ARIMA) time series is used to model the random variation of load demand. In this way, various uncertainties

including equipment failures and random generation/load variations are taken into account in the system design, which is expected to enhance system reliability in the face of different uncertainties.

In this chapter, we employ a multi-criteria approach to handle hybrid system design problems by taking into account multiple design objectives including economics, reliability, and pollutant emissions. Multi-criteria design helps the decision-maker reflect upon, articulate, and apply value judgments to determine reasonable trade-offs and thus lead to recommendations of corresponding alternatives [70], [82]. Thus, multi-criteria design provides a viable way to reach tradeoffs among these design objectives with different preferences. Also, due to the high complexity and high non-linearity of the design problem, a metaheuristics called particle swarm optimization (PSO) is adopted and improved accordingly in order to derive a set of non-dominated solutions with sufficient diversity for decision-making support. PSO has turned out to be an outstanding optimizer due to its ability to elegantly handle difficult optimization problems as well as its exceptional convergence performance.

The remainder of the chapter is organized as follows. Section B formulates the hybrid system design problem including its multiple objectives coupled with a set of design constraints. The proposed multiobjective particle swarm optimization (MOPSO) algorithm is detailed in Section C. Simulation results and sensitivity studies for designing grid-linked hybrid systems without and with system uncertainties consideration are presented in Section D and Section E, respectively. Finally, conclusions are drawn and future research direction is suggested.

B.   Problem Formulation

As shown in Figure 19, a typical hybrid generation system comprises different power sources including wind turbine generators (WTGs), PV panels (PVs), and storage batteries (SBs). These power sources have different impacts on cost, environment, and reliability. In a hybrid generation system, they are integrated together and complement one another in order to serve the load while satisfying certain economic, environmental, and reliability criteria. The hybrid system can be operated autonomously or connected to the utility grid whose power is from the conventional fossil-fuel-fired generators (FFGs). Due to space restrictions, here only grid-linked system designs will be discussed. The multi-criteria design of a stand-alone hybrid generation system can be referred to [83].
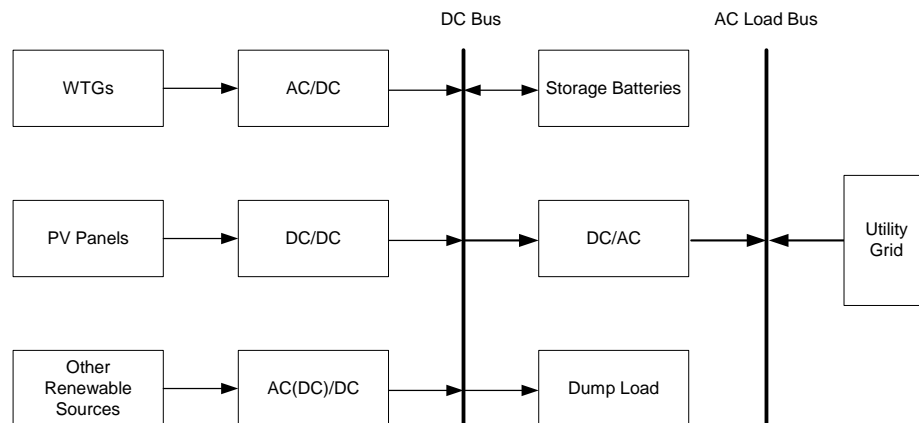

Fig. 19. Configuration of a typical hybrid generation system

The objective of this study is to achieve hybrid generation systems, which should be appropriately designed in terms of economic, reliability, and environmental measures subject to physical and operational constraints/strategies. Two design scenarios are investigated, i.e., grid-linked hybrid generation systems without and with uncertainties consideration. Here we start with the discussion of a hybrid system design

without considering uncertainties. That is, neither generator failures nor stochastic generation/load variations is considered in the design. Some of the calculations formulated in this section are applicable to the hybrid system design incorporating adequacy evaluation including uncertainties discussed in Section F.

1. Design objectives

- Objective 1: Costs

Proper cost estimation is crucial to the success of projects like hybrid generation system design [74], [75]. In this study, the total cost $COST(\$/year)$ includes initial cost, operational and maintenance (OM) cost for each type of power source, and the salvage value of each equipment should be deducted:

$$COST = \frac{\sum_{i=w,s,b}(I_i - S_{P_i} + OM_{P_i})}{N_p} + C_g \qquad (8.1)$$

where w, s, b indicates the wind power, solar power, and battery storage, respectively; I_i, S_{P_i}, OM_{P_i} are the initial cost, present worth of salvage value, and present worth of operation and maintenance cost for equipment i, respectively; $N_p(year)$ is the life span of the project; and C_g is the annual cost for purchasing power from the utility grid. Here we assume that the life time of the project does not exceed those of both WTGs and PV arrays.

1) For the WTGs,

$$I_w = \alpha_w A_w \qquad (8.2)$$

where $\alpha_w(\$/m^2)$ is the initial cost of WTGs; the present worth of the total salvage value is

$$S_{P_w} = S_w A_w \left(\frac{1+\beta}{1+\gamma}\right)^{N_p} \qquad (8.3)$$

where $S_w(\$/m^2)$ is the salvage value of WTGs per square meter, β and γ are the inflation rate and interest rate, respectively; the present worth of the total operation and maintenance cost (OM) in the project life time is

$$OM_{P_w} = \alpha_{OM_w} * A_w * \sum_{i=1}^{N_p} (\frac{1+\nu}{1+\gamma})^i \tag{8.4}$$

where $\alpha_{OM_w}(\$/m^2/year)$ is the yearly OM cost per unit area and ν is the escalation rate.

2) For the PV panels, the initial cost is

$$I_s = \alpha_s A_s \tag{8.5}$$

where $\alpha_s(\$/m^2)$ is the initial cost; the present worth of the total salvage value is

$$S_{P_s} = S_s A_s (\frac{1+\beta}{1+\gamma})^{N_p} \tag{8.6}$$

where $S_s(\$/m^2)$ is the salvage value of PVs per square meters of PV panels; the present worth of the total operation and maintenance cost (OM) in the project life time is

$$OM_{P_s} = \alpha_{OM_s} * A_s * \sum_{i=1}^{N_p} (\frac{1+\nu}{1+\gamma})^i \tag{8.7}$$

where $\alpha_{OM_s}(\$/m^2/year)$ is the yearly OM cost per unit area and ν is the escalation rate.

3) For the storage batteries, since their life span is usually shorter than that of the project, the total present worth of capital investments can be calculated as

follows:

$$I_b = \alpha_b * P_{b_{cap}} * \sum_{i=1}^{X_b} (\frac{1+\nu}{1+\beta})^{(i-1)N_b} \qquad (8.8)$$

where N_b is the life span of SBs; X_b is the number of times to purchase the batteries during the project life span N_p; the salvage value of SBs is ignored in this study; and the present worth of the total OM cost in the project life time is calculated as follows:

$$OM_{p_b} = \alpha_{OM_b} * P_{b_{cap}} * \sum_{i=1}^{N_p} (\frac{1+\nu}{1+\gamma})^i \qquad (8.9)$$

where $\alpha_{OM_b}(\$/kWh/year)$ is the yearly OM cost per kilowatthour.

4) For the grid-linked system design, the annual cost for purchasing power from the utility grid can be calculated as follows:

$$C_g = \sum_{t=1}^{T} P_{g,t} * \varphi \qquad (8.10)$$

where $P_{g,t}(\$/year)$ is the power purchased from the utility at hour t; $\varphi(\$/kWh)$ is the grid power price; and T (8760 hours) is the operational duration under consideration.

- Objective 2: Reliability

Reliability is used to assess the quality of load supply. Here Energy Index of Reliability (EIR) is used to measure the reliability of each candidate hybrid system design. EIR can be calculated from Expected Energy Not Served (EENS) as follows:

$$EIR = 1 - \frac{EENS}{E} \qquad (8.11)$$

The $EENS(kWh/year)$ for the duration under consideration T (8760 hours)

can be calculated as follows:

$$EENS = \sum_{t=1}^{T}(P_{b_{min}} - P_{b_{soc}}(t) - P_{sup}(t)) * U(t) \qquad (8.12)$$

where $U(t)$ is a step function, which is zero when the supply exceeds or equals to the demand, and equals to one if there is insufficient power in period t; $P_d(t)$ is the load demand during hour t, $P_{sup}(t) = P_{total}(t) - P_d(t)$ is the surplus power in hour t, $P_{total}(t)$ is the total power from WTGs, PVs, and FFGs during hour t:

$$P_{total}(t) = P_w(t) + P_s(t) + P_g(t) \qquad (8.13)$$

$P_{b_{soc}}(t)$ is the battery charge level during hour t, and $P_{b_{min}}$ is the minimum permitted storage level, the term $P_{b_{soc}}(t) - P_{b_{min}}$ indicates the available power supply from batteries during hour t; and provided that there is insufficient power in hour t,

$$P_g(t) = \kappa * (P_d(t) - P_w(t) - P_s(t) - P_b(t)) \qquad (8.14)$$

where $\kappa \in [0, 1]$ indicates the portion of purchased power with respect to the hourly insufficient power; or else, $P_g(t) = 0$. Note that no equipment failures and unexpected load deviations are considered in calculating the EENS, which in this design is all contributed by the fluctuations of renewable power generation.

- Objective 3: Pollutant emissions

  With the increasing concerns on environment protection, there are stricter regulations on pollutant emissions. The most important emissions considered in the power generation industry due to their highly damaging effects on the ecological environment are sulfur dioxide (SO_2) and nitrogen oxides (NO_x). These emissions can be modeled through functions that associate emissions with power production for generating units. They are dependent on fuel consumption and

take the quadratic form:

$$PE = \alpha + \beta * \sum_{t=1}^{T} P_{g,t} + \gamma * (\sum_{t=1}^{T} P_{g,t})^2 \qquad (8.15)$$

where α, β, and γ are the coefficients approximating the generator emission characteristics.

2.   Design constraints

Due to the physical or operational limits of the target system, there is a set of constraints that should be satisfied throughout system operations for any feasible solution.

- Constraint 1: Power balance constraint

  For any period t, the total power supply from the hybrid generation system must supply the total demand P_d with a certain reliability criterion. This relation can be represented by

$$P_w(t) + P_s(t) + P_b(t) + P_g(t) \geq (1 - R)P_d(t) \qquad (8.16)$$

$$P_w(t) + P_s(t) + P_b(t) + P_g(t) - P_{dump}(t) \leq P_d(t) \qquad (8.17)$$

  where P_w, P_s, P_b, P_g, $P_{dump}(t)$, and P_d are the wind power, solar power, charged/discharged battery power, power bought from grid, dumped power, and total load demand, respectively; R is the ratio of the maximum permissible unmet power with respect to the total load demand in each time instant. The transmission loss is not considered in this investigation.

  The output P_{WTG} (kW/m^2) from WTGs for wind speed V_t can be calculated

as

$$P_{WTG} = \begin{cases} 0, & V_t < V_{ci} \\ a * V_t^3 - b * P_r, & V_{ci} \leq V_t < V_r \\ P_r, & V_r \leq V_t \leq V_{co} \\ 0 & V_t > V_{co} \end{cases} \tag{8.18}$$

where $a = \frac{P_r}{V_r^3 - V_{ci}^3}$, $b = \frac{V_{ci}^3}{V_r^3 - V_{ci}^3}$, P_r is the rated power, V_{ci}, V_r, and V_{co} are the cut-in, rated, and cut-out wind speed, respectively. The real electric power from WTGs can be calculated as follows:

$$P_w = P_{WTG} * A_w * \eta_w \tag{8.19}$$

where A_w is the total swept area of WTGs and η_w is the efficiency of WTGs.

The output power $P_s(kW)$ from PV panels can be calculated as follows:

$$P_s = H * A_s * \eta_s \tag{8.20}$$

where $H(kW/m^2)$ is the horizontal irradiance, A_s is the PV area, and η_s is the efficiency of PV panels.

- Constraint 2: Bounds of design variables

The swept area of WGTs should be within a certain range:

$$A_{w_{min}} \leq A_w \leq A_{w_{max}} \tag{8.21}$$

Similarly, the area of PV arrays should also be within a certain range:

$$A_{s_{min}} \leq A_s \leq A_{s_{max}} \tag{8.22}$$

The state of charge (SOC) of storage batteries $P_{b_{soc}}$ should not exceed the capacity of storage batteries $P_{b_{cap}}$ and should be larger than the minimum permissible

storage level $P_{b_{min}}$; the total SB capacity should not exceed the allowed storage capacity $P_{b_{cap}max}$; and the hourly charge or discharge power P_b should not exceed the hourly inverter capacity $P_{b_{max}}$. As a result,

$$P_{b_{min}} \leq P_{b_{soc}} \leq P_{b_{cap}} \tag{8.23}$$

$$0 \leq P_{b_{cap}} \leq P_{b_{cap}max} \tag{8.24}$$

$$P_b \leq P_{b_{max}} \tag{8.25}$$

The amount of power bought from utility grid should be within a certain range:

$$P_{g_{min}} \leq \sum_{t=1}^{T} P_{g,t} \leq P_{g_{max}}, \tag{8.26}$$

where $P_{g_{min}}$ and $P_{g_{max}}$ are the minimum and maximum power allowed to be bought from the utility grid, respectively.

The coefficient κ indicates the portion of purchased power from utility grid with respect to the insufficient power:

$$0 \leq \kappa \leq 1 \tag{8.27}$$

3.   Problem statement

In summary, for this grid-linked system design, the objective of optimum design for renewable hybrid generation system is to simultaneously minimize $COST(A_w, S_w, P_{b_{cap}}, \kappa)$ and $E(A_w, S_w, P_{b_{cap}}, \kappa)$, as well as maximize $EIR(A_w, S_w, P_{b_{cap}}, \kappa)$, subject to the constraints (8.16)–(8.27). The design parameters that should be derived include WTG swept area $A_w(m^2)$, PV area $A_s(m^2)$, total battery capacity $P_{b_{cap}}(kWh)$, and the ratio of power purchased from grid κ.

4. Operation strategies

The power outputs from WTGs and PVs have the highest priorities to feed the load. Only if the total power from wind and solar systems is insufficient to satisfy the load demand, the storage batteries can be discharged a certain amount of energy to supply the load. If there is still not enough power to supply the load, a certain amount of power will be purchased from the utility grid. That is, the grid power has the lowest priority to feed the load. Furthermore, if there is any excess power from WTGs and PVs, the batteries will be charged to store a certain permissible amount of energy for future use. If there is surplus power from WTGs and PVs even after feeding the load and charging the SBs, the dump load will consume the spilled power.

C. The Proposed Approach

In this study, a Constrained Mixed-Integer Multi-Objective PSO (CMIMOPSO) is developed to derive a set of non-dominated solutions by appropriately combining different sources of energy subject to certain constraints.

1. CMIMOPSO

- Mixed-integer PSO: Since the target problem involves optimization of system configuration, integer numbers are used to indicate the unit sizing. The standard PSO is in fact a real-coded algorithm, thus some revisions are needed to enable it to deal with the binary-coded optimization problem. In the discrete binary PSO [32], the relevant variables are interpreted in terms of changes of probabilities. A particle flies in a search space restricted to zero and one in each direction and each v_{i_d} represents the probability of member x_{i_d} taking value 1. The update rule governing the particle flight speed can be modified accordingly by

introducing a logistic sigmoid transformation function:

$$S(v_{i_d}) = \frac{1}{1 + e^{-v_{i_d}}} \qquad (8.28)$$

The velocity can be updated according to this rule: If $rand() < S(v_{i_d})$, then $x_{i_d} = 1$; or else $x_{i_d} = 0$. The maximum allowable velocity V_{max} is desired to limit the probability that member x_{i_d} will take a one or zero value. The smaller the V_{max} is, the higher the chance of mutation is for the new individual.

- Multi-objective PSO: In this study, since a multi-objective optimization problem is concerned, the standard PSO algorithm is also modified accordingly to facilitate a multi-objective optimization approach, i.e., multi-objective particle swarm optimization (MOPSO). The Pareto-dominance concept is used to appraise the fitness of each particle and thus determine which particles should be chosen as the non-dominated solutions. For this purpose, the archiving mechanism is used to store the non-dominated solutions throughout the optimization process. The best historical solutions found by the optimizer are absorbed continuously into the archive as the non-dominated solutions generated in the past. Furthermore, to enhance the solution diversity, some diversity preserving measures such as fuzzified global best selection, and niching and fitness sharing are taken [84].

- Constrained PSO: In the proposed method, a natural constraint checking procedure called rejecting strategy is adopted to deal with the imposed constraints. When an individual is evaluated, the constraints are first checked to determine if it is a feasible candidate solution. If it satisfies all of the constraints, it is then compared with the non-dominated solutions in the archive. The concept of Pareto dominance is applied to determine if it is eligible to be chosen to

store in the archive of non-dominated solutions. As long as any constraint is violated, the candidate solution is deemed infeasible. This procedure is simple to implement, but it turned out to be quite effective in ensuring the solution feasibility while not significantly decreasing the search efficiency.

2. Representation of candidate solutions

The design variables including WTG swept area, PV area, amount of power purchased from the grid, and total SB capacity are encoded as the position value in each dimension of a particle. Several member positions indicate the coordinate of the particle in a multi-dimensional search space. Each particle is considered as a potential solution to the optimal design problem, since each of them represents a specific configuration of the hybrid generation system. Excluding $P_{b_{cap}}$, all the remaining positions are real-coded. The i-th particle (i.e., candidate design) D_i can be represented as follows:

$$D_i = [P_{w,i}, P_{s,i}, P_{b_{cap},i}, \kappa_i], \qquad i = 1, 2, \ldots, N \qquad (8.29)$$

where κ is ratio of power bought from the grid with respect to the deficit power, and the total SB capacity $P_{b_{cap}}$ is encoded using three binary bits.

3. Data flow of the optimization procedure

The computational procedure of the propose method is as follows:

- Step 1: Specify the lower and upper bounds of WTG swept area, area of PV panels, number of batteries, and other pre-determined parameters.

- Step 2: Randomly generate a population of particles. The speed and position of each particle should be initialized such that all the particles locate within the feasible search space.

- Step 3: Evaluate each particle D_i in the population based on the concept of Pareto-dominance.

- Step 4: Store the non-dominated solutions found so far in the archive.

- Step 5: Initialize the memory of each particle where a single personal best *pbest* is stored. The memory is contained in another archive.

- Step 6: Increase the iteration number by one.

- Step 7: Choose the personal best position *pbest* for each particle based on the memory record; Choose the global best *gbest* from the fuzzified region using binary tournament selection [84]. The niching and fitness sharing mechanism is also applied in order to enhance solution diversity.

- Step 8: Update the member velocity v of each individual D_i. For the real-encoded design variables,

$$
\begin{aligned}
v_{i_d}^{(t+1)} &= \chi * (w * v_i^{(t)} + c_1 * \mathrm{rand}() * (pbest_{i_d} - P_{Gi_d}^{(t)}) \\
&+ c_2 * \mathrm{Rand}() * (gbest_d - P_{Gi_d}^{(t)})), \\
& i = 1, \ldots, N; d = 1, 2.
\end{aligned}
\tag{8.30}
$$

- Step 9: Update the member position of each particle D_i based on (8.29). For real-coded variables,

$$
D_{i_d}^{(t+1)} = D_{i_d}^{(t)} + v_{i_d}^{(t+1)}
\tag{8.31}
$$

For the binary-encoded design variable, update the member position based on the updating rule for discrete variables discussed in Subsection D.1.

Following this, add the turbulence factor into the current position. For all the

positions,

$$D_{i_d}^{(t+1)} = D_{i_d}^{(t+1)} + R_T D_{i_d}^{(t+1)} \tag{8.32}$$

where R_T is the turbulence factor, which is used to enhance the solution diversity by refraining the search from undesired premature convergence.

- Step 10: Update the archive which stores non-dominated solutions according to Pareto-optimality based selection criteria [84].

- Step 11: If the current individual is dominated by the *pbest* in the memory, then keep the *pbest* in the memory; Otherwise, replace the *pbest* in the memory with the current individual.

- Step 12: If the maximum number of iterations is reached, then go to Step 13; Otherwise, go to Step 6.

- Step 13: Print out a set of Pareto-optimal solutions from the archive as the final possible system configurations.

D. A Case Study: System Design Without Incorporating Uncertainties

In this section, the tradeoff solutions are derived for a grid-linked hybrid system without incorporating system uncertainties, and some sensitivity studies are carried out.

1. System parameters

The data used in the simulation program are listed in Table XXIII [75]. The hourly wind speed patterns, the hourly insolation conditions, and the hourly load profile are shown in Figure 20. These time-series data will be used by the ARMA model [73] to derive forecasted wind speed and solar insolation, which are then used to calculate

the available wind power, solar power, and the insufficient or surplus power at each time instant.
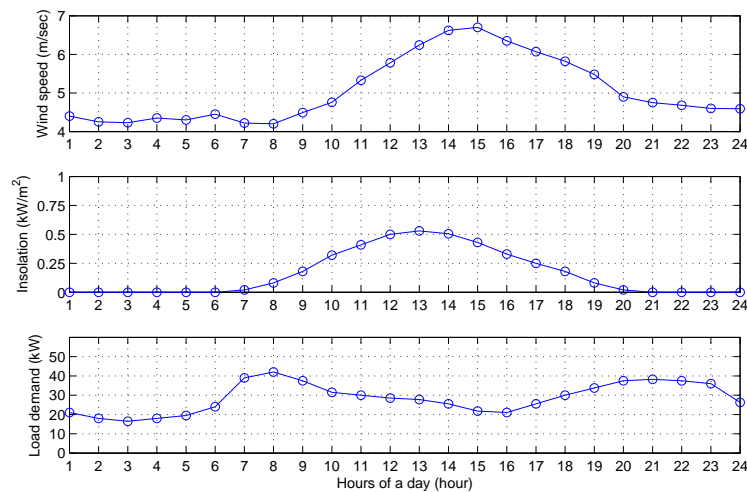

Fig. 20. Hourly mean wind speed, insolation, and load profiles

2. PSO parameters

In the simulations, both the population size and archive size are set to 100, and the maximum number of iterations is set to 500. The acceleration constants c_1 and c_2 are chosen as 1. Both turbulence factor and niche radius are set to 0.02. The inertia weight factor w decreases when the number of generations increases:

$$w = w_{max} - \frac{w_{max} - w_{min}}{iter_{max}} \times iter \tag{8.33}$$

where $iter_{max}$ is the maximum number of iterations and $iter$ is the current number of iterations. This mechanism helps achieve the balance between exploration and exploitation in the search process. The simulation program is coded using C++ and executed in a 2.20 GHz Pentium-4 processor.

3.   Simulation results

The Pareto-optimal fronts evolved using the proposed approach for bi- and tri-objective optimization problems are shown in Figure 21, and two illustrative non-dominated solutions are listed in Table XXIV.
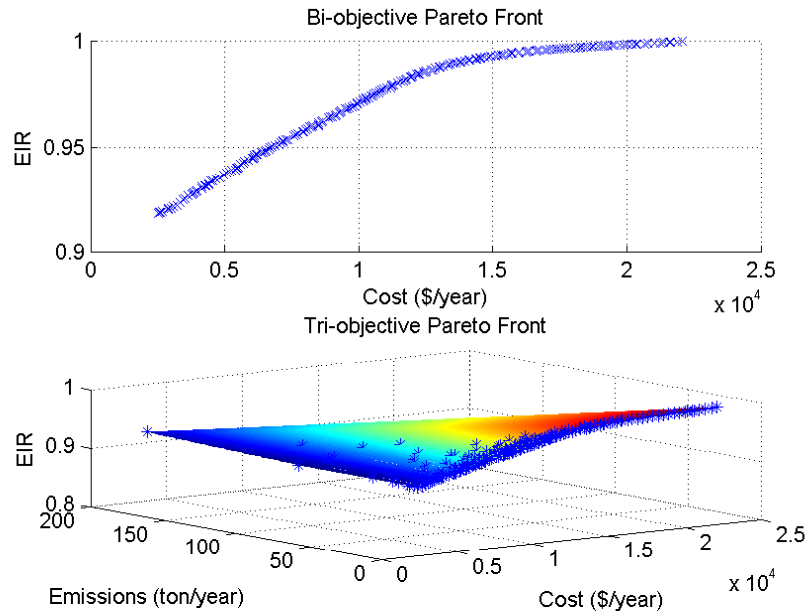

Fig. 21. Pareto fronts for bi- and tri-objective optimization scenarios

4.   Sensitivity to system parameters

Here the sensitivity analysis is carried out to examine the effects of changing the values of certain system parameters on the final non-dominated solutions derived. For instance, the mean wind speeds are changed by different multiplication factors (MFs), and different economic rates are also examined. The results are illustrated in Figure 22 and Figure 23, respectively. From Figure 22, we can appreciate the importance of site locations for a wind power plant. The simulation results shown in

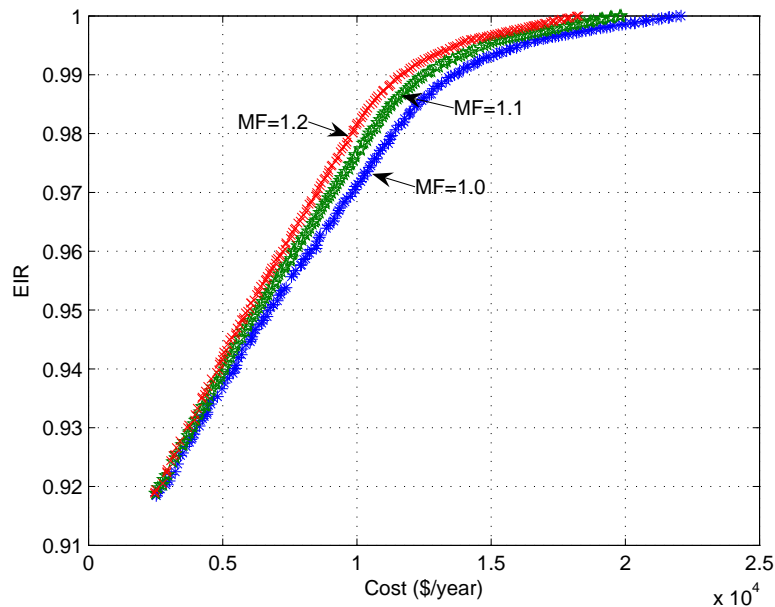Figure 23 fit with the cost estimation equations described in Section B.

Fig. 22. Pareto fronts obtained from different mean wind speeds

E.   Adequacy-constrained Design Incorporating System Uncertainties

In the previous section, a grid-linked hybrid system is designed without including uncertain factors. The design of an adequacy-constrained hybrid system using probabilistic methods is discussed in this section. Besides different problem formulations, the focal points of these two design scenarios are also different in some sense. In the previous design, the generation system with WTGs, PVs, and SBs is treated as the base system. Only if there is insufficient power, a certain amount of power can be purchased from the utility grid. Conversely, in this design, the base system is the traditional utility grid and the renewable generation system is incorporated into it. The main intention here is to investigate the impact of different penetration levels of renewable energy on the overall system performance.
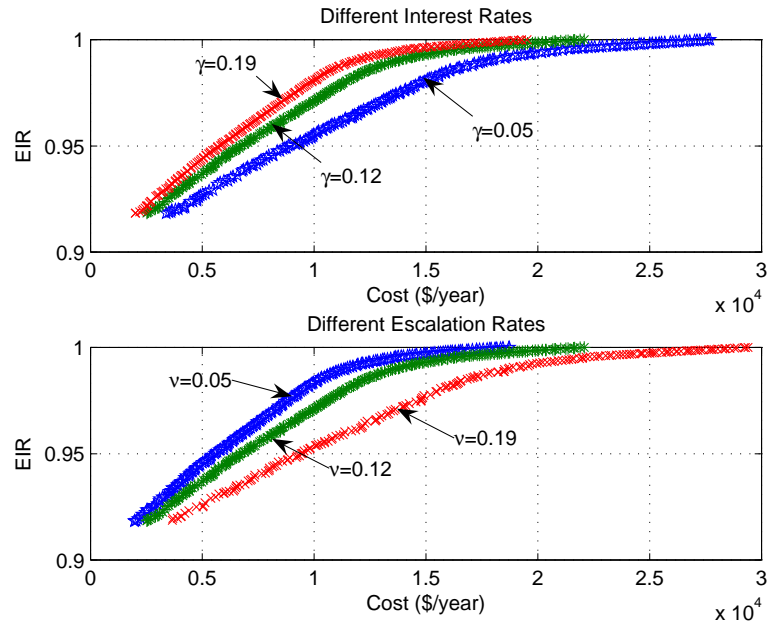
Fig. 23. Pareto fronts obtained from different economic rates

Probabilistic methods are now being used more widely in power system planning and operations due to a variety of uncertainties involved. For instance, adequacy evaluation is an important component to ensure proper operations of power systems in the presence of various uncertainties. Adequacy analysis of hybrid generating systems including time-dependent sources has been investigated in [15], [17], [18]. Here an efficient reliability evaluation technique proposed in [15] is used to calculate the reliability indices including Expected Unserved Energy (EUE), Loss of Load Expectation (LOLE), and Loss of Load Frequency (LOLF), which are three fundamental indices for adequacy assessment of generating systems. The main idea of this method is to divide the generating system into a subsystem including all the conventional units and a set of subsystems each of which contains a possibly fluctuating unconventional source. Here all the adequacy indices are calculated based on the analytical method proposed in [15], which is also introduced in Chapter V.

1. Problem formulation

In this design scenario, only WTGs and PVs are used. Thus, the total cost $COST(\$/year)$ can be changed as follows:

$$COST = \frac{\sum_{i=w,s}(I_i - S_{P_i} + OM_{P_i})}{N_p} \tag{8.34}$$

Here the cost for generating FFG power is excluded from the total cost calculation in order to examine the impact of wind and solar power penetration level on the overall system design in a more explicit fashion.

The real power balance constraint in this design scenario can be represented by

$$P_{w_t} + P_{s_t} + P_{g_t} \geq (1 - R)P_{d_t} \tag{8.35}$$

$$P_{w_t} + P_{s_t} + P_{g_t} - P_{dump_t} \leq P_{d_t} \tag{8.36}$$

Furthermore, due to the fluctuations of available wind and solar power coupled with possible generator failures, the loss of load may be caused. To ensure a certain degree of system reliability, the indices of LOLE and LOLF should also be fulfilled besides the maximization of EIR.

$$LOLE \leq LOLE_{max} \tag{8.37}$$

where $LOLE_{max}$ is the maximum LOLE allowed. In a similar manner, LOLF should also be less than or equal to the maximum value $LOLF_{max}$:

$$LOLF \leq LOLF_{max} \tag{8.38}$$

As we can see, in this study one reliability index (EUE) is used as the design objective and the other two (LOLE and LOLF) are used as design constraints to ensure the generating system adequacy, which can be computed simultaneously.

In this scenario, the objective of optimum design for hybrid generating system with time-dependent sources is to simultaneously minimize $COST(A_w, A_s)$ as well as maximize $EIR(A_w, A_s)$, subject to the constraints (8.21)–(8.22) coupled with (8.35)–(8.38). The design parameters that should be derived include total WTG swept area $A_w(m^2)$ and total PV area $A_s(m^2)$.

2. Simulation results

Three identical two-state FFGs are used together with multiple wind/solar generating units. Since solar power is much less prone to equipment failures, failures of PV cells are not considered in this investigation. In simulations, four identical WTGs are considered during the hybrid system design, and the capacity of each WTG is determined by the candidate solution under consideration. The rated FFG power (P_{FFG}) is 20 kW, and the reliability characteristics of each type of generating units are as follows: FFG failure rate (λ_{FFG}) is 0.1 day^{-1}, FFG repair rate (μ_{FFG}) is 0.9 day^{-1}, WTG failure rate (λ_{WTG}) is 0.1 day^{-1}, and WTG repair rate (μ_{WTG}) is 0.4 day^{-1}. Furthermore, $LOLE_{max}$ and $LOLF_{max}$ are set 1.5 h/week and 1 occ./week, respectively.

The computational procedure used is basically same as in the previous design, but some minor changes are needed to fit it into the current design scenario. For instance, the particle representation and design constraints should be modified accordingly. The Pareto-optimal front evolved in this design scenario using the proposed approach is shown in Figure 24. The decision-maker can choose a design solution from the derived set of non-inferior solutions based on the specific design requirement or preference. Two illustrative non-dominated solutions are listed in Table XXV. We can appreciate that the improvement of one objective is at the expense of deterioration of another objective. Thus, for any specific system design, a tradeoff between
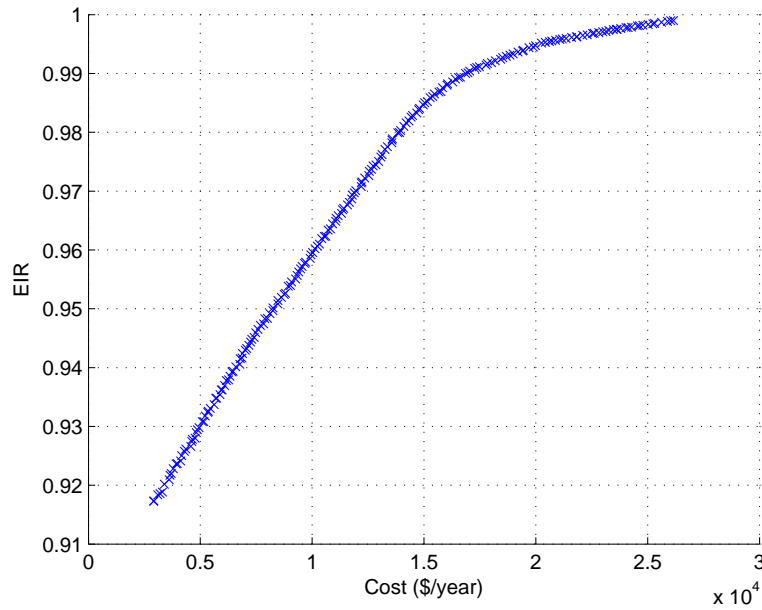
these two objectives should be reasonably made.

Fig. 24. Pareto front indicating a set of non-inferior design solutions

To examine the impacts of different wind speeds and insolations on the Pareto-optimal solutions derived, sensitivity studies are carried out. Figure 25 and Figure 26 show the tradeoff surfaces obtained in different scenarios in terms of wind speeds and solar insolations, respectively. Note that during the simulations, when different wind speeds are examined, the original insolation value is used. Likewise, when different insolations are examined, the original wind speed value is used. We can appreciate that at the same reliability level, the generating systems with the highest speed and insolation result in the lowest costs when compared with scenarios with lower wind speed and insolation. Thus, this confirms the previous observation that it is crucial to properly select power plant location when renewable sources of energy are involved. Usually plant sites with richer renewable sources of energy can cause lower generation costs.
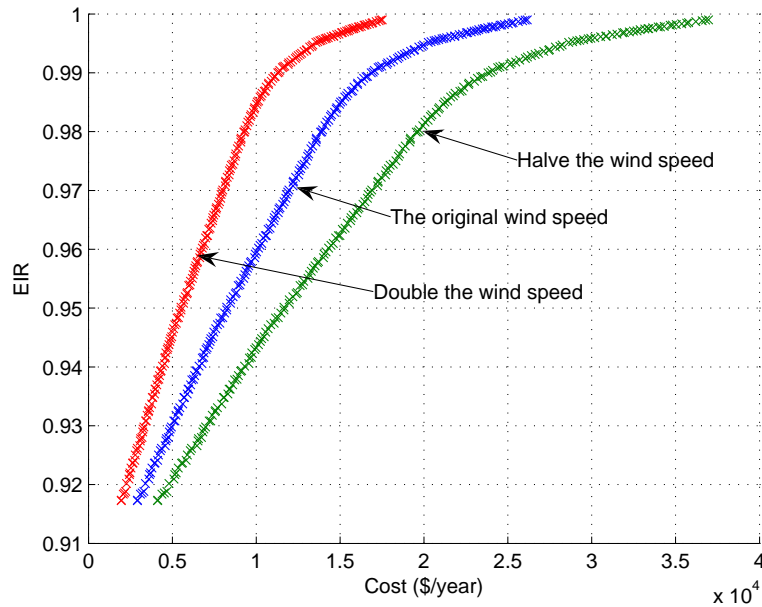
Fig. 25. Impacts of different wind speeds on Pareto fronts derived

Next, the stochastic nature of load is considered, which is modeled through a time-series method called Autoregressive Integrated Moving Average (ARIMA) [69]. Two illustrative non-dominated solutions are listed in Table XXVI, and Figure 27 shows the tradeoff surface in this design scenario. We can appreciate that the stochastic characteristic of load demand induces somewhat more costs for ensuring the same reliability level. This is understandable since random variations of load may compromise the system reliability. Also, Figure 28 shows the impacts of different wind speeds on the Pareto-optimal solutions derived. It further verifies the previous observation on the plant site selection.

F. Summary

Distributed generation using sustainable clean green power promises to considerably restructure the energy industry, which is evolving from fossil fuels towards renew-
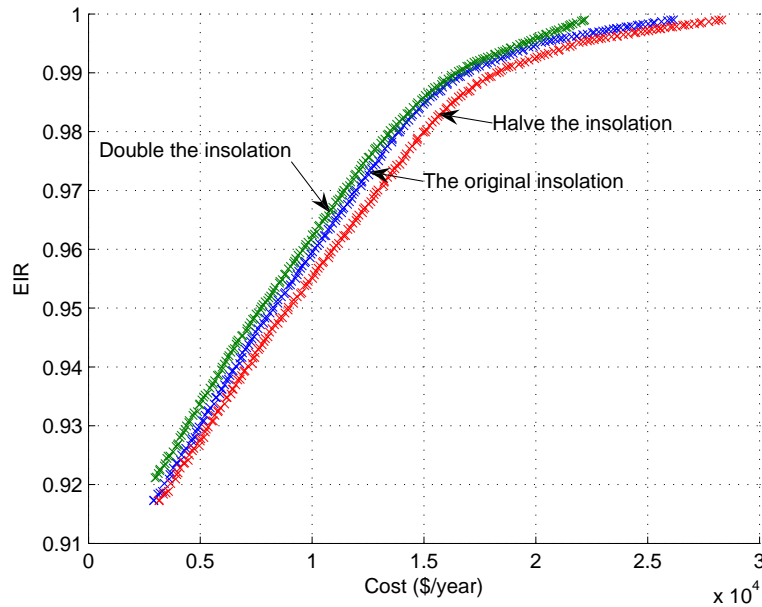
Fig. 26. Impacts of different insolations on Pareto fronts derived

ables [77]. Meanwhile, there are many open-ended problems in this field awaiting to be resolved. In this chapter, a hybrid power generation system including wind power and solar power is designed on the basis of cost, reliability, and emission criteria. A set of tradeoff solutions is obtained using the multi-criteria metaheuristic method which offers many design alternatives to the decision-maker. Moreover, in one of the designs, system uncertainties such as equipment failures and stochastic generation/load variations are considered by conducting adequacy evaluation based on probabilistic methods. In particular, the stochastic generation/load variations are modeled through time-series methods. Numerical simulations are used to illustrate the applicability and validity of the proposed MOPSO-based optimization procedure, and some sensitivity studies are also carried out. In the future studies, other more complicated design scenarios may be incorporated into system designs.
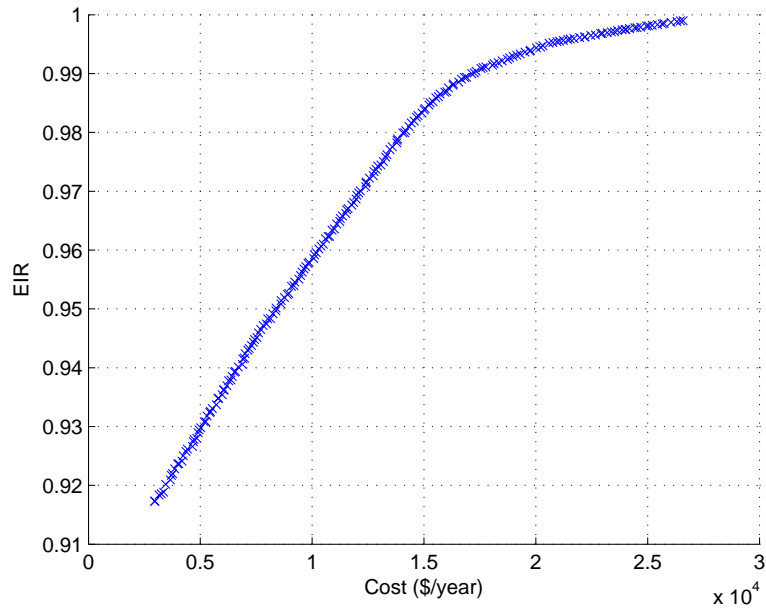
Fig. 27. Pareto front indicating a set of non-inferior design solutions considering stochastic load variations
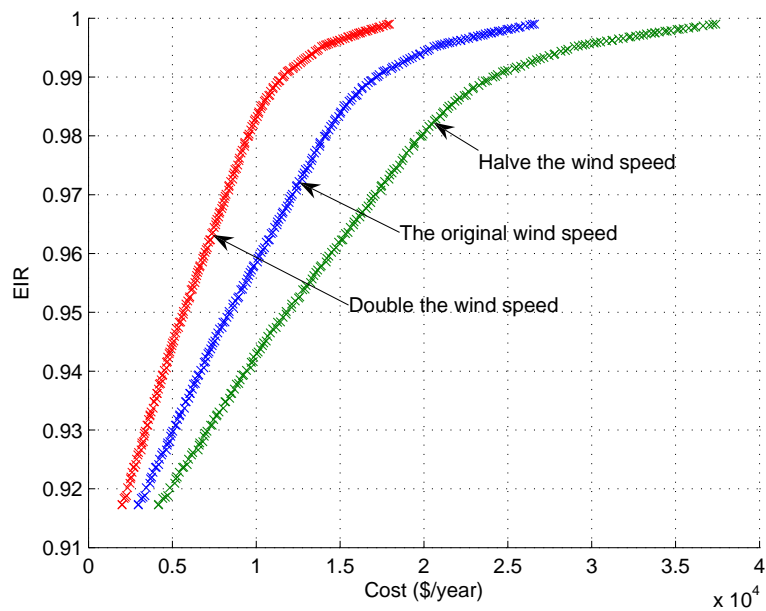

Fig. 28. Impacts of different wind speeds on Pareto fronts derived considering stochastic load variations

Table XXIII. The data used in the simulation program

System parameters	Values
Efficiency of WTG (η_w)	50%
Efficiency of PV (η_s)	16%
Efficiency of SB (η_b)	82%
Inflation rate (β)	9%
Interest rate (γ)	12%
Escalation rate (ν)	12%
Life span of project (N_p)	20 years
Life span of WTG (N_w)	20 years
Life span of PV (N_s)	22 years
Life span of SB (N_b)	10 years
PV panel price (α_s)	450\$/m^2
WTG price (α_w)	100\$/m^2
SB price (α_b)	100\$/KWh
PV panel salvage value (S_s)	45\$/m^2
WTG salvage value (S_w)	10\$/m^2
OM costs of WTG (α_{OM_w})	2.5\$/m^2/year
OM costs of PV panel (α_{OM_s})	4.3\$/m^2/year
OM costs of SB (α_{OM_b})	10\$/KWh
Cut-in wind speed (V_{ci})	2.5 m/s
Rated wind speed (V_r)	12.5 m/s
Cut-out wind speed (V_{co})	20.0 m/s
Rated WTG power (P_r)	4.0 kW
Period under observation (T)	8760 hours
Maximum swept area of WTGs ($A_{w_{max}}$)	10,000m^2
Minimum swept area of WTGs ($A_{w_{min}}$)	400m^2
Maximum area of PV panels ($A_{s_{max}}$)	200m^2
Minimum area of PV panels ($A_{s_{min}}$)	8,000m^2
Maximum conversion capacity ($P_{b_{max}}$)	3 kWh
Minimum storage level ($P_{b_{min}}$)	3 kWh
Rated battery capacity (P_{b_r})	8 kWh
Maximum total SB capacity ($P_{b_{max}}$)	40 kWh
Price of utility grid power (φ)	0.12\$/kWh

Table XXIV. Two illustrative non-dominated solutions for tri-objective optimization

Variables/objectives	Design 1	Design 2
$A_w(m^2)$	810	680
$A_s(m^2)$	40	40
$P_{b_{cap}}(kWh)$	16	16
κ	0.34	0.58
Cost ($/year)	7,919.55	7,012.10
EIR	0.9579	0.9521
Emissions (ton/year)	17.0836	59.8295

Table XXV. Two illustrative system configurations for adequacy-constrained design

Variables	Design 1	Design 2
$A_w(m^2)$	880	1020
$A_s(m^2)$	40	160
Cost ($/year)	7191.5	11233
EIR	0.9451	0.9653

Table XXVI. Two illustrative system configurations for adequacy-constrained design with load forecasting

Variables	Design 1	Design 2
$A_w(m^2)$	880	1020
$A_s(m^2)$	40	160
Cost ($/year)	7312	11418
EIR	0.9451	0.9653

CHAPTER IX

CAPACITY CREDIT ESTIMATION OF WIND POWER: FORMULATION AS
AN OPTIMIZATION PROBLEM

Significant amounts of wind power are being integrated into power grids in recent
years. However, due to intermittent characteristic of wind power, it is usually dif-
ficult to determine the appropriate penetration level to ensure a specified reliability
requirement. For this purpose, the proper calculation of wind power capacity credit
(WPCC) is of particular importance which is useful in both planning and operation
stages of hybrid power systems with multiple power sources. The capacity credit of
wind power is usually calculated based on a reliability index termed Loss of Load Ex-
pectation (LOLE). WPCC is the amount of wind power which is able to achieve the
LOLE identical to the dispatchable power sources. In this study, WPCC estimation
is formulated as an optimization problem, and an intelligent search method called
particle swarm optimization is used to automatically search out the WPCC. It has
turned out to be a viable scheme in estimating WPCC.

A. Introduction

In planning generation facilities, the planners are faced with the question of giving
appropriate credit for generating capacity from intermittent sources like wind. Es-
timation of wind power capacity credit (WPCC) due to the intermittency of wind
availability is not a sufficiently investigated area so far, and it is also a challenging
task. There are several definitions on the wind power capacity credit, one of which is
based on the system load carrying capability. Since the penetrated wind power can
be seen as "negative load", an increase in load carrying capability can be achieved
while still ensuring the original level of system reliability. The amount of this extra

load is used as a measure for capacity credit of wind power in this study.

Probabilistic methods have been more widely used in power system planning, since they are capable of incorporating various system uncertainties [1]. The estimation of wind power capacity credit is based on the reliability indices such as loss of load expectation (LOLE). Here an analytical procedure based on the mean capacity outage table is used for LOLE calculation. A trial-and-error method has been used to find out the WPCC in our previous work [85]. However, due to the complexity and nonlinearity of this problem, this method is usually not time-efficient since it demands tedious trial effort. In this work, for the first time WPCC estimation is formulated as an optimization problem, and an automatic intelligent search method is used to search for the WPCC value in a much more efficient fashion. Particle swarm optimization [8] is used for this purpose due to its proven high search efficiency in dealing with highly complex and nonlinear problems. Furthermore, a numerical study based on a practical power system is conducted to indicate the viability of the proposed method. The method is also flexible and opens up other possibilities like incorporating constraints, if needed, while computing WPCC.

The remainder of the chapter is organized as follows. Section B presents the concept and calculation of wind power capacity credit based on reliability evaluation for hybrid power-generating systems. In Section C, the proposed PSO-based WPCC estimation method is discussed in detail. Simulation results and analysis are presented and discussed in Section D. Finally, the chapter is wrapped up with the conclusion and future research suggestion.

B. Wind Power Capacity Credit

Due to the wind speed variations, the output of wind turbine generator (WTG) does not equal its rated capacity in most time periods. This creates difficulties for system planners since the effective capacity of WTG needs to be determined based on certain criteria. Quite often, reliability indices are used to measure the impact of the wind power penetration. Thus, in calculating wind power capacity credit, reliability indices such as loss of load expectation over the specified observation horizon are used to ensure that power system meets the reliability level after the wind power is integrated.

The reliability analysis of hybrid generating systems including time-dependent sources has been investigated through different methods including analytical, simulation, and artificial intelligence methods [14]–[18], [86]. These proposed reliability evaluation techniques are usually intended to calculate the reliability indices including Expected Energy Not Supplied (EENS), Loss of Load Expectation (LOLE), and Loss of Load Frequency (LOLF), which are three fundamental indices for adequacy assessment of power-generating systems. In the calculation of wind power capacity credit, usually LOLE is used as the reliability index. Thus in this chapter only LOLE will be discussed.

Assume the load is represented as a chronological sequence of N_T discrete values L_t for successive time steps $t = 1, 2, \ldots, N_T$. Each time step has equal duration $\Delta T = \frac{T}{N_T}$ where T is the entire period of observation. The LOLE of the power system without wind power integration can be calculated as follows:

$$LOLE = \Delta T \sum_{t=1}^{N_T} P_f(C_{g_t} < L_t) \tag{9.1}$$

where P_f is the loss of load probability, C_{g_t} is the capacity of conventional power

sources, L_t is the load demand in period t. The LOLE with wind power penetration can be calculated as follows:

$$LOLE = \Delta T \sum_{t=1}^{N_T} P_f[(C_{g_t} + C_{w_t}) < L_t] \qquad (9.2)$$

where C_{w_t} is the effective wind power at time instant t. In the above definition, the term $C_{g_t} + C_{w_t}$ indicates the effective total system capacity (that is, the summation of conventional sources of power and wind power at time instant t).

From the definition of reliability-based wind power capacity credit, we need to ensure the identical power system reliability (i.e., LOLE in most cases) in both situations with and without wind power penetration:

$$\sum_{t=1}^{N_T} P_f(C_{g_t} < L_t) = \sum_{t=1}^{N_T} P_f[(C_{g_t} + C_{w_t}) < (L_t + E)] \qquad (9.3)$$

where E is the capacity credit of wind power we need to find out.

C.   The Proposed Method

In the proposed method, WPCC estimation is formulated as an optimization problem, which can be solved by intelligent search algorithms.

1.   Problem formulation

The design objective is to find the WPCC variable E, which is able to minimize the difference between LOLEs of the power system with and without wind power generation. Thus, the objective function in PSO is defined as (9.4), which is to be minimized:

$$F = (\sum_{t=1}^{N_T} P_f(C_{g_t} < L_t) - \sum_{t=1}^{N_T} P_f[(C_{g_t} + C_{w_t}) < (L_t + E)])^2 \qquad (9.4)$$

This is a highly nonlinear and complex function, since LOLE calculation is needed for each potential solution.

A set of stochastic search algorithms is able to handle this optimization problem. Here particle swarm optimization (PSO) is used, which is a population-based intelligent search procedure inspired by certain social behaviors in bird groups and fish schools [8].

2. Computational procedure

In PSO, each particle is regarded as a potential solution (i.e. the wind power capacity credit), and many particles constitute a population. The dataflow diagram of the proposed method is shown in Figure 29, and the computational flow is detailed in the following.
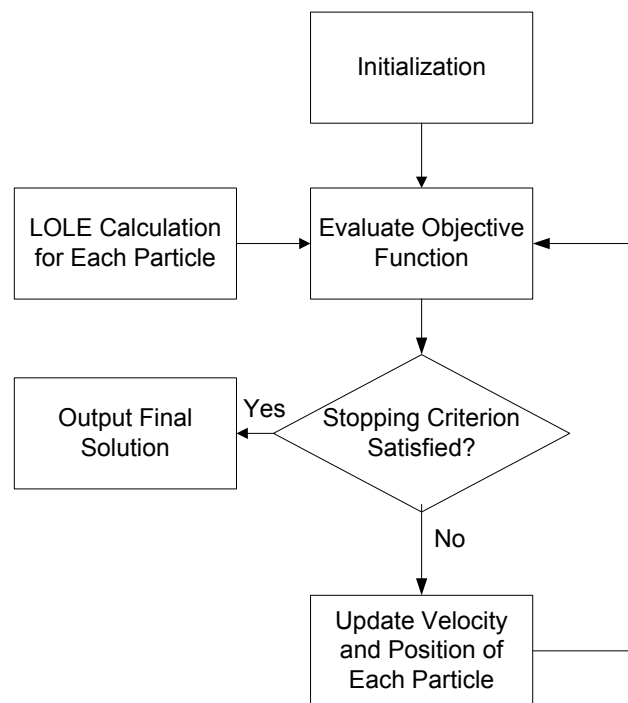

Fig. 29. Dataflow diagram of PSO-based WPCC estimation

- Step 1: Some initialization operations are carried out, including the initialization of particle velocity and position, setting of initial iteration number, and so forth. Note that to expedite the search process by seeding a feasible solution, here the initial wind power capacity credit E should fulfill the following constraint:

$$0 < E < P_w \tag{9.5}$$

  where P_w is the total wind power capacity integrated.

- Step 2: Each particle is evaluated based on the specified objective function. Note that LOLE calculation is accomplished by calling the LOLE evaluation procedure presented in Section E of Chapter V.

- Step 3: The stopping criterion is examined. If it is satisfied, then the PSO procedure stops; Or else, proceed to the next step.

- Step 4: The velocity and position of each particle are updated based on the PSO mechanism. These operations create particles of the next iteration.

- Return to step 2 until any termination criterion is satisfied.

D. A Numerical Example

A WTGs-augmented IEEE Reliability Test System (IEEE RTS-79) is used in simulations [15]. The power system has the wind power penetration of 400 MW. The number of particles used in PSO is 80, and the maximum number of iterations is used as the stopping criterion, which is set 100. Here PSO algorithm is used to find out the capacity credit E by minimizing the objective function defined in (9.4), and meanwhile reliability evaluation is conducted to calculate the LOLE for each candidate capacity credit value. When the value of objective function becomes sufficiently close

to zero satisfying the required accuracy, the last candidate capacity credit achieved is deemed as the final result. In this way, the capacity credit obtained is 163.6 MW, which is about 40.9% of the total installed wind power capacity. Obviously, this method is highly advantageous in WPCC estimation with respect to the trial-and-error method since it does not require tedious trial efforts. It is also more accurate since the objective function (9.4) can be minimized in a more effective fashion.

It should be noted that this method can also be implemented by other stochastic search algorithms including population based intelligent search (e.g., evolutionary algorithms and ant colony optimization) and non-population-based intelligent search (e.g., Tabu search and simulated annealing).

E. Summary

Due to the more significant penetration of wind power into traditional power grids in recent years, it has become necessary to calculate its capacity credit for decision-making in power system planning and operations. However, reliability-based WPCC calculation is difficult due to the problem complexity and nonlinearity. In this chapter, as a new estimation scheme, particle swarm optimization algorithm is used as a search tool to seek out the wind power capacity credit based on the reliability index LOLE. A numerical example is used to illustrate the viability of the proposed method. In the future research, other intelligent search algorithms will be used to find the most efficient one in dealing with this problem.

CHAPTER X

CONCLUSIONS AND OUTLOOK

In this chapter, conclusions will be made to summarize the work reported in this dissertation. Also, some suggestions for future investigations in this research arena will be given.

A. Conclusions

Renewable sources of energy are being integrated into the power grids due to their merits as compared with the traditional fossil-fuel-fired power generation. However, their significant penetration demands a thorough research in terms of system reliability, system cost, and environmental impact. This dissertation can be divided into two parts. In the first four chapters, some background knowledge and the motivation of this research are discussed. Then, several important and pressing topics in this research arena are explored.

- Due to the stochastic nature of wind speed, reliability of the hybrid generation system may be compromised when wind power is integrated. In Chapter V, an artificial intelligence based method called population-based intelligent search (PIS) is proposed to conduct reliability evaluation accounting for wind power penetration. Four representative PIS algorithms are used to derive out a set of most probable failure states which can be used to calculate the reliability indices. The proposed method can also be applied to more complex power systems such as multi-area systems as well as composite systems involving both power generation and transmission.

- At the power distribution level, distributed generation is being directly con-

nected to the power distribution systems for enhancing their reliability in the presence of system faults. The proper placement of both distributed generators and protective devices is crucial to maximize the system reliability using the limited hardware resources. In Chapter VI, an improved ant colony system algorithm is used to handle this complicated discrete optimization problem, where distributed generators of different sizes and reclosers are placed by optimizing a composite reliability index. The proposed method has turned out to be more effective with respect to genetic algorithm.

- Economic power dispatch is an old topic in the field of power system operations. However, when more significant amounts of wind power are being integrated into the power grid, this problem becomes more complicated due to the availability of wind power during system operations. The operational cost of wind power is very low primarily because it does not consume fossil fuels; however, its intermittency may bring certain risk to power dispatch if excessive wind power is integrated. In Chapter VII, a set of tradeoff solutions is searched by an enhanced particle swarm optimization in terms of operational cost and system risk. Here system risk is defined based on the fuzzy concept. By doing so, different operator' attitudes are incorporated to reflect their acceptance degree toward wind power integration.

- Hybrid power generation utilizing multiple energy sources is becoming more common. Different energy sources have different characteristics in terms of cost, power dispatchability, and pollutants emission. Therefore, optimum design is important to achieve an environmentally benign, operationally reliable, and economically viable hybrid generation system. In Chapter VIII, hybrid generation systems are designed based on an improved particle swarm optimization,

where multiple energy sources are used including traditional fossil-fuel-fired generators, wind turbine generators, solar panels, and storage batteries. Multiple design criteria such as system cost, system adequacy, and pollutant emissions are compromised in various design scenarios.

- Wind power is oftentimes thought of undispatchable due to its volatility. Therefore, it is highly necessary to calculate the wind-power capacity credit, which can be used by designers, operators, and planners for proper decision-making. In Chapter IX, the value of wind-power capacity credit is found out by automatic search using a PSO algorithm, which ensures that the wind power is capable of achieving the same reliability level as the dispatchable power of this capacity.

The research objectives raised in Chapter I have been examined through these case studies. Integration of renewable energy sources does have significant impacts on the conventional power systems, technically, economically, and environmentally.

- The impact of renewable energy integration on the traditional power system planning and operations is multifold, including system costs, system reliability, and pollutant emissions.

- Reliability-constrained designs are highly necessary since time-dependent energy sources may have detrimental impact on the overall system reliability. The intermittency of wind power should be included in the reliability assessment.

- Computational intelligence based optimization methods have turned out to be promising in dealing with complex and nonlinear power systems.

B.   Outlook

Renewable energy is being promoted as a solution for reducing our reliance on imported hydrocarbon fuels and cutting greenhouse gas emissions. Although wind and solar power continue to receive the most attention, these renewable resources are inherently intermittent and demand significant infrastructure and systems changes. The current power grid systems and operation methods are not yet ready for handling such fluctuations on a systematic basis. Thus, it is an infant research arena which poses great challenges, and there are still many open-ended problems. The author believes that the following several research directions are of particular importance for more significant renewables integration, which are worthy of further thorough exploration.

- System security evaluation including time-dependent sources: System adequacy dealt with in this dissertation is relevant to the existence of sufficient facilities within the system to fulfill the consumer load demand or system operational constraints. Different from the definition of system adequacy, system security is more concerned about the dynamic and transient conditions of power systems such as the sudden loss of a major generating unit and voltage instability. Power quality issues such as frequency balance, voltage stabilization, and reactive power regulation should be addressed carefully. Traditional control strategies need to be modified in order to accommodate the time-varying output from volatile sources such as wind turbine generators. For instance, appropriate voltage regulation is needed to ensure the power system stability when the wind power penetration level is high. Or else, voltage and/or reactive power excursions and oscillations may be caused.

- Forecasting models and tools for more accurate prediction of time-dependent

power productions: Unlike load forecasting which has reached very high precision, wind-speed forecasting is still relatively inaccurate. One of the major reasons lies in the lack of complete historical data of wind speed. Valid historical wind-speed database should be built for the target region. And both statistical and artificial intelligence methods should be improved to achieve more accurate wind-speed forecasting. Theoretically speaking, if the exact wind speed could be predicted (though it is not feasible in practice), the wind power becomes dispatchable just like the conventional power. Thus, accurate forecasting provides the foundation for all subsequent proper planning and operations in electric power systems, especially in large-scale integration of wind power.

- Applications of computational intelligence (CI) based optimization methods in complex power systems: Nowadays electrical power systems have become ever more complex, some analytical methods based on strict mathematical derivations oftentimes suffer from the so-called "curse of dimensionality." It means that when the system size increases, the time needed to solve the problem will increase exponentially. Thus, they will become less efficient or even unable to solve the problem when the system becomes highly complex. Approximation methods based on CI techniques can be used in these challenging scenarios, which are quite often able to achieve an adequate solution within a reasonable amount of time. Building the connections between the target problem and the mathematical tool (i.e., CI algorithms) is a key step to solving complex problems using CI techniques. Moreover, for a specific problem, the CI technique should be modified accordingly in order to achieve the best result, if necessary. Although CI has shown great promises in dealing with highly complex power systems, some "killer applications" are desirable to corroborate its superiority in

handling some kinds of practical problems. Meanwhile, more theoretic research should be carried out to justify its performance (e.g., convergence, optimality, sensitivity to initial values, etc.) in a more systematic fashion.

Other important research directions in this field include integrated energy resources management, integration of energy storage devices, as well as systematic modeling and simulation studies of grid integration to ensure optimization in management and practices.

REFERENCES

[1] G. J. Anders, *Probability Concepts in Electric Power Systems*, New York: Wiley, 1990.

[2] C. Singh and R. Billinton, *System Reliability Modelling and Evaluation*, London: Hutchinson Educational Publishers, 1977.

[3] N. Gubbala and C. Singh, "Models and considerations for parallel implementation of Monte Carlo simulation methods for power system reliability evaluation," *IEEE Transactions on Power Systems*, vol. 10, no. 2, pp. 779–787, 1995.

[4] C. Singh and L. F. Wang, "Role of artificial intelligence in the reliability evaluation of electric power systems," in *Proceedings of IEEE International Conference on Electrical and Electronics Engineering (ELECO07)*, Bursa, Turkey, 2007, pp. 1–8.

[5] N. Jenkins, R. Allan, P. Crossley, D. Kirschen and G. Strbac, *Embedded Generation*, IEE Power and Energy Series 31, Stevenage, UK: The Institution of Electrical Engineers, 2000.

[6] S. Kirkpatrick, C. D. Jr. Gelatt, and M. P. Vecchi, "Optimization by simulated annealing," *Science*, vol. 220, no. 4598, pp. 671–680, 1983.

[7] D. E. Goldberg, *Genetic Algorithm in Search, Optimization, and Machine Learning*, Reading, MA: Addison-Wesley, 1989.

[8] J. Kennedy and R. Eberhart, "Particle swarm optimization," in *IEEE Proceedings of the International Conference on Neural Networks*, Perth, Australia, 1995, pp. 1942–1948.

[9] M. Dorigo and T. Stutzle, *Ant Colony Optimization*, Cambridge: The MIT Press, 2004.

[10] L. N. de Castro, and J. Timmis, *Artificial Immune Systems: A New Computational Intelligence Approach*, London: Springer, 2002.

[11] L. N. de Castro and F. J. Von Zuben, "Learning and optimization using the clonal selection principle," *IEEE Transactions on Evolutionary Computation*, vol. 6, no. 3, June, pp. 239–251, 2002.

[12] J. Mitra (Editor), *IEEE Tutorial on Electric Delivery System Reliability Evaluation*, IEEE Power Engineering Society General Meeting, San Francisco, CA, Publication number 05TP175, 2005.

[13] N. Samaan and C. Singh, "Adequacy assessment of power system generation using a modified simple genetic algorithm," *IEEE Transactions on Power Systems*, vol. 17, no. 4, pp. 974–981, 2002.

[14] E. N. Dialynas and A. V. Machias, "Reliability modelling interactive techniques of power systems including wind generating units," *Electrical Engineering*, vol. 72, no. 1, pp. 33–41, 1989.

[15] S. Fockens, A. J. M. van Wijk, W. C. Turkenburg, and C. Singh, "Reliability analysis of generating systems including intermittent sources," *International Journal of Electric Power & Energy Systems*, vol. 14, no. 1, pp. 2–8, 1992.

[16] E. S. Gavanidou, A. G. Bakirtzis, and P. S. Dokopoulos, "A probabilistic method for the evaluation of the performance of wind-diesel energy systems," *IEEE Transactions on Energy Conversion*, vol. 7, no. 3, pp. 418–425, 1992.

[17] C. Singh and Y. Kim, "An efficient technique for reliability analysis of power systems including time dependent sources," *IEEE Transactions on Power Systems*, vol. 3, no. 3, pp. 1090–1094, 1988.

[18] C. Singh and A. Lago-Gonzalez, "Reliability modeling of generation systems including unconventional energy sources," *IEEE Transactions on Power Apparatus & Systems*, vol. PAS-104, no. 5, pp. 1049–1056, 1985.

[19] G. Tina, S. Gagliano, and S. Raiti, "Hybrid solar/wind power system probabilistic modelling for long-term performance assessment," *Solar Energy*, vol. 80, pp. 578–588, 2006.

[20] C. Singh, X. Luo, and H. Kim, "Power system adequacy and security calculations using Monte Carlo Simulation incorporating intelligent system methodology," *Proceedings of the 9th International Conference on Probabilistic Methods Applied to Power Systems*, Stockholm, Sweden, 2006, pp. 1–9.

[21] N. Gubbala and C. Singh, "A fast and efficient method for reliability evaluation of interconnected power systems - preferential decomposition method," *IEEE Transactions on Power Systems*, vol. 9, no. 2, pp. 644–652, 1994.

[22] M. Pereira, M. Macceira, G. C. Oliveira, and L. M. V. G. Pinto, "Combining analytical models and Monte-Carlo techniques in probabilistic power system analysis," *IEEE Transactions on Power Systems*, vol.7, no.1, pp. 265–272, 1992.

[23] C. Singh and J. Mitra, "Composite system reliability evaluation using state space pruning," *IEEE Transactions on Power Systems*, vol. 12, no. 1, pp. 471–479, 1997.

[24] N. Samaan and C. Singh, "Genetic algorithms approach for the assessment of composite power system reliability considering multi-state components," in *Pro-

ceedings of the 9th International Conference on Probabilistic Methods Applied to Power Systems, Ames, Iowa, 2004, pp. 64–69.

[25] H.-G. Beyer, H.-P. Schwefel, and I. Wegener, *How to Analyse Evolutionary Algorithms*, Technical Report No. CI-139/02, Dept. of Computer Science, University of Dortmund, Dortmund, Germany, August, 2002.

[26] F. Liang and W. H. Wong, "Real-parameter evolutionary Monte Carlo with applications to Bayesian mixture models," *Journal of the American Statistical Association*, vol. 96, no. 454, pp. 653–666, 2001.

[27] A. Cercueil and O. Francois, "Monte Carlo simulation and population-based optimization," in *Proceedings of IEEE Congress on Evolutionary Computation*, Seoul, Korea, 2001.

[28] A. P. Engelbrecht, *Fundamentals of Computational Swarm Intelligence*, Chichester, England: John &Wiley Sons, Ltd., 2005.

[29] A. C. G. Melo, M. V. F. Pereira, and A. M. Leite da Silva, "A conditional probability approach to the calculation of frequency and duration in composite reliability evaluation," *IEEE Transactions on Power Systems*, vol. 8, no. 8, pp. 1118–1125, 1993.

[30] C. Singh, "Rules for calculating the time-specific frequency of system failure," *IEEE Transactions on Reliability*, vol. R-30, pp. 364–366, 1981.

[31] IEEE Committee Report, "IEEE reliability test system," *IEEE Transactions on Power Apparatus and Systems*, vol. PAS-98, no. 6, pp. 2047–2054, 1979.

[32] J. Kennedy and R. Eberhart, "A discrete binary version of the particle swarm optimization," in *IEEE Proceedings of the International Conference on Systems,*

Man, and Cybernetics, Orlando, FL, 1997, pp. 4104–4108.

[33] R. E. Brown, *Electric Power Distribution Reliability*, New York: Marcel Dekker, Inc., 2002.

[34] G. Celli, E. Ghiani, S. Mocci, and F. Pilo, "A multiobjective evolutionary algorithm for the sizing and siting of distributed generation," *IEEE Transactions on Power Systems*, vol. 20, no. 2, pp. 750–757, May 2005.

[35] R. C. Dugan, T. E. McDermott, and G. J. Ball, "Planning for distributed generation," *IEEE Industry Applications Magazine*, March/April, 2001.

[36] H. L. Willis, and W. G. Scott, *Distributed Power Generation: Planning and Evaluation*, New York: Marcel Dekker, 2000.

[37] A. Pregelj, M. Begovic, A. Rohatgi, and D. Novosel, "On optimization of reliability of distributed generation-enhanced feeders," in *Proceedings of the 36th Hawaii International Conferences on System Sciences*, IEEE Computer Society, [CD-ROM], 2002, pp. 1–6.

[38] C. Blum, and M. Dorigo, "The hyper-cube framework for ant colony optimization," *IEEE Transactions on Systems, Man, and Cybernetics–Part B: Cybernetics*, vol. 34, no. 2, pp. 1161–1172, 2004.

[39] W. Kuo and R. Wan, "Recent advances in optimal reliability allocation," *IEEE Transactions on Systems, Man, and Cybernetics–Part A: Systems and Humans*, vol. 37, no. 2, pp. 143–156, 2007.

[40] K. M. Sim and W. H. Sun, "Ant colony optimization for routing and load-balancing: survey and new directions," *IEEE Transactions on Systems, Man, and Cybernetics–Part A: Systems and Humans*, vol. 33, no. 5, pp. 560–572, 2003.

[41] J.-P. Chiou, C.-F. Chang, and C.-T. Su, "Ant direction hybrid differential evolution for solving large capacitor placement problems," *IEEE Transactions on Power Systems*, vol. 19, no. 4, November, pp. 1794–1800, 2004.

[42] S. C. Chu, J. F. Roddick, and J. S. Pan, "Ant colony system with communication strategies," *Information Sciences*, Vol. 167, nos 1-4, pp. 63–76, 2004.

[43] J. F. Gomez, H. M. Khodr, P. M. De Oliveira, L. Ocque, J. M. Yusta, R. Villasana, and A. J. Urdaneta, "Ant colony system algorithm for the planning of primary distribution circuits," *IEEE Transactions on Power Systems*, vol. 19, no. 2, May, pp. 996–1004, 2004.

[44] J.-H. Teng and Y.-H. Liu, "A novel ACS-based optimum switch relocation method," *IEEE Transactions on Power Systems*, vol. 18, no. 1, February, pp. 113–120, 2003.

[45] J. G. Vlachogiannis, N. D. Hatziargyriou, and K. Y. Lee, "Ant colony system-based algorithm for constrained load flow problem," *IEEE Transactions on Power Systems*, vol. 20, no. 3, August, pp. 1241–1249, 2005.

[46] Lj. A. Kojovic and R. D. Willoughby, "Integration of distributed generation in a typical USA distribution system," in *Proceedings of the 16th CIRED*, 2001, pp. 1–5.

[47] J. Wan, *Nodal Load Estimation for Electric Power Distribution Systems*, Ph.D. Dissertation, Department of Electrical and Computer Engineering, Drexel University, PA, July, 2003.

[48] P. K. Hota and S. K. Dash, "Multiobjective generation dispatch through a neuro-fuzzy technique," *Electric Power Components and Systems*, vol. 32, pp. 1191–1206,

2004.

[49] T. Jayabarathi, K. Jayabarathi, D. N. Jeyakumar, and T. Raghunathan, "Evolutionary programming techniques for different kinds of economic dispatch problems," *Electric Power System Research*, vol. 73, pp. 169–176, 2005.

[50] K. Y. Lee, A. S. Yome, and J. H. Park, "Adaptive Hopfield neural networks for economic load dispatch," *IEEE Transactions on Power Systems*, vol. 13, no. 2, pp. 519-526, 1998.

[51] Z.-L. Gaing, "Particle swarm optimization to solving the economic dispatch considering the generator constraints," *IEEE Transactions on Power Systems*, vol. 18, no. 3, pp. 1187–1195, 2003.

[52] E. A. DeMeo, W. Grant, M. R. Milligan, and M. J. Schuerger, "Wind plant integration: costs, status, and issues," *IEEE Power & Energy Magazine*, November/December, pp. 38–46, 2005.

[53] J. Douglas, "Putting wind on the grid," *EPRI Journal*, pp. 6–15, Spring 2006.

[54] P. B. Eriksen, T. Ackermann, H. Abildgaard, P. Smith, W. Winter, and R. Garcia, "System operation with high wind penetration," *IEEE Power & Energy Magazine*, November/December, pp. 65–74, 2005.

[55] R. Piwko, D. Osborn, R. Gramlich, G. Jordan, D. Hawkins, and K. Porter, "Wind energy delivery issues," *IEEE Power & Energy Magazine*, November/December, pp. 67–56, 2005.

[56] J. C. Smith, "Wind of change: issues in utility wind integration," *IEEE Power & Energy Magazine*, November/December, pp. 20–25, 2005.

[57] R. Zavadil, N. Miller, A. Ellis, and E. Muljadi, "Making connections: wind generation challenges and progress," *IEEE Power & Energy Magazine*, pp. 26–37, November/December, 2005.

[58] V. Miranda, and P. S. Hang, "Economic dispatch model with fuzzy constraints and attitudes of dispatchers," *IEEE Transactions on Power Systems*, vol. 20, no. 4, Nov., pp. 2143–2145, 2005.

[59] J. Kennedy and R. Eberhart, *Swarm Intelligence*, San Francisco: Morgan Kaufmann Publishers, 2001.

[60] K. E. Parsopoulos, and M. N. Vrahatis, "Particle swarm optimization method in multi-objective problems," in *Proceedings of the ACM Symposium on Applied Computing*, Madrid, Spain, 2002, pp. 603–607.

[61] X. Hu, and R. Eberhart, "Multiobjective optimization using dynamic neighborhood particle swarm optimization," in *Proceedings of the IEEE Congress on Evolutionary Computation*, Honolulu, Hawaii, 2002, pp. 1677–1681.

[62] X. Hu, R. C. Eberhart, and Y. Shi, "Particle swarm with extended memory for multiobjective optimization," in *Proceedings of the IEEE Swarm Intelligence Symposium*, Indianapolis, Indiana, 2003, pp. 193–197.

[63] C. A. Coello Coello, and M. S. Lechuga, "MOPSO: A proposal for multiple objective particle swarm optimization," in *Proceedings of IEEE Congress on Evolutionary Computation*, Honolulu, HI, 2002, pp. 1051–1056.

[64] S. Mostaghim, and J. Teich, "Strategies for finding good local guides in multi-objective particle swarm optimization (MOPSO)," in *IEEE Proceedings of the 2003 Swarm Intelligence Symposium*, Indianapolis, IN, 2003, pp. 26–33.

[65] D. S. Liu, K. C. Tan, C. K. Goh, and W. K. Ho, "A multiobjective memetic algorithm based on particle swarm optimization," *IEEE Transactions on Systems, Man, and Cybernetics–Part B: Cybernetics*, vol. 37, no. 1, pp. 42–50, 2007.

[66] E. Zitzler, K. Deb, and L. Thiele, "Comparison of multiobjective evolutionary algorithms: Empirical results," *Evolutionary Computation*, vol. 8, no. 2, pp. 173–195, 2000.

[67] J. R. Schott, "Fault Tolerant Design Using Single and Multicriteria Genetic Algorithm Optimization," M.S. Thesis, Dept. Aeronautics and Astronautics, Massachusetts Inst. Technol., Cambridge, MA, May 1995.

[68] D. A. Van Veldhuizen, "Multiobjective Evolutionary Algorithms: Classifications, Analyzes, and New Innovation," Ph.D. Dissertation, Dept. Elec. Comput. Eng., Air Force Inst. Technol., Wright-Patterson AFB, OH, May 1999.

[69] H. K. Alfares, and M. Nazeeruddin, "Electric load forecasting: literature survey and classification of methods," *International Journal of Systems Science*, vol. 33, no. 1, pp. 23–34, 2002.

[70] B. A. Akash, R. Mamlook, and M. S. Mohsen, "Multi-criteria selection of electric power plants using analytical hierarchy process," *Electric Power Systems Research*, vol. 52, pp. 29–35, 1999.

[71] J. P. Barton and D. G. Infield, "Energy storage and its use with intermittent renewable energy," *IEEE Transactions on Energy Conversion*, vol. 19, no. 2, pp. 441–448, 2004.

[72] G. N. Bathurst and G. Strbac, "Value of combining energy storage and wind in short-term energy and balancing markets," *Electric Power System Research*, vol.

67, pp. 1–8, 2003.

[73] G. E. P. Box and G. M. Jenkins, *Time Series Analysis: Forecasting and Control*, San Francisco: Holden Day, 1976.

[74] R. Chedid, H. Akiki, and S. Rahman, "A decision support technique for the design of hybrid solar-wind power systems," *IEEE Transactions on Energy Conversion*, vol. 13, no. 1, pp. 76–83, March, 1998.

[75] R. Chedid and S. Rahman, "Unit sizing and control of hybrid wind-solar power systems," *IEEE Transactions on Energy Conversion*, vol. 12, no. 1, pp. 79–85, March, 1997.

[76] E. A. DeMeo, W. Grant, M. R. Milligan, and M. J. Schuerger, "Wind plant integration: costs, status, and issues," *IEEE Power & Energy Magazine*, pp. 38–46, November/December, 2005.

[77] W. EI-Khattam and M. M. A. Salama, "Distributed generation technologies, definitions, and benefits," *Electric Power System Research*, vol. 71, pp. 119–128, 2004.

[78] M. A. EI-Sayes, M. G. Osman, and S. S. Kaddah, "Assessment of the economic penetration levels of photovoltaic panels, wind turbine generators and storage batteries," *Electric Power Systems Research*, vol. 27, pp. 233–246, 1993.

[79] W. Kellogg, M. H. Nehrir, G. Venkataramanan, and V. Gerez, "Optimal unit sizing for a hybrid wind/photovoltaic generating system," *Electric Power Systems Research*, vol. 39, pp. 35–38, 1996.

[80] W. Kellogg, M. H. Nehrir, G. Venkataramanan, and V. Gerez, "Generation unit sizing and cost analysis for stand-alone wind, photovoltaic, and hybrid wind/PV

systems," *IEEE Transactions on Energy Conversion*, vol. 13, no. 1, pp. 70–75, 1998.

[81] T. Senjyu, D. Hayashi, N. Urasaki, and T. Funabashi, "Optimum configuration for renewable generating systems in residence using genetic algorithm," *IEEE Transactions on Energy Conversion*, vol. 21, no. 2, June, pp. 459–466, 2006.

[82] T. J. Stewart, "A critical survey on the status of multiple criteria decision making theory and practice," *OMEGA*, vol. 20, no. 5/6, pp. 569–586, 1992.

[83] L. F. Wang, and C. Singh, "Compromise between cost and reliability in optimum design of an autonomous hybrid power system using mixed-integer PSO algorithm," in *IEEE Proceedings of International Conference on Clean Electrical Power (ICCEP07)*, Capri, Italy, May, 2007, pp. 682–689.

[84] L. F. Wang and C. Singh, "Environmental/economic power dispatch using a fuzzified multi-objective particle swarm optimization algorithm," *Electric Power Systems Research*, vol. 77, no. 12, pp. 1654–1664, 2007.

[85] L. F. Wang and C. Singh, "Calculation of wind power capacity credit based on reliability evaluation using population-based intelligent search," *IEEE Proceedings of the 10th International Conference on Probabilistic Methods Applied to Power Systems (PMAPS08)*, Rincon, Puerto Rico, May 2008, pp. 1–6.

[86] L. F. Wang and C. Singh, "Population-based intelligent search in reliability evaluation of generation systems with wind power penetration," *IEEE Transactions on Power Systems*, in press, 2008.

VITA

Lingfeng Wang obtained his B.Eng and M.Eng degrees from Zhejiang University, China in 1997 and 2000, respectively. He also has an M.Eng degree from National University of Singapore in 2002. His research interests include integration of renewable energy sources, electric power and energy systems, computational intelligence, and industrial informatics.

His permanent address is:

Lingfeng Wang

You Chen Nong #7, Shen Dang

Haiyan County, Jiaxing City

Zhejiang Province, P.R. China 314311

The typist for this thesis was Lingfeng Wang.